Structure-biological function study of 17β-hydroxysteroid dehydrogenase type 1 and reductive steroid enzymes: inhibitor design targeting estrogen-dependent diseases

Thèse

Tang Li

Doctorat en médecine moléculaire
Philosophiæ doctor (Ph. D.)

Québec, Canada

Résumé

La 17β-HSD1 catalyse l'activation de l'œstrogène le plus actif, l'estradiol, ainsi que la désactivation de la dihydrotestosterone, l'androgène le plus puissant. Cette enzyme est considérée comme une cible prometteuse pour le traitement des maladies dépendantes des œstrogènes. Malgré des décennies de recherches, aucun inhibiteur ciblant la 17β-HSD1 n'a encore atteint le stade clinique. De plus, le mécanisme de l'inhibition du substrat de la 17β-HSD1, qui peut être utilisé pour faciliter la conception d'inhibiteur, n'est toujours pas bien démontré de manière structurelle. Ici, nous avons Co-cristallisé trois inhibiteurs de différence, à savoir l'EM-139, le 2-MeO-CC-156 et le PBRM, avec la 17β-HSD1 et avons résolu ces structures cristallines. L'inhibiteur réversible EM-139 s'est révélé moins stable dans le site de liaison aux stéroïdes, avec seulement la fraction du noyau stéroïdien de l'inhibiteur présentant une densité d'électron définissable. La fraction volumineuse de 7α-alkyle de l'inhibiteur, qui limite son activité anti-œstrogénique, n'est pas définie dans la densité électronique, peut compromettre l'effet inhibiteur de l'inhibiteur sur l'enzyme. Quant à l'inhibiteur réversible, le 2-MeO-CC-156, il interagit de manière similaire que le CC-156 avec l'enzyme. Cependant, avec la présence du groupe 2-MeO, le pouvoir inhibiteur de la 17β-HSD1 est nettement inférieur à celui du CC-156. L'analyse du complexe ternaire PBRM avec la 17β-HSD1 montre clairement la formation d'une liaison covalente entre l'His^{221} et la chaîne latérale bromoethyl de l'inhibiteur, donnant un aperçu des interactions moléculaires bénéfiques qui favorisent la liaison et l'avènement de N-alkylation ultérieur dans le site catalytique de l'enzyme. En outre, le groupe bromoethyl en position C-3 du PBRM justifie son profil non œstrogénique, ralentit son métabolisme et assure son action spécifique de la 17β-HSD1 par la formation d'une liaison covalente avec Nε du résidu His^{221}. Nous avons aussi Co-cristallisé la 17β-HSD1 avec l'œstrone ainsi qu'avec l'analogue de l'œstrone et du cofacteur NADP+, la structure a révélé un mode de liaison inversé de l'œstrone dans l'enzyme, jamais trouvé dans les complexes d'estradiol. L'analyse structurale a démontré que His^{221} est le résidu clé responsable de la réorganisation et de la stabilisation de l'œstrone liée de manière inversée, conduisant à la formation d'un complexe sans issue. Ainsi, sur la base du mécanisme d'inhibition du substrat et de l'analyse computationnelle, une novelle entité chimique (SX7) est proposée qui peut inhiber la 17β-HSD1 et former un complexe sans issue. De plus, avec un grand nombre d'échantillons cliniques, nous avons démontré la modulation et la corrélation d'expression significative de plusieurs enzymes clés de conversion des stéroïdes, supportant les 17β-HSD1 et 17β-HSD7 réductrices comme cibles prometteuses et la nouvelle thérapie combinée ciblant les 11β-HSD2 et 17β- HSD7.

Abstract

Human 17β-hydroxysteroid dehydrogenase type 1 (17β-HSD1) catalyzes the activation of the most potent estrogen estradiol as well as the deactivation of the most active androgen dihydrotestosterone, and is considered as a promising target for the treatment of estrogen-dependent diseases such as endometriosis, breast cancer, endometrial cancer and ovarian cancer. Despite decades of research, no inhibitor targeting 17β-HSD1 has yet reached the stage of clinical trials. Moreover, the structure-biological function of the substrate inhibition of 17β-HSD1, which can be used to facilitate the inhibitor design, is still not well demonstrated. Here we co-crystallized three different inhibitors, namely EM-139, 2-MeO-CC-156 and PBRM, with 17β-HSD1 and solved the structures of these complexes. The reversible inhibitor EM-139 showed high mobility in the steroid binding site with only its steroid core moiety could be defined in the electron density. The bulky 7α-alkyl moiety of the inhibitor, which guarantees its anti-estrogenic activity but unable to be defined in the electron density, may compromise the inhibitory effect of the inhibitor on the enzyme. As for the reversible inhibitor 2-MeO-CC-156, it interacts similarly to CC-156 with the enzyme. However, in the presence of the 2-MeO group, it shows much less inhibitory potency to 17β-HSD1 as compared to the CC-156. The analysis of the PBRM ternary complex with 17β-HSD1 clearly shows an unambiguous continuity of electron density from the side chain of His^{221} to the bound PBRM, demonstrating the formation of a covalent bond between the Nε of His^{221} and the C-31 ($BrCH_2$) of the inhibitor. This result provides insight into beneficial molecular interactions that favor the binding and subsequent N-alkylation event in the enzyme catalytic site. Also, the bromoethyl group at position C-3 of the PBRM warrants its non-estrogenic profile, slows down its metabolism, and secures the specific action of 17β-HSD1 through the formation of a covalent bond with Nε of residue His^{221}. Meanwhile, we co-crystallized 17β-HSD1 with estrone as well as with estrone and cofactor analog NADP+, revealed a reversely orientated binding mode of estrone in the enzyme, never found in reported estradiol complexes. Structural analysis demonstrated that His^{221} is the key residue responsible for the reorganization and stabilization of the reversely bound estrone, leading to the formation of a dead-end complex. Thus, based on the substrate inhibition mechanism and computational analysis, a chemical entity (SX7) is proposed that may inhibit 17β-HSD1 and form a dead-end complex. Furthermore, with large number clinical samples, we demonstrated the significant expression modulation and expression correlation of several key steroid-converting enzymes, supporting the reductive 17β-HSD1 and 17β-HSD7 as promising targets and the new combined therapy targeting 11β-HSD2 and 17β-HSD7.

Table des matières

Liste des figures

Liste des figures, tableaux, illustrations

Liste des abréviations

2-MeO-CC-156	2methoxy-16β-(m-carbamoylbenzyl)-E2
3β-diol	5α-androstane-3β,17β-diol
4-dione	androstenedione
5-diol	5-androstenediol; androst-5-ene-3β,17β-diol
5-diol-FA	5-diol fatty acid
5-diol-S	5-diol sulfate
ACTH	adrenocorticotropic hormone
A-dione	5α-androstane-3,17-dione
ADT	androsterone
AIs	aromatase inhibitors
AKR	aldo-ketoreductase
AR	androgen receptor
BC	breast cancer
$C_{12}E_8$	octaethylene glycol monododecyl ether
CC-156	16β-m-carbamoylbenzyl-E2
CRH	corticotropin releasing hormone
DHEA	dehydroepiandrosterone
DHEAS	dehydroepiandrosterone sulfate
DHT	dihydrotestosterone
DMF	Dimethylformamide

E1	Estrone
E1S	estrogen sulfate
E2	Estradiol
EDD	estrogen-dependent disease
EM-139	N-n-Butyl-N-methyl-ll-(16'α-chloro3',17'β-dihydroxyestra-1',3',5'(10')-trien-7'α-yl)undecanamide
epi-ADT	epiandrosterone
ER	estrogen receptor
EREs	estrogen responsive elements
FSH	follicle-stimulating hormone
GnRH	gonadotropin-releasing hormone
GSC	Genome Sequencing Centers
HSD	hydroxysteroid dehydrogenase
HTS	high throughput sequencing
LH	luteinizing hormone
mg	microgram
ml	microliter
NAD+	nicotinamide adenine dinucleotide
NADP+	nicotinamide adenine dinucleotide phosphate
NIH	National Institute of Health
nm	nanometer

nM	nanomolar
OD	optical density
PAGE	polyacrylamide gel electro phoresis
PBRM	3-(2-bromoethyl)-16β-(m-carbamoylbenzyl)-17β-hydroxy-1,3,5(10)-estratriene
PDB	protein data bank
*p*NPA	*p*-nitro phenyl acetate
*p*NPB	*p*-nitro phenyl butyrate
*p*NPD	*p*-nitro phenyl decanoate
*p*NPL	*p*-nitro phenyl dodecanoate
*p*NPM	*p*-nitro phenyl myristate
*p*NPP	*p*-nitro phenyl palmitate
P_{PH}	polyhedron promoter
pro-S	prochiral S configuration
RhB	rhodamine B
RhB-OOe	RhB-olive oil
RNA-seq	RNA sequencing
RoDH-1	Ro dehydrogenase 1
SDR	short chain dehydrogenase/reductase
SDS	sodium dodecyl sulfate
SG	space group
Sult2B1	sulfotransferase 2B1

T	testosterone
TCGA	The Cancer Genome Atlas
Testo	testosterone
UGT1A1	uridine glucuronosyl transferase 1A1
UGT2B28	uridine glucuronosyl transferase 2B28
UV	ultra-violet
β-DDM	n-Dodecyl-β-D-Maltoside
β-ME	β-mercaptoethanol
β-OG	n-octyl-β-D-glucoside
μM	micromolar

Remerciements

I would like to convey my immeasurable gratitude to my director of research, professor Sheng-Xiang Lin, for his meticulous guidance and enlightening discussions that helped me overcome all the difficulty and enabled me to present this thesis. I greatly appreciate his trustiness and supports for giving me this inspiring and challenging project. His diligent directions and interactive concept helped me greatly during my study, and I will certainly benefit from that in my future career. I also sincerely appreciate the following person and organisations for supporting my doctoral study to obtain the degree of Doctor of Philosophy (Ph.D.). The Ph.D. study will light up my future career in scientific research and practise.

I would like to thank all the members in Dr. Lin's Lab. I express my gratitude to Dre. Ming Zhou for her help in protein purification and crystallization; to Mr. Jean-François Theriault for his help in enzyme kinetics; to Mr. Jian Song for his help in binding study and growing rLcn6 crystals; to Dr. Preyesh Stephen for his help in Crif1-CDK2 project; to Miss. Xiaoye San and Ruixuan Wang for their inspiriting discussion in diagnosis and treatment of breast and ovarian cancers. I would like to thank Dr. Dao-Wei Zhu for his help in familiar with the surroundings and his advices in protein purification and crystallization. As well as Dr. Xiaoqiang Wang, Dre. Dan Xu and Dre. Juliette Adjo Aka for their advices and discussion in cell experiments.

I would like to thank Dr. Donald Poirier. I sincerely appreciate the knowledge from him in the field of medicinal chemistry, especially for the inhibitor design. I would like to thank Dr. Rong Shi for his help in collecting an X-ray diffraction dataset at the CLS synchrotron. I would like to thank Dr. Alexandre Brunet in the Laboratory of Flow-cytometry for his advice in preparing the sample and analysing the results. I also appreciated Dre. Sylvie Bourassa and Dre. Florence Roux-Dalvai for their advice and discussion in mass spectrometry experiment design and sample preparation. I would like to thank Mr. Martin Thibault for his help in analysing image of western blot.

I would like to thank all administration staffs in the Research Center of CHU de Quebec (CHUL). Thank Mme Nicole Almeras for taking care of the registration and financial documents. Thank Mme Marianne Roberge for her help in the order of experiment materials and reagents.

Finally, I am very grateful to my family, especially to my beloved son Guanrui Li and wife Juan Liu as well as my parents. It is your love that encouraging and supporting me during my studies.

Avant-propos

This thesis is submitted to the “Faculté des études supérieures de l'Université Laval” for the requirement of a doctor’s degree in science. The thesis is written in English, except for the summary as well as the abstract of each article, which are in French. Two articles have been published by Journal of Physical Chemistry Letters and Health, respectively. The other three are being submitted for publication or in preparation.

In the introductory section, four major estrogen-dependent diseases were reviewed. The biosynthesis of estrogens, mostly estradiol, and the role of 17β-HSD1 in estrogen activation as well as inactivation of androgen are summarized. The structural and kinetic studies as well as the development of 17β-HSD1 inhibitor design are also discussed. The hypothesis and objectives are described in the end of this chapter.

The Chapter I: “Tang Li, René Maltais, Donald Poirier, Sheng-Xiang Lin. Combined Biophysical Chemistry Reveals a New Covalent Inhibitor with a Low-Reactivity Alkyl Halide. *Journal of Physical Chemistry Letters* (2017 IF: 8.7). 2018 Aug; 9:5275-5280. doi: 10.1021/acs.jpclett.8b02225.” I conducted all the experiments and wrote the manuscript, and I’m the first author of this article. In this chapter, the crystal structures of 17β-HSD1 with two inhibitors (PBRM and 2-MeO-CC-156) were described. This study constructed the first example of N-alkylation between a human enzyme and a low-reactivity alkyl halide derivative, which opens the door to a new design of alkyl halide-based specific covalent inhibitors as potential therapeutic agents.

The Chapter II: “Tang Li, Dao-Wei Zhu, Fernand Labrie and Sheng-Xiang Lin. Crystal structures of human 17β-hydroxysteroid dehydrogenase type 1 complexed with the dual-site inhibitor EM-139. *Health*. 2018 Aug; 10(8):1079-89. doi: 10.4236/health.2018.108081.” I processed the crystal diffraction data to solve the complex structure and wrote the manuscript, and I’m the first author of this article. In this chapter, the 17β-HSD1 binary complex with the inhibitor EM-139 was described. The interaction between the steroid moiety of the inhibitor and the enzyme was analyzed. The influence of its bulky 7α-alkyl side chain to its inhibitory effect in 17β-HSD1 was also discussed.

The Chapter III: “Tang Li, Preyesh Stephen, Dao-Wei Zhu, Rong Shi, Sheng-Xiang Lin. Crystal structures of human 17β-hydroxysteroid dehydrogenase type 1 complexed with estrone and cofactor reveal the mechanism of substrate inhibition. *FEBS Journal*. 2019. Doi: 10.1111/febs.14784.” I conducted all the experiments except for the crystallization of the 17β-HSD1-E1 binary complex. I wrote the manuscript, and I’m the first author of this article. In this chapter, the crystal structures of 17β-HSD1 in complex with E1 and with/without cofactor analog NADP+ were described. Based on the E1 binary and ternary complex structures as well as previously published 17β-HSD1 complexes with other ligands, the mechanism of the long observed substrate inhibition of 17β-HSD1 has been discussed.

The Chapter IV: “Tang Li, Zhongjun Li, Sheng-Xiang Lin. Remarkable steroid-converting enzyme and receptor regulations in large number breast tumor samples: molecular correlation and combined therapies (Article under submission).” I conducted the data analysis and wrote the manuscript, and I’m the first author of this article. In this chapter, the cDNA sequencing data from the public cohort The Cancer Genome Atlas Breast Invasive Carcinoma (TCGA-BRCA) was extracted and statistically analyzed, and identified several key steroid-converting enzymes which are significantly up-regulated in cancer samples. Close expression correlations of the enzymes were also found, suggesting combined therapy for breast cancer treatment.

In the conclusion, I interactively discussed 17β-HSD1 structure-function study from inhibitor interactions to the mechanism of enzyme regulation. Besides, I also discussed the use of cDNA sequencing data in breast cancer research.

The references of introduction and conclusion are listed after the conclusion section. References of publications are listed after the text of each article.

In the end of the thesis is the appendix: “Tang Li, Wenfa Zhang, Jianhua Hao, Mi Sun, Sheng-Xiang Lin. Cold-active extracellular lipase: expression in Sf9 insect cells, homogenization, and catalysis. *Biotechnol Rep (Amst)*. 2018; 21:e00295. doi:10.1016/j.btre.2018.e00295.” I conducted all the experiments and wrote the manuscript, and I’m the first author of this article. In this article, I expressed a novel cold-active marine lipase in Sf9 insect cells. After purification, I carefully characterized its enzymatic properties, such as the optimum temperature and pH ranges, substrate specificity, the effects of detergents, organic solvents as well as enzyme inhibitors. These results will facilitate its application in industries.

Introduction

1 Estrogen-dependent disease

1.1 Breast cancer

Breast cancer (BC) is the most commonly diagnosed cancer in women worldwide, and one of the leading cause of cancer death in women[1]. BC can also occur in man, but it is rare [1]. It has estimated that 268,670 patients will be diagnosed BC in 2018 in the United States, among which 99% were women (**Figure 1**)[2]. The estimated number of death from BC in women is 40,920, ranking the second among all estimated deaths from cancers[2]. The incidence of BC is estimated to increase based on the trend of the past ten years (**Figure 2**)[2-12]. Similar situation was also observed in Canada, about 26,300 female patients will be diagnosed BC, which account for 25% of all cancers in 2017 (Canadian breast cancer statistics 2017, http://www.cancer.ca/en/cancer-information/cancer-type/breast/statistics/). The majority of female patients diagnosed with BC are above 45 years old, and mostly after menopause[13]. Among incidences of all BCs, around 60% in premenopausal women and 75% in postmenopausal women are initially estrogen-dependent[14-15]. There is a multistep process involved in the occurrence of BC, which starts from normal cells through hyperplasia, premalignant change, in situ carcinoma, progression of primary BC and to metastasis formation (**Figure 3**)[16]. During this progression process, hormones such as estrogen, progesterone and prolactin, stimulate cell proliferation through their receptors mediated signaling pathways as well as induced genetic damage and mutations[16-17].

Estimated New Cases				Estimated Deaths		
Breast	266,120	30%		Lung & bronchus	70,500	25%
Lung & bronchus	112,350	13%		Breast	40,920	14%
Colon & rectum	64,640	7%		Colon & rectum	23,240	8%
Uterine corpus	63,230	7%		Pancreas	21,310	7%
Thyroid	40,900	5%		Ovary	14,070	5%
Melanoma of the skin	36,120	4%		Uterine corpus	11,350	4%
Non-Hodgkin lymphoma	32,950	4%		Leukemia	10,100	4%
Pancreas	26,240	3%		Liver & intrahepatic bile duct	9,660	3%
Leukemia	25,270	3%		Non-Hodgkin lymphoma	8,400	3%
Kidney & renal pelvis	22,660	3%		Brain & other nervous system	7,340	3%
All Sites	**878,980**	**100%**		**All Sites**	**286,010**	**100%**

Figure 1 Ten leading cancer types for the estimated new cancer cases and deaths in women in United States, 2018 (Siegel et al., 2018).

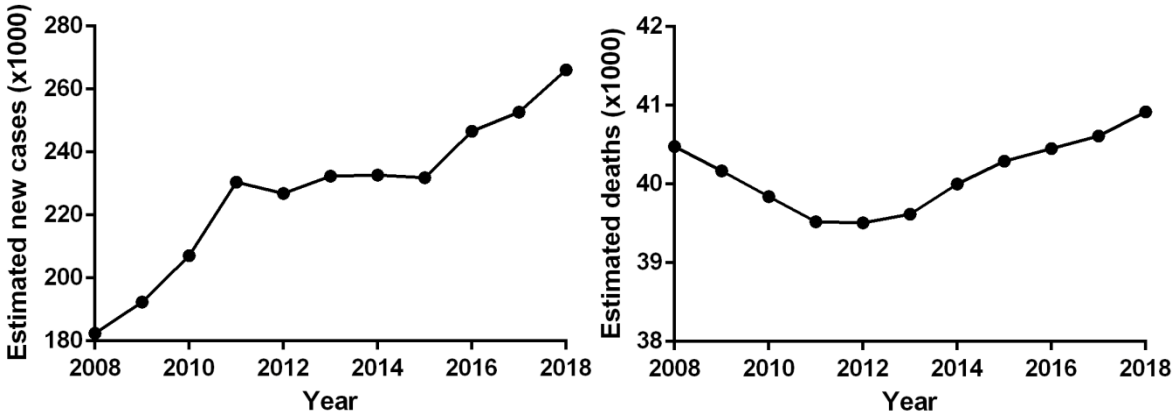

Figure 2 The time course of the estimated new BC cases and deaths in women in the United States (Jemal et al., 2008-2010; Siegel et al., 2011-2018).

Estradiol (E2) is the most biologically potent natural estrogen. In estrogen dependent human breast cancers, E2 plays a critical role in the proliferation and development of carcinoma cells and it is actually essential for some of these carcinomas to continue growth[18]. The primary biological effects of estrogen are mediated by two distinct nuclear receptors, estrogen receptor (ER)α[19] and ERβ[20], which encoded by unique genes and function in the nucleus as ligand-dependent transcription factors. ERα is mainly responsible for the effects of estrogens on normal and malignant breast tissues. Its role in promoting proliferation of BC cells is well characterized, through either membrane and cytoplasmic signaling cascades[21] or transcriptional regulation[22]. In contrast, the role of ERβ in BC is not clearly understood but seems to act as an antagonist of ERα activity, attenuating the proliferation stimulation effect of estrogen[23-25].

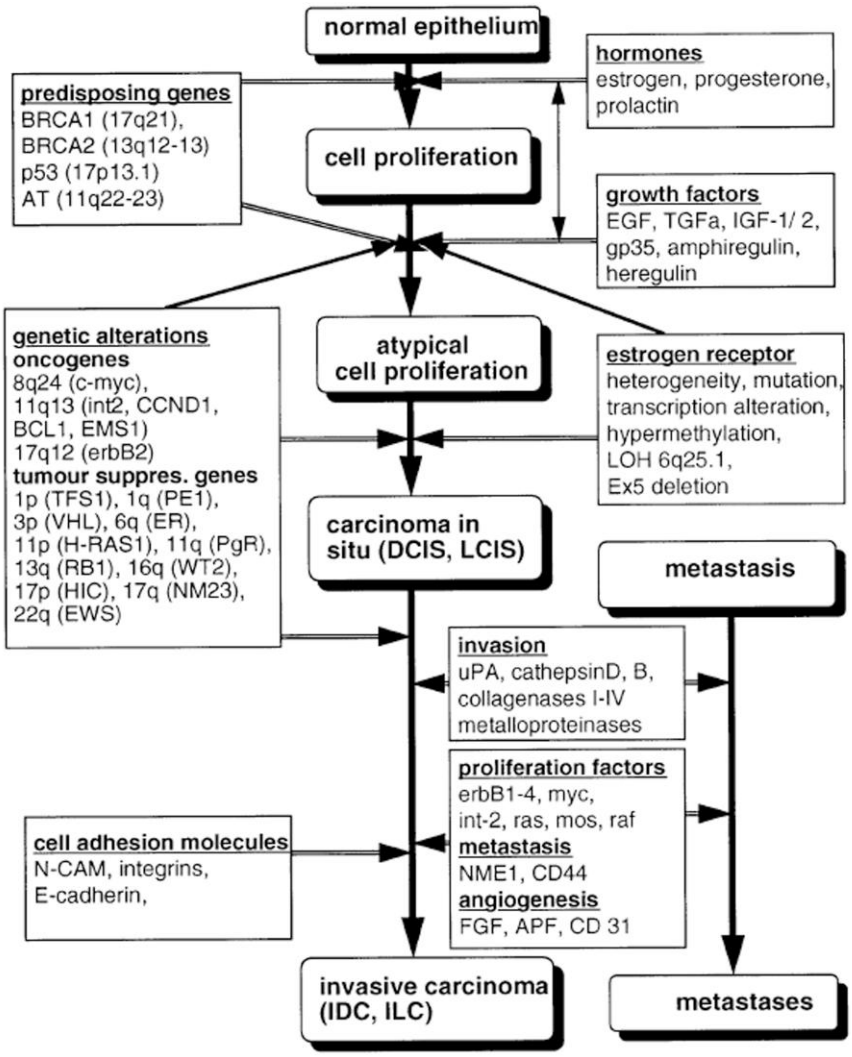

Figure 3 Model of the multistep carcinogenesis in BC (Beckmann et al., 1997).

1.2 Endometrial cancer

Endometrial cancer is one of the most common gynecologic malignancies. It ranks to be the fourth most diagnosed cancers in women after breast, lung, and colorectal cancers, and was expected to have more than 63,000 new cases in US in 2017 (**Figure 1**)[12]. The death rate for endometrial cancer almost doubled during the past two decades[26]. Endometrial cancer is commonly classified into two types based on the dualistic model of endometrial cancer tumorigenesis described by Bokhman[27]. Type I commonly develops in women before menopause in an estrogen-dependent manner. In contrast, type II endometrial cancer majorly develops in postmenopausal women in an estrogen-independent manner[28]. The pathogenesis of type I endometrial cancer is through atypical endometrial hyperplasia, whereas type II endometrial cancer is proposed to be generated directly from normal endometrium[28]. Most patients diagnosed with endometrial adenocarcinoma are between

the ages of 50 and 60 years, and 90% of women diagnosed with endometrial cancer are after age of 50, mostly after menopause[26, 29]. About 80% of endometrial cancers are estrogen-dependent[30] and the most potent estrogen, estradiol (E2), is suggested to play an important role in the pathogenesis of the disease by increasing the mitotic activity of endometrial cells[31].

1.3 Endometriosis

Endometriosis is an estrogen-activated gynecological disease characterized by the presence of endometrial-like tissue growing outside the uterine cavity, typically on the pelvic peritoneum, ovaries, and uterosacral ligaments, and in the rectovaginal septum and vesico-uterine fold[32]. Severe disease may lead to deformation of pelvic anatomy and extensive pelvic adhesions, often associated with pelvic pain and infertility[32]. Endometriosis is initially considered largely as a benign condition, while the wide opinion nowadays is that endometriosis is a neoplastic condition which can develop into specific type of invasive ovarian cancer[33-34]. It is estimated that 6 to 10% of diagnosed endometriosis are in premenopausal women, whereas the frequency rises up to 50% of women with infertility[32]. Endometriosis is a multifactorial disease. Its pathogenesis involves estrogen overexposure, angiogenesis, inflammation, genetic predisposition, and environmental exposure to pollutants[35-40]. It has been demonstrated that estrogen plays a central role in the development and maintenance of endometriosis by promoting the growth of ectopic tissue[41]. In premenopausal patient, the depression of E2 levels through gonadotropin-releasing hormone analogues (GnRH-a) leads to the relieving of pains and regression of endometriotic lesions, which relapsed with the recovery of E2 when the therapy discontinues[42]. While in postmenopausal women, the administration of hormone replacement therapy may lead to the relapse of endometriosis[43].

1.4 Ovarian cancer

Ovarian cancer is the fifth most lethal of all gynecological malignancies in western country with more than 14,000 estimated death in 2017 in The United States (**Figure 1**)[12]. As more than 80% of all diagnosed ovarian cancers are in women above age 50, it is mainly considered to be a disease of postmenopausal women[44]. About 90% of malignant ovarian tumors are epithelial ovarian cancer[45]. Epidemiological data show that estrogen exposure and metabolism are involved in the stimulation and pathogenesis of ovarian cancer, and patients taking estrogen-only hormone replacement therapy have a higher risk of ovarian cancer[44, 46-48]. Cell studies confirmed that ovarian cancer cells share several estrogen regulation pathways with other estrogen-associated cancers such as endometrial cancer and breast cancer, and anti-estrogen intervention suppresses the proliferation of ovarian cancer cells *in vitro* and *in vivo*[49-51]. Moreover, estrogen was demonstrated to promote ovarian cancer cell migration and invasion through activating the PIK3/AKT pathway expression and down-regulating nm23-H1 expression[52].

2 Origins of estradiol

The origins of E2 in women can be divided into two sources, one is secreted from the ovary, and another is locally biosynthesized from the adrenal precursor dehydroepiandrosterone (DHEA), dehydroepiandrosterone-sulfate (DHEAS) and androstenedione in the peripheral tissues[51]. In premenopausal women, circulating E2 is produced primarily by the ovaries[53], and DHEAS is produced primarily by the adrenal glands[54]. As for the DHEA, half of it is produced by adrenal glands, 20% originates from the ovaries and the other 30% is converted from DHEAS in peripheral tissues by sulfatase[55]. The production of androstenedione is equally contributed by the adrenals and the ovaries[56] (**Figure 4A**). After menopause, when the ovaries become atrophied and cease to act, E2 no longer functions as a circulating hormone. Thus, E2 in postmenopausal women is produced only from precursor steroids of the adrenal glands in an intracrine manner to peripheral sites, which include breast, bone, vascular smooth muscle, and various sites in the brain (**Figure 4B**)[51, 57]. Moreover, it is increasingly being recognised in EDDs that these tumor tissues are not just passively dependent on circulating levels of E2 but rather generate it locally from precursors in an active fashion[58-59].

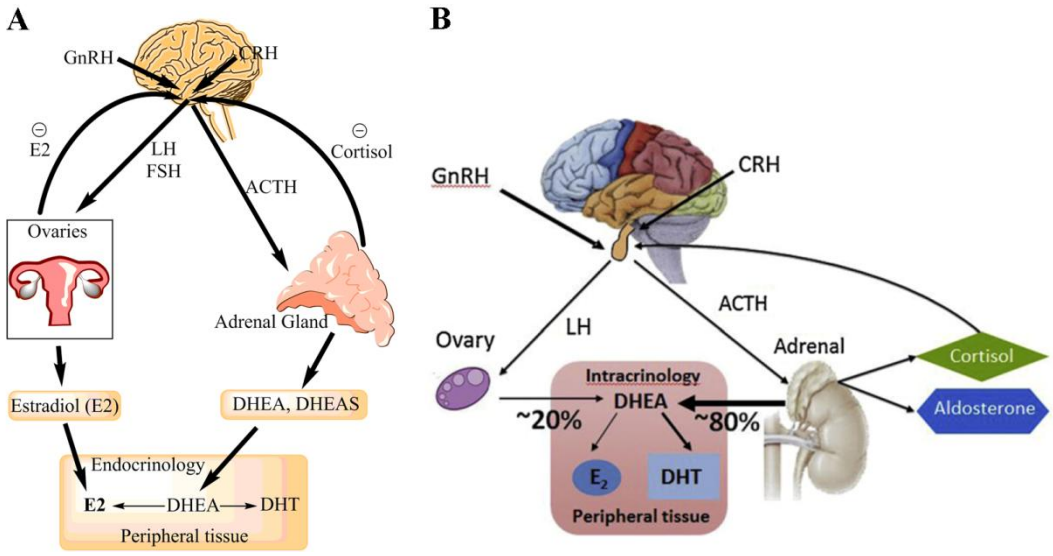

Figure 4 Schematic representations of sex hormones synthesis regulations in pre- (A) and postmenopausal (B) women. GnRH, gonadotropin releasing hormone; LH, luteinizing hormone; FSH, follicle-stimulating hormone; CRH, corticotropin releasing hormone; ACTH, adrenocorticotropic hormone; T, testosterone; DHT, dihydrotestosterone; DHEA, dehydroepiandrosterone; E2, estradiol (Labrie 2015).

3 The role of 17β-HSD1

17β-HSD1 belongs to the short-chain dehydrogenase/reductase (SDR) family[60]. The major function of this enzyme is the activation of estrone (E1) to the most potent estrogen E2 (**Figure 5**) [61], which is known to play a pivotal role in the occurrence and development of estrogen-dependent diseases (EDDs). It can also catalyze the conversion of DHEA into 5-androstene-3β,17β-diol (5-diol), which has been suggested to be the main estrogen after menopause[62]. Beside the ability of activating estrogen, 17β-HSD1 can also inactivate androgens. It has been demonstrated that 17β-HSD1 can transform the most potent androgen dihydrotestosterone (DHT) into a weak estrogen 5α-Androstane-3β,17β-diol (3β-diol), a reaction which has been proposed to become more important after menopause and may be involved in aromatase inhibitor (AI) resistance[63-65]. 17β-HSD1 is the most active enzyme in terms of the production of E2[66-67]. The over-expression of 17β-HSD1 as well as the increased estrogen/androgen ratio indicates the pivotal role of the enzyme in breast cancer[68-69], endometrial cancer[30, 70], endometriosis [71], and ovarian cancer[72]. Thus, inhibition of 17β-HSD1 is considered as a promising therapeutic approach for the treatment of these diseases.

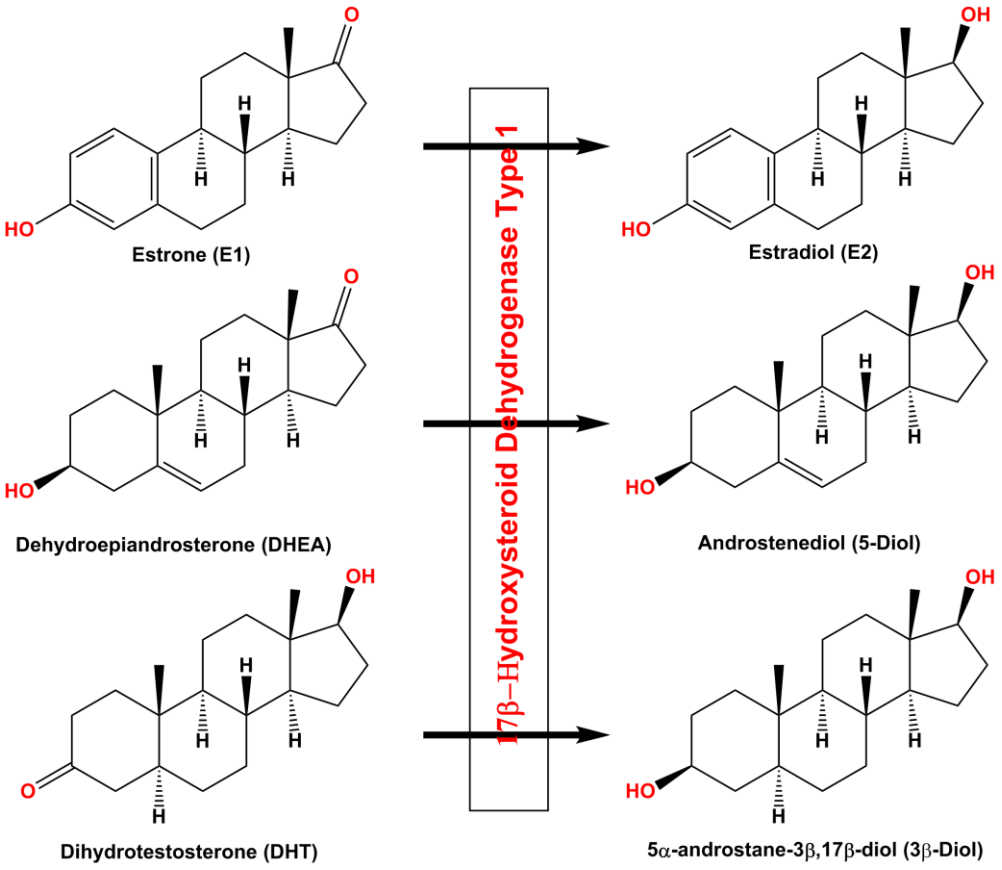

Figure 5 Human 17β-HSD1 catalyze the conversion of E1 to E2, DHEA to 5-Diol, and DHT to 3β-Diol (Dumont et al., 1992; Aka et al., 2010).

4 Structural studies of 17β-HSD1

17β-HSD1 is the first human steroid-converting enzyme whose three-dimensional structure has been solved. 17β-HSD1 consists of 328 amino acids with a molecular weight of 34.5kDa. This membrane-associated enzyme is acting as a homodimer and possesses a conserved Tyr-X-X-X-Lys sequence as a SDR family member and a Ser residue at the active site[66, 73]. The first crystallization of human estrogenic 17β-HSD1 was reported by Zhu and co-workers in 1993[74]. The three-dimensional structure of the enzyme was published in 1995[75]. Since then, there are 22 17β-HSD1 structures deposited into the protein data bank (PDB), some in complex with substrate or inhibitor, some in complex with cofactor, and some in combination with cofactor and substrate/inhibitor (**Table 1**). This has led to the atomic level description of the substrate and cofactor binding cavities of the enzyme and a detailed understanding of its mechanism of action, as well as the molecular basis for the estrogen-specificity of the enzyme[76-78].

The core of 17β-HSD1 structure is consisting of seven-stranded parallel β-sheet (βA to βG) surrounded by six parallel α-helices (αB to αG), evenly distributed by the two sides of the β-sheet (**Figure 6**). The structure of the protein generally forms into two segments: the first segment, βA to βF, is a classic Rossmann fold, responsible for cofactor binding; the second segment, βD to βG, is partly in the Rossmann fold, governs steroid substrate binding[75]. The C-terminus of 17β-HSD1 (285-327) cannot be defined in all published structures and residues 190-199 have very poor density or even no density in many structures (1FDS, 1FDU, 1FDV, 1FDW, 1JTV, 1QYV, 1QYW, 1QYX, 3DEY, 3KLM, 3KLP, 3KM0).

Table 1 Previously published 17β-HSD1 structures

PDB code	ligand	Cofactor	Resolution(Å)	SG	Other	Author	βFαG'-loop
1A27	EST	NAP	1.9	C2		Mazza	Closed
1BHS			2.2	C2		Ghosh	Semi-opend
1DHT	DHT		2.24	C2		Han	Opened
1EQU	EQI	NAP	3.0	P212121		Sawicki	Closed
1FDS	EST		1.7	C2		Breton	-
1FDT	EST	NAP	2.2	C2	SO4	Breton	Closed
1FDU	EST	NAP	2.7	P21	SO4	Mazza	-
1FDV		NAD	3.1	P21	SO4	Mazza	-
1FDW	EST		2.7	C2		Mazza	-
1I5R	HYC		1.6	C2	GOL	Qiu	Closed
1IOL	EST		2.3	C2		Azzi	Opened
1JTV	TES		1.54	C2	GOL	Gangloff	-
1QYV		NAP	1.81	C2	GOL	Shi	-
1QYW	5SD	NAP	1.63	C2	GOL	Shi	-
1QYX	ASD	NAP	1.89	C2	GOL	Shi	-
3DEY	DHT		1.7	C2	GOL	Mazumdar	-
3DHE	AND		2.3	C2		Han	Opened

3HB4	E2B		2.21	C2		Mazumdar	Closed
3HB5	E2B	NAP	2.0	C2		Mazumdar	Closed
3KLM	DHT		1.7	C2	GOL	Aka	-
3KLP	B81		2.5	C2		Mazumdar	-
3KM0	AOM	NAP	2.3	C2		Mazumdar	-

EST, estradiol; NAP, NADP; B81, 5-Androstenediol; AOM, 5α-Androstane-3β,17β-diol (3β-diol); 5SD, 5α-Androstane-3,17-dione (5α-Adione); ASD, 4-Androstene-3,17-dione (4-dione); TES, testosterone (T); AND, Dehydroepiandrosterone (DHEA); EQI, Equilin; HYC, EM-1745. SG, space group.

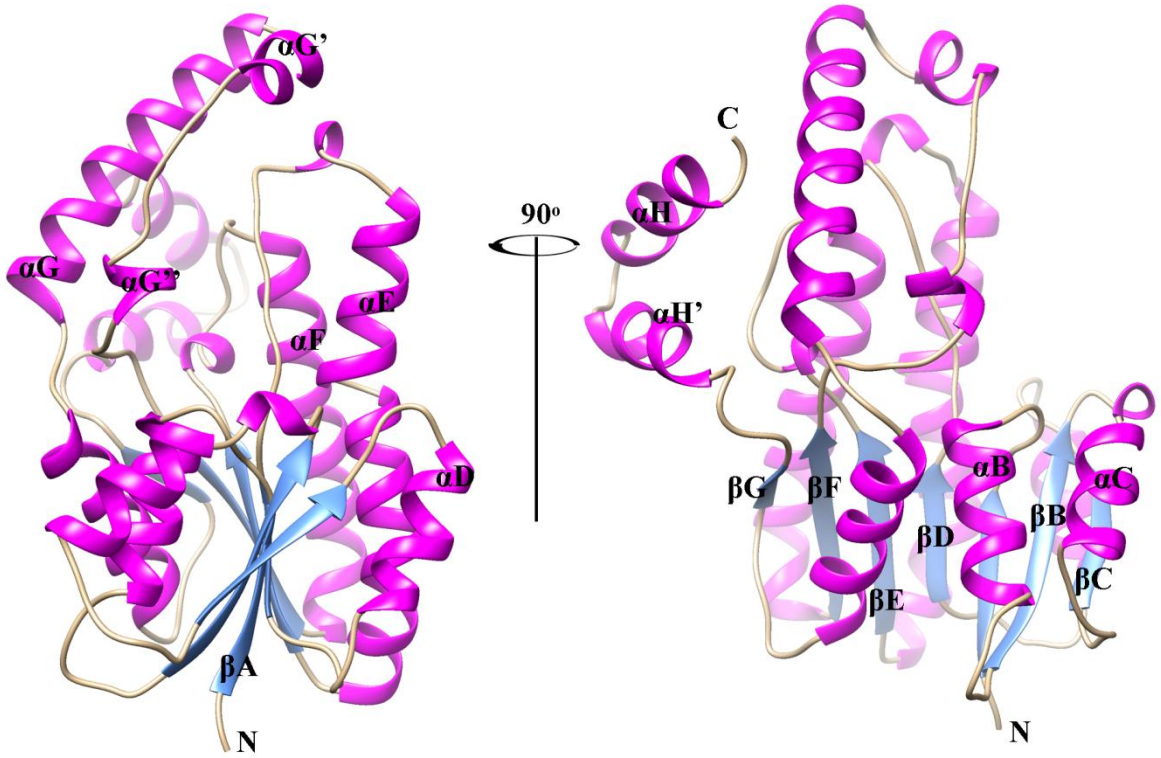

Figure 6 Stereo ribbon presentation of human 17β-HSD1 structure. The α-helices are represented as magenta coils and designated as αB to αH, β-strands are blue arrows and marked as βA to βF, and loops and turns are drawn as gray ropes. The N-terminus and the C-terminus of the protein molecule are indicated (Ghosh et al., 1995).

Table 2 The ratio of kinetic constants of 17β-HSD1 variants vs. that of wild type enzyme

Enzyme variants	Estradiol to Estrone[a]			Estrone to Estradiol[b]			Effects on the enzyme	Reference
	Specific activity	K_m	V_{max} or K_{cat}	Specific activity	K_m	V_{max} or K_{cat}		
H221A	0.12	2.23	0.11	0.18	3.57	0.33	Remarkably reduce the catalytic activity	Puranen et al.[73]
H210A	1.17			0.97			No significant difference	
H213A	0.92			1.02			No significant difference	
H210A+H213A	0.72	1.08	0.50	0.50	0.90	0.56	Decrease the V_{max} by 50%	
Y155A	2.43E-03	5.32	5.88E-03	4.51E-04	2.69	2.55E-04	Almost completely inactivate the enzyme, critical for hydride transfer	
C54A	0.92			0.93			No significant difference	
A237V	0.89			0.95			No significant difference	
S312V	1.12			1.08			No significant difference	
S134A		1.20	1.07		0.87	0.49	Its phosphorylation has no effect on the catalytic properties of the enzyme	Puranen et al.[79]
S142A		2.30	4.50E-03		1.20	5.21E-03	Almost completely inactivate the enzyme, critical for hydride transfer	
K159A		2.35	4.15E-03		0.83	2.93E-03	Almost completely inactivate the enzyme, critical for hydride transfer	
E282A		0.71	0.74		0.82	1.16	His^{221} is critical for the catalytic activity *in vitro*, but neither His^{221} nor Glu^{282} is critical for substrate recognition *in vivo*	
H221AE282A		1.63	0.10		3.70	0.36		
E282Q		0.79	0.72		0.48	0.73		
H221AE282Q		1.87	0.17		2.72	0.49		
L111EV113F			ND			ND	Results in an inactive aggregated protein	
A170E+F172			ND			ND		
H221L		3.53	0.20		4.50	0.44	Not essential to substrate binding, but is important for enzyme specificity	Mazza et al.[80]
H221Q		3.33	0.67		2.33	0.65		
L149V		2.17	0.05		10.0	0.04	Primary contribute to the discrimination of C-19 steroids and estrogens	Han et al.[81]
S12K		8.14	0.35		0.44	0.77	Increase the enzyme's preference for NADP(H)	Huang et al.[82]
L36D		7.03	1.85		285.56	2.32	Switch the enzyme's cofactor preference from NADPH to NAD	
H221A		6.75	0.40		30	0.47	Weaken the apparent affinity for estrone	
E282A		1.25	0.53		0.5	0.59	No significant difference	
S142C		ND	ND		ND	ND	Fully inactive the enzyme	
S142G		4.5	0.04		145	0.02	Abolish most of the enzyme's activities	
C10S					1.51	1.13	Stabilizing interactions in the cofactor binding site	Nashev et al.[83]

[a], NAD+ was used as cofactor in the kinetic tests. [b], NADPH was used as cofactor in the kinetic tests. ND, undetectable. Some of the 17β-HSD1 kinetic data were reported by Jin et al.[67]

4.1 Substrate recognition

The substrate recognition domain of 17β-HSD1 structure is buried under the flexible loop located between βF and αG', and delimited by the C-terminal region. The tunnel-like substrate binding cavity is composed majorly by hydrophobic residues, such as Leu[96], Val[143], Met[147], Leu[149], Pro[150], Pro[187], Val[225], Phe[226], Phe[259], Leu[262], Leu[263] and Met[279], as well as polar residues Asn[152] and Tyr[218]. The βFαG'-loop acts as a lid covering the entry of the cavity. This segment is highly flexible and unable to be defined in twelve 17β-HSD1 structures. While in the rest ten structures, it shows three possible conformations, including the closed, semi-opened and opened conformation (**Table 1**). Interestingly, all structures with the presence of cofactor analog NADP+ adopt a closed conformation, whereas structures only with natural steroid ligands exhibit an opened conformation, which suggests the modulation role of cofactor on the conformation of the loop. Moreover, the loop region in structures complexed with inhibitor CC-156 (E2B) and EM-1745 also has a close conformation even without cofactor. Only the apoenzyme has a semi-opened conformation at this flexible loop region. In the close conformation, residue Phe[192] from the loop region forms a T-stacking conformation with residue Tyr[155], providing extra contacts for stabilizing the bound ligand[84]. The roles of residues from the active site of 17β-HSD1 have been investigated by mutagenesis and kinetic experiments which are summarized in **Table 2**. Residue His[221] as well as Tyr[155]/Ser[142] are critical for steroid substrate recognition through their hydrogen bonds with the O3 and O17 of the ligand, respectively. Residue Glu[282] is supposed to play the same important role as the His[221] does since it might also form a hydrogen bond with the O3 of the bound steroid[79], as showed in the E2 complex structure[76]. However, the variant E282A in Huang et al.'s experiment did not show any significant modification in kinetics[82]. In contrast, residue Leu[149] plays an important role for the discrimination of C-19 steroids and estrogens. Steroid ligand is stabilized by hydrogen bonds between O3 and His[221]/Glu[282] at the recognition end, as well as between O17 and Tyr[155]/Ser[142] at the catalytic end of the cavity.

4.2 Catalytic mechanism of 17β-HSD1

The kinetics of 17β-HSD1 follows the common chemical mechanism: a reversible hydride transfer from NADPH to a ketosteroid or a hydride transfer from a hydroxysteroid to NADP+, which is achieved by a proton shift for charge equalization. Based on mutational and structural studies, three conserved amino acids, Tyr[155], Lys[159] and Ser[142] (catalytic triad), and a water molecule have been identified to be essential for the catalytic process[73, 75-76]. Previous kinetic studies, which was measuring the rate of isotopic exchange between substrate-product pairs while varying concentrations of unlabeled reactants, demonstrated that the binding of substrate and cofactor is random during the reaction[85]. Therefore, three hypotheses of the catalytic mechanisms of 17β-HSD1 have been proposed: one is a simultaneous transformation of proton and hydride; the other two are stepwise processes which differed in the intermediate presence of either a carbocation or an

oxyanion (**Figure 7**)[86]. The proton relay is mediated by the phenyl ring of Tyr[155], an electrostatic interaction between the protonated side chain of Lys[159] and a hydrogen-bond network involving Lys[159], Asn[114] and two water molecules[87]. Phe[192] may also involve in this step by forming a T-shape conformation with Tyr[155] to increase the acidity of the phenol group of Tyr[155] (84).

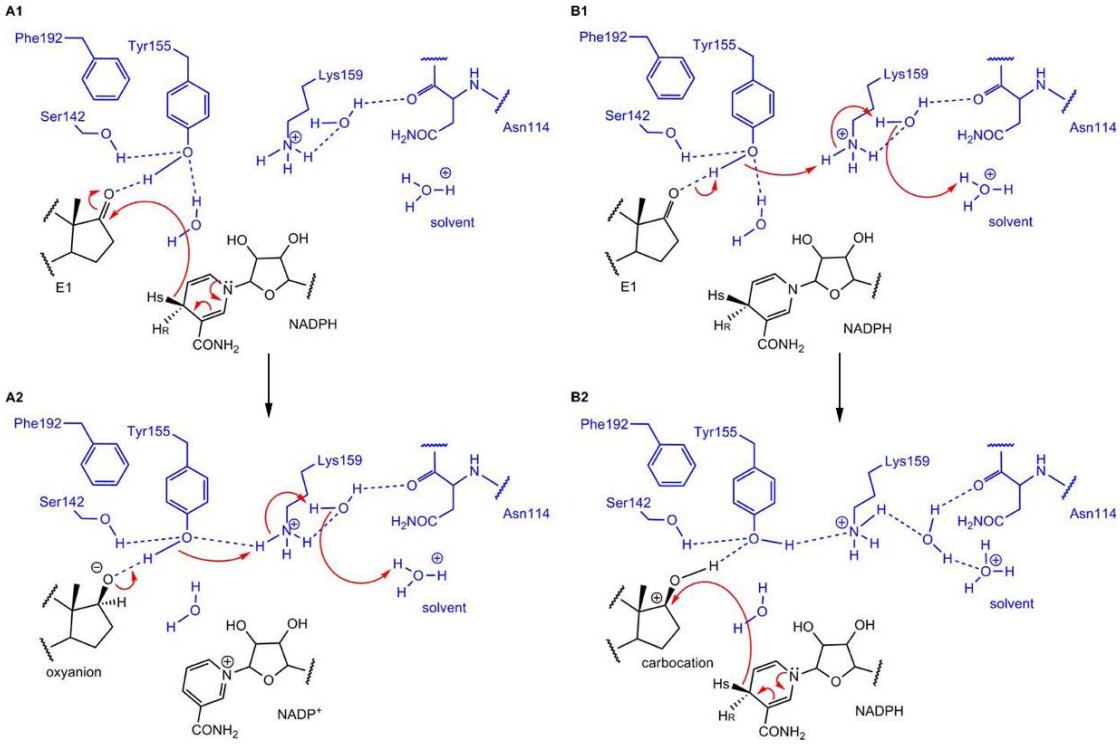

Figure 7 Two possible stepwise catalytic mechanisms for 17β-HSD1. (A) In the first step the prochiral S configuration (*pro*-S) hydride of NADPH is transferred to the α-face of E1 at the planar C17 carbon (A1), resulting in an energetically favorable aromatic system; subsequently the resultant oxyanion is protonated by the acidic OH group of Tyr[155] (A2). (B) In the first step the keto oxygen of E1 is protonated by the acidic OH of Tyr[155] (B1); then the resultant carbocation accepts the *pro*-S hydride of NADPH at the α-face (B2). Hydrogen bonds are represented in dashed lines (Marchais-Oberwinkler et al., 2011)..

4.3 Inhibitors of 17β-HSD1

The development of inhibitors of 17β-HSD1 began in the 1970s and gradually gained momentum thereafter before culminating in the first decade of the 2000s[88]. Despite the number of years of research, no inhibitor has yet reached the stage of clinical trials. The general properties of a good inhibitor should be highly potent and non-estrogenic. Also, it should be selective to 17β-HSD1 over the other 17β-HSD isozymes, especially 17β-HSD2, which catalyzes the reverse reaction (eg. oxidation of estrogens)[89]. The development of 17β-HSD1 inhibitor can generally be concluded into four different series (**Figure 8**). The first series of 17β-HSD1 inhibitors

were E2 derivatives bearing a bromoalkyl side chain at the 16α-position represented by the compound EM-251[90]. This irreversible competitive inhibitor EM-251 on 17β-HSD1 has an IC_{50} of about 320 nM, but was proven to have estrogenic activity on the estrogen sensitive human breast cancer cell line ZR-75-1[91]. A modification at the C6 position of E2 has led to the development of a second series of reversible inhibitors. These inhibitors have a thiaheptamamide side chain at the 6β-position of E2, and were represented by the compound EM-678 (IC_{50}=0.17μM) which was found to be more potent than the substrate E1 itself[92]. Similar as the first series inhibitors, it also has an estrogen effect[92-93]. Based on the binding energies of both the cofactor and substrate sites[94], as well as the three dimensional-structure of 17β-HSD1[75-76], a third series of inhibitors from E2-adenosine hybrids were developed. These molecules are represented by compound EM-1745. This compound has an E2 moiety to interact with the substrate-binding site and an adenosine moiety to interact with the cofactor binding site, which is connected by an eight methylene groups side chain[95]. Though it has a high inhibitory activity on purified 17β-HSD1 (IC_{50}=52nM), there are some major drawbacks such as difficulty to penetrate the cell membrane and weak competition ability against NADPH in intact cells [96]. Further studies focused on a benzyl group at the 16β-position of E2, which is proven to be efficient in improving the inhibitory activity, yielded the 16β-*m*-carbamoylbenzyl-E_2 (CC-156), which is the most potent 17β-HSD1 inhibitor by far with an IC_{50} value of 44nM for the conversion of E1 into E2[97]. However, this fourth series of compounds was demonstrated to have estrogenic activity. It stimulated the proliferation of estrogen receptor positive cell line MCF-7 and T-47D cells[97]. To reduce the unwanted estrogenic activity of CC-156, a series of modification at position 2, 3 and 7 have been made and assessed, yielding the compound 18 (2-MeO-CC-156)[97] which is less potent (IC_{50} of about 230nM) than CC-156 but bearing no estrogenic activity, and a new potent nonestrogenic compound named as 3-(2-bromoethyl)-16β-(m-carbamoylbenzyl)-17β-hydroxy-1,3,5(10)-estratriene (PBRM)[98-99]. The latter did neither inhibit other 17β-HSDs nor CYP3A4[100], and demonstrated to form a covalent bond with 17β-HSD1. A long delay period (i.e. 3-5 days) was required to restore the 17β-HSD1 activity in cells after they had been treated with PBRM[101]. Moreover, further investigation demonstrated its efficiency in both breast cancer cells and human tumor xenografts in nude mice[99-100].

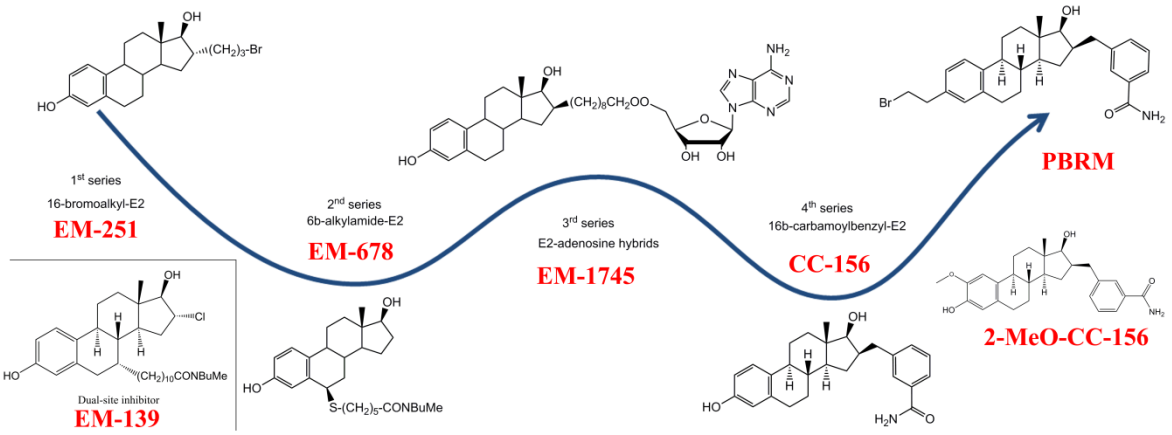

Figure 8 Key inhibitors of 17β-HSD1 from different Series (Poirier 2011).

Other than the inhibitors with a steroidal scaffold, several classes of non-steroidal 17β-HSD1 inhibitors have also been reported, such as the phytoestrogens[102-103], gossypols[104-105], thiophenepyrimidinones[106], (hydroxyphenyl)naphthols[107-109], and bis(hydroxyphenyl)heterocycles[110-112]. Among these non-sterodial inhibitors, the bicyclic substituted hydroxyphenylmethanones (BSHs) exhibited high inhibitory activity toward the 17β-HSD1 enzyme[113-114]. The following structural optimized (5-(3,5-dichloro-4-methoxyphenyl)thiophen-2-yl)(2,6-difluoro-3-hydroxyphenyl)methanone displayed a subnanomolar IC_{50} towards the enzyme as well as high selectivity over other enzymes, especially the 17β-HSD2[89], and estrogen receptors[115], making it a promising candidate for following development as a therapeutic agent.

Beside the traditional 17β-HSD1 inhibitors, a series of E2 derived pure antiestrogens bearing a 7α-alkylamide side chain and a D-ring modification (a halogen atom or a double bond) were reported to exert potent inhibitory effects on 17β-HSD1 activities[116]. These compounds were defined as dual-site inhibitor which represented by compound EM-139[116]. Although the inhibition on 17β-HSD1 activities was obtained with this series of inhibitors, the lack of selectivity for other enzymes compromised their potential in clinical utilities[117].

5 The role of 17β-HSD7

17β-HSD7 is another important multi function enzyme in the reductive 17β-HSDs. Like 17β-HSD1, it catalyzes the formation of E2 from E1 and performs a more significant role in the inactivation of DHT into 3β-diol[118-119]. 17β-HSD7 was reported to be primarily involved in cholesterol synthesis[120-121], and was suggested to be predominantly involved in cholesterol metabolism rather than in sex steroid synthesis [122-123]. However, experiment conducted by Mr. Thériault in Prof. Lin' lab demonstrated that inhibiting E1 to E2 activity of the enzyme by inhibitor is not blocking its zymosterol to zymosterone activity (unpublished data). Moreover, unlike aromatase, which converts testosterone (T) to E2 and is mostly expressed in stromal cells, 17β-HSD7 is

principally expressed and modulated in epithelial cancer cells such as MCF-7 and T47D[124]. Furthermore, recent *in vitro* and *in vivo* experiments demonstrated that inhibition of 17β-HSD7 can induce cell cycle arrest and trigger cell apoptosis in BC cells, and auto-downregulation feedback of the enzyme, leading to significant shrinkage of xenograft tumors[118, 124]. Furthermore, recent kinetic study showed that 17β-HSD7 has a K_m value of 5.2±0.4 μM which is much higher than the value of 17β-HSD1 (0.03±0.01 μM); while the k_{cat} value of 17β-HSD7 (2.9±0.4 s^{-1}) is much lower that the value of 17β-HSD1 (0.0063±0.0003 s^{-1})[67, 125]. As a result, the K_{cat}/K_m value of 17β-HSD7 is 80,000 times lower than the value of 17β-HSD1, indicating that these two reductive steroid enzymes may responsible of the E1 to E2 conversion at different substrate (E1) levels.

6 Statistical Analysis of RNA sequencing Data in Cancer Research

DNA sequencing technologies have been advanced during recent years due to the development of high throughput sequencing (HTS) technologies which can sequence multiple DNA molecules in parallel[126]. They enable simultaneous sequencing of millions of DNA molecules and are widely applied on genomics, epigenomics and transcriptomics[127]. RNA sequencing (RNA-seq) provides a profound advantage over other methods on cancer diagnosis and classification, prediction of response to therapy and prognosis, as well as unveiling the molecular bases of tumorigenesis[128]. Moreover, transcriptomic profiling through RNA-seq will facilitate the development of personalized treatment for cancer patients through the molecular classification of subtypes[128]. The Cancer Genome Atlas (TCGA) is a community resource project launched in 2005 by the National Institute of Health (NIH) as a pilot project aiming to discover and catalogue major cancer-causing genome alterations in large cohorts through large-scale genome sequencing and integrated multi-dimensional analyses. The Genome Sequencing Centers (GSCs) of TCGA performed large-scale DNA sequencing on two complementary DNA (cDNA) samples from every TCGA cancer case: one from the tumor specimen and the second from non-malignant tissue to serve as a control. The TCGA database is currently the largest database of cancer genetic information of over 30 kinds of human tumours[129]. TCGA database provides the most complete clinical information of each patient, and is widely used in many studies[130-131].

7 Working Hypothesis and Research Objectives

7.1 Hypothesis

7.1.1 PBRM inhibiting 17β-HSD1 activity would be through the formation of a covalent bond with the enzyme. The interactions of the three inhibitors (PBRM, 2-MeO-CC-156 and EM-139) with 17β-HSD1 would have significant difference.

7.1.2 The substrate inhibition of 17β-HSD1 would be due to the formation of a dead-end complex which is involving the binding of a reversely oriented E1 and the enzyme.

7.1.3 The analysis of RNA sequencing data would unveil potential new target and combined therapy for breast cancer treatment.

7.2 Objectives

Objective one: To elucidate the structural detail of representative inhibitors interacting with 17β-HSD1, such as EM-139, 2-Meo-CC-156 and PBRM. To achieve this, we have expressed and purified the recombinant 17β-HSD1 protein with Sf9 cells, which then was used in co-crystallization with these inhibitors in the presence or absence of cofactor analog NADP+. The crystal structures of the three complexes were determined and analyzed.

Objective two: To identify the mechanism of the substrate inhibition of 17β-HSD1 and *in silico* design of inhibitors based on this information. To reach this goal, we have co-crystallized the purified 17β-HSD1 with E1, in the presence or absence of cofactor analog NADP+. After determination of the binary and ternary complex structures, a comparative analysis with previously reported E2/testosterone complexes will be performed to elucidate the substrate inhibition mechanism, followed by computer assisted inhibitor design.

Objective three: To use RNA-seq data from large number clinical samples from TCGA-BRCA cohort to identify novel targets or combined therapy for breast cancer treatment.

Chapitre 1 Combined biophysical chemistry reveals a new covalent inhibitor with a low-reactivity alkyl halide

1.1 Résumé

La 17β-HSD1 joue un rôle central dans la progression des maladies liées aux œstrogènes en raison de son implication dans la biosynthèse des œstrogènes, en particulier de l'estradiol, constituant une cible thérapeutique importante pour le traitement endocrinien. Auparavant, le composé principal 16β-(m-Carbamoylbenzyl)-E2 (CC-156) était décrit comme un puissant inhibiteur de 17β-HSD1 dans la transformation de l'œstrone en estradiol. Cependant, l'activité œstrogénique de l'inhibiteur a compromis son potentiel de développement ultérieur. Une modification à la position C-2 du CC-156 a produit un inhibiteur non œstrogénique, le 2-MeO-CC-156, avec beaucoup moins de puissance d'inhibition que celle d'origine. Des recherches plus poussées à la position C-3 du CC-156 donnent un nouvel inhibiteur irréversible, non estrogénique, puissant et stéroïdien, le 3-(2-bromoethyl)-16β-(*m*-carbamoylbenzyl)-17β-hydroxy-1,3,5(10)-estratriene (PBRM). Dans cette publication, nous rapportons les structures des complexes ternaires de la 17β-HSD1 avec le NADP+ et l'inhibiteur 2-MeO-CC-156 ou le PBRM.

1.2 Abstract

17β-Hydroxysteroid dehydrogenase type 1 (17β-HSD1) plays a pivotal role in the progression of estrogen-related diseases for its involvement in the biosynthesis of estrogens, especially estradiol, constituting a valuable therapeutic target for endocrine treatment. Previously, the lead compound 16β-(m-Carbamoylbenzyl)-E2 (CC-156) was described as a potent 17β-HSD1 inhibitor of the transformation of estrone into estradiol. However, the estrogenic activity of the inhibitor compromised its potential for further development. A modification at the position C-2 of CC-156 produced a non-estrogenic inhibitor 2-MeO-CC-156, with a much less potency as compared with the original one. Further investigation at the position C-3 of CC-156 yield a new potent and steroidal non-estrogenic irreversible inhibitor 3-(2-bromoethyl)-16β-(m-carbamoylbenzyl)-17β-hydroxy-1,3,5(10)-estratriene (PBRM). In the present paper, we report structures of the ternary complexes of 17β-HSD1 with NADP+ and inhibitor 2-MeO-CC-156 and PBRM. In the 17β-HSD1-2-MeO-CC-156-NADP+ complex, the presence of a methoxy group at C-2 of the inhibitor significantly reduces its estrogenic effect in estrogen-depended cancer cells, however it also impedes the essential hydrogen bond at the recognition end of the ligand binding pocket, significantly decreasing its inhibitory activity to the enzyme. For the 17β-HSD1-PBRM-NADP+ complex, the hydrogen bond between O-19 of the inhibitor and Oγ of Ser^{142} is much weaker as compared with that of CC-156 complex, contributing to its relatively high IC_{50} to 17β-HSD1 activity. However, the bromoethyl group at position C-3 of the inhibitor warrants its non-estrogenic profile, and secures its

selectivity of 17β-HSD1 through the formation of a covalent bond with Nε of residue His[221], suggesting its potential as a therapeutic agent for EDDs.

1.3 Introduction

Covalent inhibitors (CIs) are more beneficial than noncovalent ones because of the reduced risk of drug resistance, extended inhibition effect, increased efficiency with lower doses, and fewer side effects[1]. However, despite these advantages, toxicity issues encountered with the first generation of CIs related to their high reactivity, low specificity of action, and some immunogenicity response resulted in resistance from the pharmaceutical industry[2]. Nevertheless, the approval of more specific and safe targeted CIs in the past decade led to a resurgence of interest in the pharmaceutical research field[3-4]. However, the design of such inhibitors remains a challenge, considering that a high binding affinity for the targeted protein, as well as an inherent reactivity, are two essential elements that must be combined in a single molecular entity to obtain a valuable drug candidate. Even if some covalent drugs have been documented bearing a low-reactivity group that could lead to alkylation in a particular molecular context[5], the electrophilic group incorporated into CI is generally highly reactive (α,β-unsaturated ketone, α-haloketone, cyanamide, fluorophosphate, and epoxide), with the inconvenience of increasing the risk of off-target and nonspecific tagging[6]. The use of less reactive electrophile groups is thus suitable for increasing the level of CI specificity[2, 7-9].

Most CI drugs are based on the reactivity of cysteine[10], the strongest nucleophile among natural amino acids (AAs), allowing the alkylation of a large diversity of electrophiles[11]. However, because of its low abundance or an inaccessible position in the enzyme catalytic site, other nucleophilic residues have been exploited for covalent inhibition, such as lysine, serine, tyrosine, threonine, aspartate, and glutamate[12-13]. One uncommon case is the histidine (His) residue, which, despite its good nucleophilicity and its presence at the catalytic site of many enzymes[14], has been very rarely exploited in CI design[15].

17β-hydroxysteroid dehydrogenase type 1 (17β-HSD1) catalyzes the final step of the transformation of estrone (E1) to estradiol (E2), the most potent estrogen, and is considered a promising therapeutic target for endocrine treatment[16-21]. This enzyme also catalyzes the reduction of dehydroepiandrosterone (DHEA) into 5-androstene-3β,17β-diol (5-diol) and dihydrotestosterone (DHT) into 5α-androstane-3β,17β-diol (3β-diol), which has been suggested to become more important after menopause, and may be involved in aromatase inhibitor resistance[16, 21-23]. It is well-known that E2 stimulates breast cancer and also plays a crucial role in other estrogen-related diseases such as ovarian cancer, endometriosis, and endometrial cancer[24-25]. Thus, the blockade of the biosynthesis of E2 is considered to be a valuable therapeutic approach for treating estrogen-dependent diseases[24-26].

Previous reports have described 16β-(*m*-carbamoylbenzyl)-E2 (CC-156) (**Figure 1.1**) as a potent competitive and reversible inhibitor of 17β-HSD1 with an IC_{50} value of 44 nM[27]. Unfortunately, this compound has an estrogenic activity observed by the proliferation of the stimulation of estrogen receptor (ER) positive cell lines MCF-7 and T-47D[27]. To reduce this unwanted estrogenic activity, further development was then engaged to modify the E2 scaffold of CC-156. The addition of a methoxy (MeO) group at position C-2 of CC-156, which produced 2-MeO-CC-156 (**Figure 1.1**), was efficient in attenuating estrogenic activity but was unfavorable for enzyme inhibition[27]. A more promising strategy next focused on the chemical modification of the C-3 phenolic group, which is known to be important for the binding of the E2 scaffold to ER[28], and resulted in the discovery of PBRM (**Figure 1.1**), the first nonestrogenic irreversible inhibitor of 17β-HSD1[29]. Further investigations demonstrated the PBRM efficiency in both breast cancer cells and human breast tumor xenografts in nude mice[30-31], as well as interspecies differences of 17β-HSD1 inhibition[32]. Kinetic studies classified PBRM as a competitive and irreversible inhibitor of 17β-HSD1, and a covalent binding of PBRM with 17β-HSD1 was then demonstrated by using a 17α-tritiated derivative of PBRM[32]. Furthermore, a molecular modeling study investigating interspecies inhibitory activity of PBRM noted His^{221} as a potential key AA involved in the formation of a covalent bond with the bromoethyl side chain. Interestingly, as an indication of the applicability of the bromoethyl group for developing a specific CI drug, PBRM possesses the expected properties of a CI, such as an extended inhibition action and a very low promiscuity rate[33]. The bromoethyl side chain also provides a reduced in vitro CYP metabolism in comparison to its phenolic analog (CC-156), which is translated by a higher in vivo bioavailability for PBRM[29].

Despite the indirect evidence of an alkylation between PBRM and 17β-HSD1, the existence and the exact configuration of expected covalent bonds remain to be proven. This was especially significant, considering the predicted low reactivity between a His residue and a primary alkyl halide, even more in a physiological environment[32]. Obviously, the demonstration of the capacity of a common and accessible functional group like a primary alkyl halide to act as a reagent for the N-alkylation of an enzyme could demonstrate the viability of such a weak electrophile group for the development of a new type of selective CI. In fact, very few documented examples of an enzyme alkylation by a primary alkyl halide derivative have been reported to date, including a case of *O*-alkylation from a carboxylate group of Asp^{106} residue for haloalkane dehalogenase tagging[34] and a suspected S-alkylation from Met^{193} of 16α-bromopropyl-E2 leading to an irreversible inhibition of 17β-HSD1[35-36]. Importantly, the primary alkyl halide electrophile group must not be confused with activated alkyl halide units, like the highly reactive N-ethylhalide of “nitrogen mustard” agents, which form a covalent bond via the formation of an intermediate aziridinium very reactive species that reacts with the DNA nitrogenous base[37], or with benzyl halide[38-39] and α-halo ketone[40] groups, which are not specific, albeit useful in labeling affinity agents for enzyme characterization[41-42].

1.4 Results and Discussion

Analysis of PBRM molecular interactions before the His^{221} N-alkylation

The inhibitor PBRM bears a bromoethyl side chain at position C-3, making the inhibitor a little longer compared to CC-156's. However, since the core structure of PBRM, especially the C-16 benzylamide moiety, is the same as that of CC-156, we expected the major conformational modifications during the binding of PBRM had happened at the recognition end (His^{221}, Glu^{282}) of the steroid binding site[43-44]. We were therefore interested in investigating the interaction of the bromoethyl chain with His^{221} before the N-alkylation event. Besides, the Met^{279} could possibly act as a nucleophile over the bromoethyl chain, considering that the distance between the C-3 of phenolic OH at C-3 in CC-156 and Met^{279} (3.97 Å) is similar to with His^{221} (3.45 Å) (data from CC-156 ternary complex[45]).

The pseudo PBRM complex structures were visually built from the CC-156 ternary complex structure using *SeeSAR* software. In the CC-156 complex, the Glu^{282} side chain faces the binding site to make a hydrogen bond with the inhibitor, leaving no space to build the bromoethyl side chain on CC-156. Since Glu^{282} is a solvent-exposed flexible residue with a high average B-factor value of 40.6 Å^2, we modeled its conformation to have the side chain exposed to the solvent (as described in the Experimental Section). Moreover, with the existence of side chains from His^{221} and Met^{279}, the bromide from generated poses of PBRM maintained at least a van der Waals distance from them, which is too long to overcome the force field limitations that do not allow for covalent reactions between the bromoethyl moiety and the side chains. To explore the possible positions of the bromoethyl side chain before the subsequent N-alkylation reaction, residues His^{221} and Met^{279} were mutated into Ala, which has a smaller side chain. The best poses with the highest estimated affinity using this binding site conformation are presented in **Figure 1.2 A,B**. The distance from the CH_2 of the bromoethyl side chain to the NH of the His^{221} side chain is about 2.5 Å, whereas that distance to the S of Met^{279} is 2.0 Å. This result urges us to engage co-crystallization experiment for 17β-HSD1-PBRM to clarify the mechanism.

Because no example of N-alkylation between an enzyme and a primary alkyl halide has been reported to date and also to rule out the possibility of the Met^{279} of 17β-HSD1 to act as nucleophile over the primary alkyl halide (**Figure 1.2**), we thus seized this opportunity and engaged cocrystallization experiments of PBRM with 17β-HSD1 to prove the capacity of such a weak electrophile to form a covalent bond with the suspected His^{221} residue, an AA rarely exploited in design of CI drugs[15].

Structure determination of enzyme-inhibitor complex crystals

The space group identified for all the crystals was $P2_12_12_1$ with a dimer in one asymmetric unit representing the functional unit of the enzyme[46-47]. Two ternary complexes, 17β-HSD1–2-MeO-CC-156–NADP$^+$ and 17β-

HSD1–PBRM–NADP+, were refined to 2.1 and 2.2 Å, respectively. The two models show good stereochemistry[48], and the quality of the final refined models can be accessed from the statistics in **Table 1.1**. The models of 17β-HSD1 with PBRM (F0D) and 2-MeO-CC-156 (F0A) ternary complexes show very clear electron density for almost all residues, except for the C-terminal end of the protein (residues 286–327) as well as the flexible loop region from Ala[191] to Gly[198], as observed in other 17β-HSD1 complexes[21, 43, 49-50]. The active-site structure of both inhibitor complexes for the A subunit is shown in **Figure 1.3**.

Comparison of 2-MeO-CC-156 and CC-156 ternary complexes

The presence of a methoxy group at position C-2 in 2-MeO-CC-156 introduces a strong hydrophobic interaction with residue Leu[262] with the distance of 3.15 Å between C-32 (CH_3 of MeO) of inhibitor and Cδ of the AA residue. This interaction causes the inhibitor to shift 1.04 Å at the O-4 end and to rotate by approximately 4.8° at the steroid core and 3.5° at the benzylamide ring, as compared to the position of the CC-156 complex when superimposing the 2-MeO-CC-156 complex with the previously reported CC-156 ternary complex (PDB ID 3HB5) by Cα atoms (**Figure 1.4A**)[45].

The side chain of Glu[282], used to make a hydrogen bond with the inhibitor in the CC-156 ternary complex, adopts a conformation facing the outside of the protein. Thus, no hydrogen bond can form between the AA residue and 2-MeO-CC-156. Besides, the movement of the O-4 at the end of 2-MeO-CC-156 forces the imidazole side chain of His[221] to shift away by 1.49 Å for the Nε as compared with the position of the Cε of His[221] in CC-156 complex. The hydrogen bond between the inhibitor and His[221], which is important for ligand recognition and orientation[51], is established in the 2-MeO-CC-156 complex with a distance of 2.86 Å (**Table 1.2**). However, the movement of the side chain of His[221] toward the solvent leads to the decrease of its stability (average *B*-factor of 49.0 $Å^2$ of the AA residue as compared with 39.0 $Å^2$ of the subunit) compared with its counterpart (average *B*-factor of 30.7 $Å^2$ of the AA residue as compared with 29.8 $Å^2$ of the subunit) in the CC-156 complex.[45] Indeed, when 0.1 μM inhibitor concentration was used, 2-MeO-CC-156 inhibited 37% of the transformation of E1 into E2, whereas CC-156 inhibited 77% of the same reaction[27]. This is in agreement with the relatively high flexibility of the bound 2-MeO-CC-156 (average *B*-factor, 54.9 Å) as compared to CC-156 (average *B*-factor, 35.6 Å). The hydrogen bonding with Ser[142] is conserved in the 2-MeO-CC-156 complex, as in the CC-156 ternary complex.

For the benzylamide ring, the π–π interaction between Tyr[155] and the ring is conserved (**Figure 1.4A**). The distance between $Cε_2$ of Tyr[155] and C-23 of 2-MeO-CC-156 is 3.50 Å, and the distance between the centroid of the two phenyl rings is about 4.4 Å, a little bit longer than the distances observed in the CC-156 ternary complex (4.3 Å). Nevertheless, three hydrogen bonds between the carboxamide group of the inhibitor and Leu[95] and Asn[152] residues are presented (**Figure 1.4A** and **Table 1.2**). However, it is more reasonable that the

O-29 of the carboxamide (CON) group of the inhibitor acts as an acceptor forming a hydrogen bond with N of Leu^{95}, whereas the N-30 (CON) acts as a donor forming two hydrogen bonds with O of Leu^{95} and Oδ of Asn^{152} (**Table 1.2**). Thus, the CON group in 2-MeO-CC-156 adopts a conformation of 180° flip, as compared with that in the CC-156 ternary complex (**Figure 1.4A**).

Enzyme interaction with $NADP^+$ in ternary complexes

Similar to the previously described model[50], only the adenine ring, the ribose and phosphate groups of $NADP^+$ molecule can be unambiguously identified in the electron densities of the 17β-HSD1–2-MeO-CC-156–$NADP^+$ ternary structure (**Figure 1.3A**). The NMN moiety of the $NADP^+$ molecules missing from the densities was omitted from the final models. It indicates that the major interaction between the $NADP^+$ and enzyme happens at the ADP part, in agreement with previous the structure-function study[44]. As compared with the $NADP^+$ molecule in CC-156 ternary complex, the 2'-phosphate group attached to the adenine ribose in 2-MeO-CC-156 ternary complexes has moved 3.7 Å toward the position of Nη of Arg^{37} in CC-156 complex, and is stabilized by the water bridged hydrogen bond with the N of Arg^{37} and Asp^{38} as well as the Oγ of Thr^{41}. As a result, the side chain of Arg^{37} has moved to the protein surface and stabilized by forming a hydrogen bond with Oδ of Asp^{38}. Two important hydrogen bonds between the adenine ring and residues Asp^{65} and Val^{66} are conserved in 2-MeO-CC-156 ternary complex, as well as the hydrogen bond between the O-3 attached to the adenine ribose and Oγ of Ser^{12}. No obvious different interaction was observed at the $NADP^+$ binding site in the PBRM complex, as compared with that of the 2-MeO-CC-156 complex. Similarly, the electron density map of the nicotinamide and the attached ribose of the $NADP^+$ molecule are unable to define (**Figure 1.3B**). The hydrogen bonds with surrounding residues Ser^{11}, Ser^{12}, Asp^{65} and Val^{66}, as well as the water bridged hydrogen bond with residues Asp^{38} and Thr^{41} stabilized the ADP moiety of the $NADP^+$ molecule. No direct interaction was observed between the bound inhibitor and cofactor molecule in the ternary complex.

Comparison of PBRM and CC-156 ternary complexes

In the 17β-HSD1–PBRM–$NADP^+$ ternary structure, an unambiguous continuity of electron density from the side chain of His^{221} to the bound PBRM is observed in both subunits, indicating the formation of a covalent bond between the Nε of His^{221} and the C-31 ($BrCH_2$) of PBRM (**Figure 1.3B**). The structure overlay of the complex with CC-156 complex shows a slight shifting at the C-3 end of PBRM (0.66 Å) as well as the imidazole side chain of His^{221} (0.89 Å) as compared with the positions of their counterparts in the CC-156 complex, indicating the dynamic process favoring the formation of the covalent bond between them. The slight movement of the steroid core of PBRM and side chain of His^{221} is caused by the formation of their covalent bond (**Figure 1.4B**). As a result, the distance of the hydrogen bond between O-19 of the inhibitor and Oγ of Ser^{142} increased to 3.22 Å (**Table 1.2**). The hydrogen bond with Ser^{142} is one of the three major interactions in

which the potent inhibitor CC-156 interacts with 17β-HSD1[30], the increased distance of the bond thus indicating a less favored interaction of the inhibitor with the enzyme.

Similar to CC-156 and 2-MeO-CC-156 complexes, the π–π interaction between the benzylamide ring of PBRM and the side chain of Tyr[155] is conserved. The distance between $C\varepsilon_2$ of Tyr[155] and C-23 in the benzylamide ring of PBRM (3.35 Å) is slightly shorter than that in both the CC-156 (3.45 Å) and 2-MeO-CC-156 (see above) complexes. Besides, the distance of the centroid of the two phenyl rings (4.32 Å) is almost the same as in the CC-156 complex. The carboxamide group of PBRM adopts the same conformation as 2-MeO-CC-156 described previously, making three hydrogen bonds with Leu[95] and Asn[152] residues (**Figure 1.4B**). The distance of the three hydrogen bonds in the PBRM complex is similar to that in the CC-156 complex (**Table 1.2**), indicating their important role in the inhibitor binding to the enzyme. These molecular interactions are thus sufficiently favorable to bring the bromoethyl side chain of PBRM in proximity to His[221] and to favor the reaction between these two complementary groups. In fact, such a reaction between an alkyl halide and a relatively poor nucleophile like His is not possible under physiological conditions. Even in the laboratory, excess amounts of imidazole or His were found to be unable to react with PBRM at room temperature[32]. The proximity effect is thus a crucial factor to allow this unfavorable event, as has been previously demonstrated for low-reactivity electrophile groups in CI reactivity[9].

1.5 Conclusion

The present study illustrates the structural details of different inhibitory mechanisms of two potent 17β-HSD1 inhibitors, the reversible inhibitor 2-MeO-CC-156 and the irreversible inhibitor PBRM, as compared to CC-156. The results strongly support PBRM as a promising and selective new drug candidate for the adjuvant therapy of estrogen-dependent diseases. All these represent a breakthrough in the long history of the 17β-HSD1 inhibitor search. Also, and in a broader way, this is the first report of a specific N-alkylation between a His residue and a low-reactivity alkyl halide-based inhibitor, which supports the viability of such an approach toward the development of specific CIs.

1.6 Experimental Procedures

Materials. pFastBac™1 vector, DH10Bac™ Competent *E. coli*, Gibco® *Spodoptera frugiperda* Sf9 cells, Sf-900™ III SFM (serum free medium), Sf-900 Medium (1.3X), Cellfectin® II Reagent, PureLink™ HiPure Plasmid Maxiprep Kit, Ni-NTA Agarose were purchased from Thermo Fisher Scientific Corporation. The I-Max serum free medium for insect cells was purchased from Wisent Bioproducts. Albumin standard was purchased from Thermo Scientific. Protease inhibitor cocktail, sodium chloride, NAD^+, $NADP^+$, PMSF, β-octylglucoside (β-OG), estrone, trizma base, disodium ethylenediamine tetraacetate (EDTA), glycerol, phenylmethylsulphonyl (PMSF), polyethylene glycol 8000 (PEG-8K), dithiothreitol (DTT) and potassium phosphate monobasic were

obtained from Sigma-Aldrich. MonoQ (HR 5/5) column and Blue Sepharose® 6 Fast Flow resin were obtained from GE Healthcare Life Sciences. Antibiotic such as ampicillin, kanamycin, gentamicin, tetracycline, and penicillin-streptomycin were obtained from Thermo Scientific. Bradford Protein Assay kit and Protein Marker were purchased from Bio-Rad. The DU-80 spectrophotometer was from Beckman Coulter.

Recombinant virus preparation. 17β-HSD1 gene (*HSD17B1*) was first subcloned into pFastBac™1 donor plasmid through *RsrII* and *XhoI* double digestion to generate the pFastBac-HSD17B1 recombinant donor plasmid, which has then transformed into DH10Bac™ *E.Coli* competent cell to form the recombinant Bacmid-HSD17B1 shuttle plasmid. The integrity of these recombinant plasmids was confirmed by sequencing, which was provided by the genome sequencing and genotyping platform of the CHU de Québec - Research Center (Québec, QC, Canada).

17β-HSD1 expression and purification. Sf9 cells were maintained at 27 °C in stationary T-flasks and were passaged to 150 × 20 mm dishes for protein expression. Cells were infected with virus at a multiplicity of infection (MOI) of 0.1 to 1 pfu to produce virus stocks or at a MOI ≥10 for maximal protein expression. Recombinant 17β-HSD1 was purified by a fast preparation procedure modified from a previously described method[52-53]. Briefly, enzyme purification consisted in two FPLC steps using Blue-Sepharose affinity and Mono-Q anion exchange columns. β-OG was added to the protein fraction thus obtained to stabilize the enzyme[54]. The protein concentration was measured by the Bradford method and its activity was measured by the oxidation of E2 to E1[52].

Inhibitors 2-MeO-CC-156 and PBRM. The reversible and irreversible 17β-HSD1 inhibitors 2-MeO-CC-156 and PBRM, respectively, were synthesized from commercially available estrone, as previously reported[27, 29-30].

Co-crystallization. Ternary complex samples were prepared according to the repeated concentration and dilution method of Zhu *et al*[55] to saturate 17β-HSD1 in high concentration with hydrophobic steroid. In brief, purified enzyme was subjected to a buffer change procedure via Centricon. The added buffer contains 0.06% (w/v) β-OG, 1 mM $NADP^+$ and 25 μM of different inhibitors. The obtained complex samples were then concentrated to 20 mg/ml and used for crystal growth. Crystals were obtained using hanging-drop method with 400 μl of well solution consisting in 24% - 29% (w/v) PEG8K, 100 mM Tris buffer (pH 7.5 – 7.8) and 50 mM KH_2PO_4 at 27 ºC.

Data collection and structure determination. Data collection was carried out using MAR CCD 165 mm detector at APS beamline 31-LRL-CAT at 100 K using a wavelength of 0.979 Å. Mineral oil was used as the cryoprotectant. The datasets were intergraded using *MOSFLM*[56] and scaled with *SCALA*[57] from the *CCP4* suite[58]. The structures were solved by molecular replacement with *MOLREP*[59] using the coordinate of 17β-

HSD1, with the highest current resolution (PDB code 1JTV)[60], as the search model. The structure parameters for the inhibitor 2-MeO-CC-156 and PBRM were generated using the *Sketcher* from *CCP4* suite and were refined using *REFMAC5*[61]. The complex structures were subjected to multiple rounds of auto-refinement using *REFMAC5* and manual refinement using *Coot*[62]. The quality of the final models was evaluated with *PROCHECK*[63]. The structure figures were prepared with the *PyMOL*[64].

Manual edition using *SeeSAR*. The manual compound edition was performed using *SeeSAR*[65] software. The crystal structure of 17β-HSD1 in complex with CC-156 and NADP was taken from PDB code 3HB5[45]. Inhibitor PBRM shares its core structure with CC-156. We thus chose to use the *SeeSAR* to build the pseudo PBRM complex structure from CC-156 in the CC-156 complex. The binding poses of PBRM were generated with *SeeSAR*, its geometry optimized by the Hydrogen bond and Dehydration (HYDE)[66] as implemented in the software and ranked according to their estimated affinity to the binding site. Before the visual building of PBRM from CC-156, the system's energy was minimized using UCSF *Chimera*[67] software after the side chain of Glu^{282} was modified using Dunbrack[68] backbone-dependent rotamer library in *Chimera* in which the highest probability conformer not facing the binding site was selected. The mutation of His^{221} and Met^{279} to Ala was done, respectively using the rotamer tool in UCSF *Chimera*, and no further energy minimization was required.

Notes

The authors declare no competing financial interests.

The PDB ID of 17β-HSD1-2-MeO-CC-156-$NADP^+$ and 17β-HSD1-PBRM-$NADP^+$ are 6CGC and 6CGE, respectively.

ACKNOWLEDGMENT

The authors would like to acknowledge the CIHR's support (MOP97917) to Sheng-Xiang Lin, Donald Poirier and Charles Jean Doillon.

1.7 Reference

1. Bauer, R. A., Covalent Inhibitors in Drug Discovery: from Accidental Discoveries to Avoided Liabilities and Designed Therapies. *Drug. Discov. Today* **2015,** *20* (9), 1061-1073.

2. Johnson, D. S.; Weerapana, E.; Cravatt, B. F., Strategies for Discovering and Derisking Covalent, Irreversible Enzyme Inhibitors. *Future medicinal chemistry* **2010,** *2* (6), 949-964.

3. Singh, J.; Petter, R. C.; Baillie, T. A.; Whitty, A., The Resurgence of Covalent Drugs. *Nature reviews. Drug discovery* **2011,** *10* (4), 307-317.

4. Baillie, T. A., Targeted Covalent Inhibitors for Drug Design. *Angew. Chem., Int. Ed. Engl.* **2016,** *55* (43), 13408-13421.

5. Lei, J.; Zhou, Y.; Xie, D.; Zhang, Y., Mechanistic Insights into a Classic Wonder Drug--Aspirin. *J. Am. Chem. Soc.* **2015,** *137* (1), 70-73.

6. De Cesco, S.; Kurian, J.; Dufresne, C.; Mittermaier, A. K.; Moitessier, N., Covalent Inhibitors Design and Discovery. *Eur. J. Med. Chem.* **2017,** *138*, 96-114.

7. Lopes, F.; Santos, M. M. M.; Moreira, R., Designing Covalent Inhibitors: A Medicinal Chemistry Challenge. In *Biomedical Chemistry: Current Trends and Developments*, Vale, N., Ed. De Gruyter Open Ltd: Warsaw/Berlin, 2015; pp 44-59.

8. Long, M. J. C.; Aye, Y., Privileged Electrophile Sensors: A Resource for Covalent Drug Development. *Cell Chem. Biol.* **2017,** *24* (7), 787-800.

9. Kobayashi, T.; Hoppmann, C.; Yang, B.; Wang, L., Using Protein-Confined Proximity to Determine Chemical Reactivity. *J. Am. Chem. Soc.* **2016,** *138* (45), 14832-14835.

10. Backus, K. M.; Correia, B. E.; Lum, K. M.; Forli, S.; Horning, B. D.; Gonzalez-Paez, G. E.; Chatterjee, S.; Lanning, B. R.; Teijaro, J. R.; Olson, A. J.; Wolan, D. W.; Cravatt, B. F., Proteome-Wide Covalent Ligand Discovery in Native Biological Systems. *Nature* **2016,** *534* (7608), 570-574.

11. Marino, S. M.; Gladyshev, V. N., Analysis and Functional Prediction of Reactive Cysteine Residues. *J. Biol. Chem.* **2012,** *287* (7), 4419-4425.

12. Shannon, D. A.; Weerapana, E., Covalent Protein Modification: The Current Landscape of Residue-Specific Electrophiles. *Curr. Opin. Chem. Biol.* **2015,** *24*, 18-26.

13. Powers, J. C.; Asgian, J. L.; Ekici, O. D.; James, K. E., Irreversible Inhibitors of Serine, Cysteine, and Threonine Proteases. *Chem. Rev.* **2002,** *102* (12), 4639–4750.

14. Liao, S. M.; Du, Q. S.; Meng, J. Z.; Pang, Z. W.; Huang, R. B., The Multiple Roles of Histidine in Protein Interactions. *Chem. Cent. J.* **2013,** *7* (1), 44.

15. Liu, S.; Widom, J.; Kemp, C. W.; Crews, C. M.; Clardy, J., Structure of Human Methionine Aminopeptidase-2 Complexed with Fumagillin. *Science* **1998,** *282* (5392), 1324-1327.

16. Lin, S. X.; Chen, J.; Mazumdar, M.; Poirier, D.; Wang, C.; Azzi, A.; Zhou, M., Molecular Therapy of Breast Cancer: Progress and Future Directions. *Nat. Rev. Endocrinol.* **2010,** *6* (9), 485-493.

17. Moeller, G.; Adamski, J., Integrated View on 17beta-Hydroxysteroid Dehydrogenases. *Mol. Cell Endocrinol.* **2009,** *301* (1-2), 7-19.

18. Lin, S. X.; Poirier, D.; Adamski, J., A Challenge for Medicinal Chemistry by the 17β-Hydroxysteroid Dehydrogenase Superfamily: An Integrated Biological Function and Inhibition Study. *Curr. Top. Med. Chem.* **2013,** *13* (10), 1164-1171.

19. Aka, J. A.; Zerradi, M.; Houle, F.; Huot, J.; Lin, S. X., 17beta-Hydroxysteroid Dehydrogenase Type 1 Modulates Breast Cancer Protein Profile and Impacts Cell Migration. *Breast Cancer Res.* **2012,** *14*, R92.

20. Zhang, C. Y.; Chen, J.; Yin, D. C.; Lin, S. X., The Contribution of 17beta-Hydroxysteroid Dehydrogenase Type 1 to the Estradiol-Estrone Ratio in Estrogen-Sensitive Breast Cancer Cells. *PLoS One* **2012,** *7* (1), e29835.

21. Aka, J. A.; Mazumdar, M.; Chen, C. Q.; Poirier, D.; Lin, S. X., 17beta-Hydroxysteroid Dehydrogenase Type 1 Stimulates Breast Cancer by Dihydrotestosterone Inactivation in Addition to Estradiol Production. *Mol. Endocrinol.* **2010,** *24* (4), 832-845.

22. Simard, J.; Vincent, A.; Duchesne, R.; Labrie, F., Full Oestrogenic Activity of C19-Δ5 Adrenal Steroids in Rat Pituitary Lactotrophs and Somatotrophs. *Mol. Cell Endocrinol.* **1988,** *55*, 233-242.

23. Hanamura, T.; Niwa, T.; Gohno, T.; Kurosumi, M.; Takei, H.; Yamaguchi, Y.; Ito, K.; Hayashi, S., Possible Role of the Aromatase-Independent Steroid Metabolism Pathways in Hormone Responsive Primary Breast Cancers. *Breast Cancer Res. Treat.* **2014,** *143* (1), 69-80.

24. Marchais-Oberwinkler, S.; Henn, C.; Moller, G.; Klein, T.; Negri, M.; Oster, A.; Spadaro, A.; Werth, R.; Wetzel, M.; Xu, K.; Frotscher, M.; Hartmann, R. W.; Adamski, J., 17beta-Hydroxysteroid Dehydrogenases (17beta-HSDs) as Therapeutic Targets: Protein Structures, Functions, and Recent Progress in Inhibitor Development. *J. Steroid Biochem. Mol. Biol.* **2011,** *125* (1-2), 66-82.

25. Poirier, D., 17β-Hydroxysteroid Dehydrogenase Inhibitors: A Patent Review. *Expert. Opin. Ther. Pat.* **2010,** *20* (9), 1123-1145.

26. Brodie, A.; Njar, V.; Macedo, L. F.; Vasaitis, T. S.; Sabnis, G., The Coffey Lecture: Steroidogenic Enzyme Inhibitors and Hormone Dependent Cancer. *Urol. Oncol.* **2009,** *27* (1), 53-63.

27. Laplante, Y.; Cadot, C.; Fournier, M. A.; Poirier, D., Estradiol and estrone C-16 derivatives as inhibitors of type 1 17beta-hydroxysteroid dehydrogenase: blocking of ER+ breast cancer cell proliferation induced by estrone. *Bioorganic & medicinal chemistry* **2008,** *16* (4), 1849-60.

28. Fang, H.; Tong, W.; Shi, L. M.; Blair, R.; Perkins, R.; Branham, W.; Hass, B. S.; Xie, Q.; Dial, S. L.; Moland, C. L.; Sheehan, D. M., Structure−Activity Relationships for a Large Diverse Set of Natural, Synthetic, and Environmental Estrogens. *Chem. Res. Toxicol.* **2001,** *14* (3), 280-294.

29. Maltais, R.; Ayan, D.; Trottier, A.; Barbeau, X.; Lague, P.; Bouchard, J. E.; Poirier, D., Discovery of a Non-Estrogenic Irreversible Inhibitor of 17beta-Hydroxysteroid Dehydrogenase Type 1 from 3-Substituted-16beta-(m-carbamoylbenzyl)-estradiol Derivatives. *J. Med. Chem.* **2014,** *57* (1), 204-222.

30. Maltais, R.; Ayan, D.; Poirier, D., Crucial Role of 3-Bromoethyl in Removing the Estrogenic Activity of 17beta-HSD1 Inhibitor 16beta-(m-Carbamoylbenzyl)estradiol. *ACS Med. Chem. Lett.* **2011,** *2* (9), 678-681.

31. Ayan, D.; Maltais, R.; Roy, J.; Poirier, D., A New Nonestrogenic Steroidal Inhibitor of 17beta-Hydroxysteroid Dehydrogenase Type I Blocks the Estrogen-Dependent Breast Cancer Tumor Growth Induced by Estrone. *Mol. Cancer Ther.* **2012,** *11* (10), 2096-2104.

32. Trottier, A.; Maltais, R.; Ayan, D.; Barbeau, X.; Roy, J.; Perreault, M.; Poulin, R.; Lague, P.; Poirier, D., Insight into the Mode of Action and Selectivity of PBRM, a Covalent Steroidal Inhibitor of 17beta-Hydroxysteroid Dehydrogenase Type 1. *Biochem. Pharmacol.* **2017,** *144*, 149-161.

33. Maltais, R.; Trottier, A.; Roy, J.; Ayan, D.; Bertrand, N.; Poirier, D., Pharmacokinetic Profile of PBRM in Rodents, a First Selective Covalent Inhibitor of 17beta-HSD1 for Breast Cancer and Endometriosis Treatments. *J. Steroid Biochem. Mol. Biol.* **2018,** *178*, 167-176.

34. Los, G. V.; Encell, L. P.; McDougall, M. G.; Hartzell, D. D.; Karassina, N.; Zimprich, C.; Wood, M. G.; Learish, R.; Ohana, R. F.; Urh, M.; Simpson, D.; Mendez, J.; Zimmerman, K.; Otto, P.; Vidugiris, G.; Zhu, J.; Darzins, A.; Klaubert, D. H.; Bulleit, R. F.; Wood, K. V., HaloTag: A Novel Protein Labeling Technology for Cell Imaging and Protein Analysis. *ACS Chem. Biol.* **2008,** *3* (6), 373-382.

35. Tremblay, M. R.; Poirier, D., Overview of a Rational Approach to Design Type I 17beta-Hydroxysteroid Dehydrogenase Inhibitors without Estrogenic Activity: Chemical Synthesis and Biological Evaluation. *J. Steroid Biochem. Mol. Biol.* **1998,** *66* (4), 179-191.

36. Sam, K. M.; Boivin, R. P.; Tremblay, M. R.; Auger, S.; Poirier, D., C16 and C17 Derivatives of Estradiol as Inhibitors of 17beta-Hydroxysteroid Dehydrogenase Type 1: Chemical Synthesis and Structure-Activity Relationships. *Drug. Des. Discov.* **1998,** *15* (3), 157-180.

37. Polavarapu, A.; Stillabower, J. A.; Stubblefield, S. G.; Taylor, W. M.; Baik, M. H., The Mechanism of Guanine Alkylation by Nitrogen Mustards: A Computational Study. *J. Org. Chem.* **2012,** *77* (14), 5914-5921.

38. Katzenellenbogen, J. A.; McGorrin, R. J.; Tatee, T.; Kempton, R. J.; Carlson, K. E.; Kinder, D. H., Chemically Reactive Estrogens: Synthesis and Estrogen Receptor Interactions of Hexestrol Ether Derivatives and 4-Substituted Deoxyhexestrol Derivatives Bearing Alkylating Functions. *J. Med. Chem.* **1981,** *24* (4), 435-450.

39. Rogers, G. A.; Shaltiel, N.; Boyer, P. D., Facile Alkylation of Methionine by Benzyl Bromide and Demonstration of Fumarase Inactivation Accompanied by Alkylation of a Methionine Residue. *J. Biol. Chem.* **1976,** *251* (18), 5711-5717.

40. Ruddraraju, K. V.; Zhang, Z. Y., Covalent Inhibition of Protein Tyrosine Phosphatases. *Mol. Biosyst.* **2017,** *13* (7), 1257-1279.

41. Glazer, A. N.; Delange, R. J.; Sigman, D. S., Chemical Modification of Proteins: Selected Methods and Analytical Procedures. In *Laboratory Techniques in Biochemistry and Molecular Biology*, Work, T. S.; Work, E., Eds. Elsevier B.V.: 1976; Vol. 4, pp 135-166.

42. Shaw, E., Chemical Modification by Active-Site-Directed Reagents. In *The Enzymes*, 3 ed.; Boyer, P. D., Ed. Academic Press: New York and London, 1970; Vol. 1, pp 91-146.

43. Azzi, A.; Rehse, P. H.; Zhu, D. W.; Campbell, R. L.; Labrie, F.; Lin, S. X., Crystal Structure of Human Estrogenic 17β-Hydroxysteroid Dehydrogenase Complexed with 17β-Estradiol. *Nat. Struct. Biol.* **1996,** *3*, 665-668.

44. Huang, Y. W.; Pineau, I.; Chang, H. J.; Azzi, A.; Bellemare, V.; Laberge, S.; Lin, S. X., Critical Residues for the Specificity of Cofactors and Substrates in Human Estrogenic 17β-Hydroxysteroid Dehydrogenase 1: Variants Designed from the Three-Dimensional Structure of the Enzyme. *Mol. Endocrinol.* **2001,** *15* (11), 2010-2020.

45. Mazumdar, M.; Fournier, D.; Zhu, D. W.; Cadot, C.; Poirier, D.; Lin, S. X., Binary and Ternary Crystal Structure Analyses of a Novel Inhibitor with 17beta-HSD type 1: A Lead Compound for Breast Cancer Therapy. *Biochem. J.* **2009,** *424* (3), 357-366.

46. Sawicki, M. W.; Erman, M.; Puranen, T.; Vihko, P.; Ghosh, D., Structure of the Ternary Complex of Human 17beta-Hydroxysteroid Dehydrogenase Type 1 with 3-hydroxyestra-1,3,5,7-tetraen-17-one (Equilin) and NADP+. *Proc. Natl. Acad. Sci. USA* **1999,** *96* (3), 840-845.

47. Lin, S. X.; Yang, F.; Jin, J. Z.; Breton, R.; Zhu, D. W.; Luu-The, V.; Labrie, F., Subunit Identity of the Dimeric 17β-Hydroxysteroid Dehydrogenase from Human Placenta. *J. Biol. Chem.* **1992,** *267*, 16182-16187.

48. Kleywegt, G. J.; Jones, T. A., Phi/Psi-Chology: Ramachandran Revisited. *Structure* **1996,** *4* (12), 1395-1400.

49. Breton, R.; Housset, D.; Mazza, C.; Fontecilla-Camps, J. C., The Structure of a Complex of Human 17β-Hydroxysteroid Dehydrogenase with Estradiol and NADP+ Identifies Two Principal Targets for the Design of Inhibitors. *Structure* **1996,** *4*, 905-915.

50. Shi, R.; Lin, S. X., Cofactor Hydrogen Bonding onto the Protein Main Chain is Conserved in the Short Chain Dehydrogenase/Reductase Family and Contributes to Nicotinamide Orientation. *J. Biol. Chem.* **2004,** *279* (16), 16778-16785.

51. Han, Q.; Campbell, R. L.; Gangloff, A.; Huang, Y. W.; Lin, S. X., Dehydroepiandrosterone and Dihydrotestosterone Recognition by Human Estrogenic 17β-Hydroxysteroid Dehydrogenase. *J. Biol. Chem.* **2000,** *275*, 1105-1111.

52. Yang, F.; Zhu, D. W.; Wang, J. Y.; Lin, S. X., Rapid Purification Yielding Highly Active 17β-Hydroxysteroid Dehydrogenase: Application of Hydrophobic Interaction and Affinity Fast Protein Liquid Chromatography. *J. Chromatogr. B Biomed. Sci. Appl.* **1992,** *582*, 71-76.

53. Zhu, D. W.; Lee, X.; Breton, R.; Ghosh, D.; Pangborn, W.; Duax, W. L.; Lin, S. X., Crystallization and Preliminary X-ray Diffraction Analysis of the Complex of Human Placental 17β-Hydroxysteroid Dehydrogenase with NADP+. *J. Mol. Biol.* **1993,** *234* (1), 242-244.

54. Zhu, D. W.; Lee, X.; Labrie, F.; Lin, S. X., Crystal Growth of Human Estrogenic 17β-Hydroxysteroid Dehydrogenase. *Acta Crystallogr. D Biol. Crystallogr.* **1994,** *50* (4), 550-555.

55. Zhu, D. W.; Azzi, A.; Rehse, P.; Lin, S. X., The Crystallogenesis of a Human Estradiol Dehydrogenase-Substrate Complex. *J. Cryst. Growth* **1996,** *168*, 275-279.

56. Leslie, A. G. W.; Powell, H. R., *Processing Diffraction Data with Mosflm*. Springer Netherlands: 2007.

57. Evans, P., Scaling and Assessment of Data Quality. *Acta Crystallogr. D Biol. Crystallogr.* **2006,** *62* (Pt 1), 72-82.

58. Winn, M. D.; Ballard, C. C.; Cowtan, K. D.; Dodson, E. J.; Emsley, P.; Evans, P. R.; Keegan, R. M.; Krissinel, E. B.; Leslie, A. G.; McCoy, A.; McNicholas, S. J.; Murshudov, G. N.; Pannu, N. S.; Potterton, E. A.; Powell, H. R.; Read, R. J.; Vagin, A.; Wilson, K. S., Overview of the CCP4 Suite and Current Developments. *Acta Crystallogr. D Biol. Crystallogr.* **2011,** *67* (Pt 4), 235-242.

59. Vagin, A.; Teplyakov, A., Molecular Replacement with MOLREP. *Acta Crystallogr. D Biol. Crystallogr.* **2010,** *66* (Pt 1), 22-25.

60. Gangloff, A.; Shi, R.; Nahoum, V.; Lin, S. X., Pseudo-Symmetry of C19 Steroids, Alternative Binding Orientations, and Multispecificity in Human Estrogenic 17beta-Hydroxysteroid Dehydrogenase. *FASEB J.* **2003,** *17* (2), 274-276.

61. Murshudov, G. N.; Skubak, P.; Lebedev, A. A.; Pannu, N. S.; Steiner, R. A.; Nicholls, R. A.; Winn, M. D.; Long, F.; Vagin, A. A., REFMAC5 for the Refinement of Macromolecular Crystal Structures. *Acta Crystallogr. D Biol. Crystallogr.* **2011,** *67* (Pt 4), 355-367.

62. Emsley, P.; Lohkamp, B.; Scott, W. G.; Cowtan, K., Features and Development of Coot. *Acta Crystallogr. D Biol. Crystallogr.* **2010,** *66* (Pt 4), 486-501.

63. Laskowski, R. A.; MacArthur, M. W.; Moss, D. S.; Thornton, J. M., PROCHECK: A Program to Check the Stereochemical Quality of Protein Structures. *J. Appl. Crystallogr.* **1993,** *26* (2), 283-291.

64. *The PyMOL Molecular Graphics System, Version 2.0 Schrödinger, LLC.*

65. *SeeSAR version 7.3; BioSolveIT GmbH, Sankt Augustin, Germany, 2018*.

66. Schneider, N.; Lange, G.; Hindle, S.; Klein, R.; Rarey, M., A Consistent Description of Hydrogen Bond and Dehydration Energies in Protein-Ligand Complexes: Methods Behind the HYDE Scoring Function. *J. Comput. Aided. Mol. Des.* **2013,** *27* (1), 15-29.

67. Pettersen, E. F.; Goddard, T. D.; Huang, C. C.; Couch, G. S.; Greenblatt, D. M.; Meng, E. C.; Ferrin, T. E., UCSF Chimera--a Visualization System for Exploratory Research and Analysis. *J. Comput. Chem.* **2004,** *25* (13), 1605-1612.

68. Dunbrack, R. L., Rotamer Libraries in the 21st Century. *Curr. Opin. Struct. Biol.* **2002,** *12* (4), 431-440.

Figures and Legends

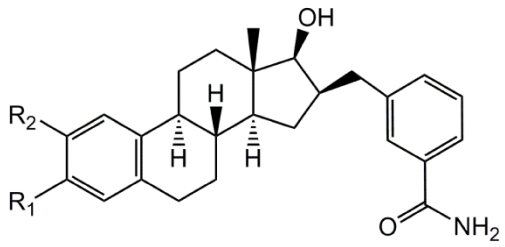

CC-156 (R_1 = OH, R_2 = H): Reversible Inhibitor
2-MeO-CC-156 (R_1 = OH, R_2 = OCH_3): Reversible Inhibitor
PBRM (R1 = CH_2CH_2Br, R_2 = H): Irreversible Inhibitor

Figure 1.1. Three potent steroidal inhibitors of 17β-HSD1: 16β-(*m*-carbamoylbenzyl)-E2 (CC-156), 2-methoxy-16β-(*m*-carbamoylbenzyl)-E2 (2-MeO-CC-156), and 3-(2-bromoethyl)-16β-(*m*-carbamoyl benzyl)-17β-hydroxy-1,3,5(10)-estratriene (PBRM).

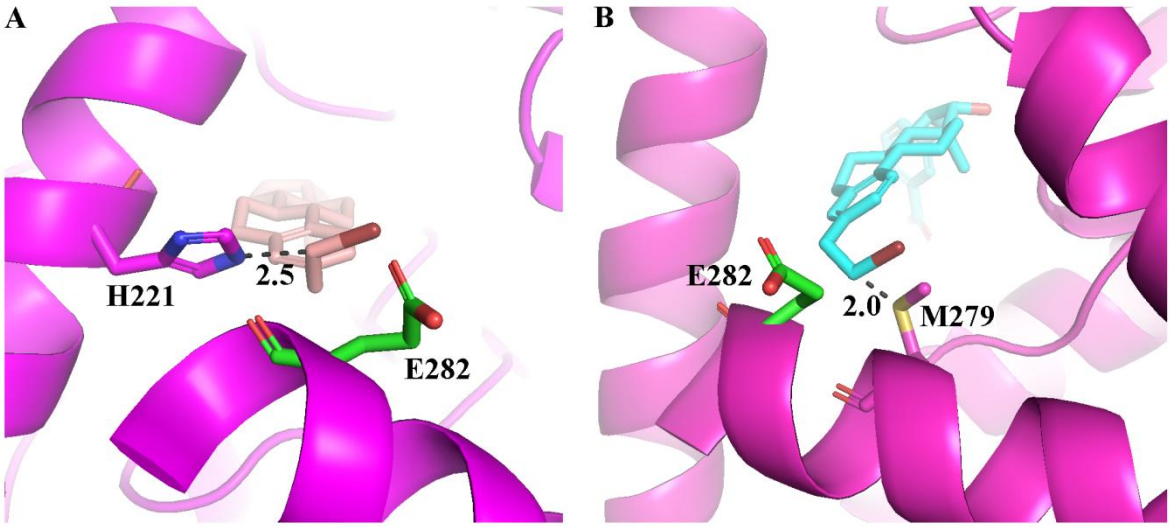

Figure 1.2. Results from the *in silico* building of PBRM at the binding site of 17β-HSD1. The binding site conformation of CC-156 ternary complex structure is represented (magenta) with Glu^{282} side chain solvent-oriented (labelled and colored in green). His^{221} and Met^{279} residues are labelled and shown in sticks in (A) and (B) respectively. The best pose of manually built PBRM with (A) His^{221} mutated into Ala, and (B) Met^{279} mutated into Ala are represented by pink and blue sticks, respectively. The distance from the CH_2 of the bromoethyl side chain to (A) the NH of His^{221} side chain, and (B) the S of Met^{279} side chain are labelled.

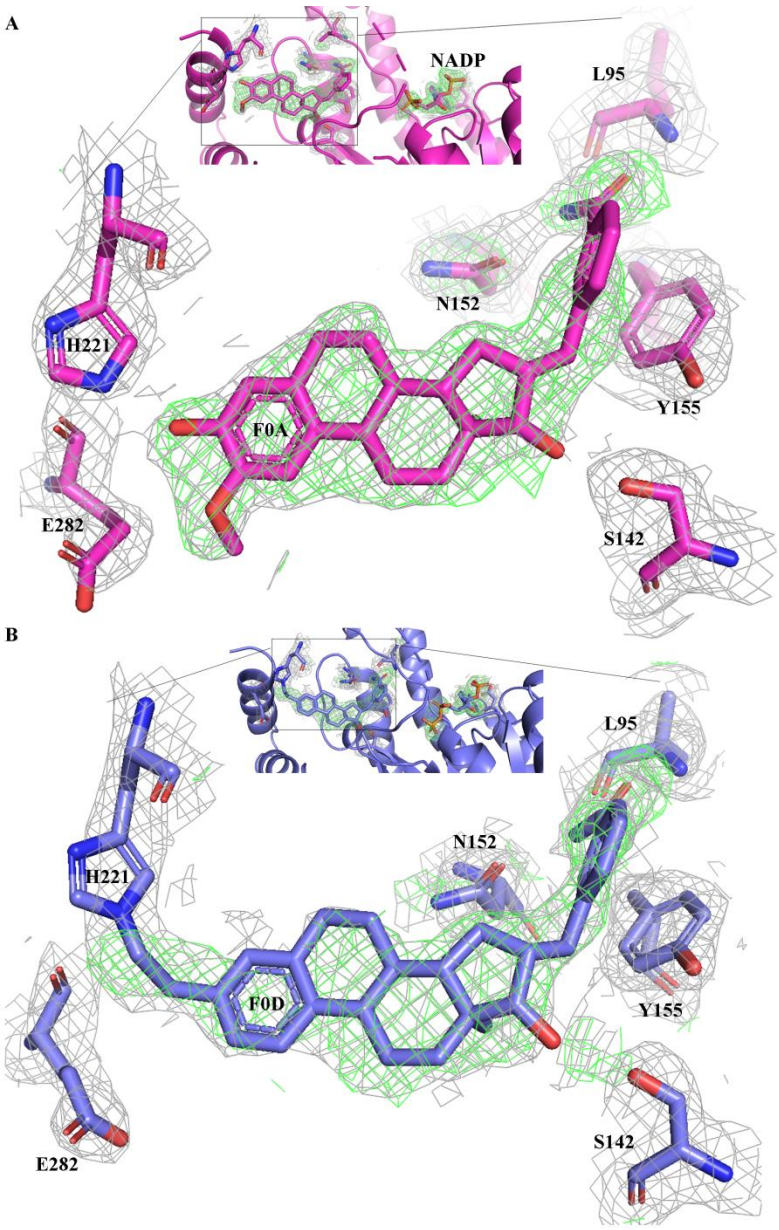

Figure 1.3. View of the active sites within the A subunit of 2-MeO-CC-156 (A) and PBRM (B) ternary complex structures. Inhibitors 2-MeO-CC-156 (F0A) and PBRM (F0D) and cofactor $NADP^+$ are shown in their omit F_o-F_c and $2F_o$-F_c electron densities. The side chains of important residues Leu^{95}, Ser^{142}, Asn^{152}, Tyr^{155}, His^{221}, and Glu^{282} are shown in their $2F_o$-F_c electron densities. $2F_o$-F_c maps are drawn in gray and contoured at 1σ; F_o-F_c maps are drawn in green and contoured at 2.5σ. The backbones of the A subunit in 2-MeO-CC-156 and PBRM complexes are shown in magenta and blue, respectively.

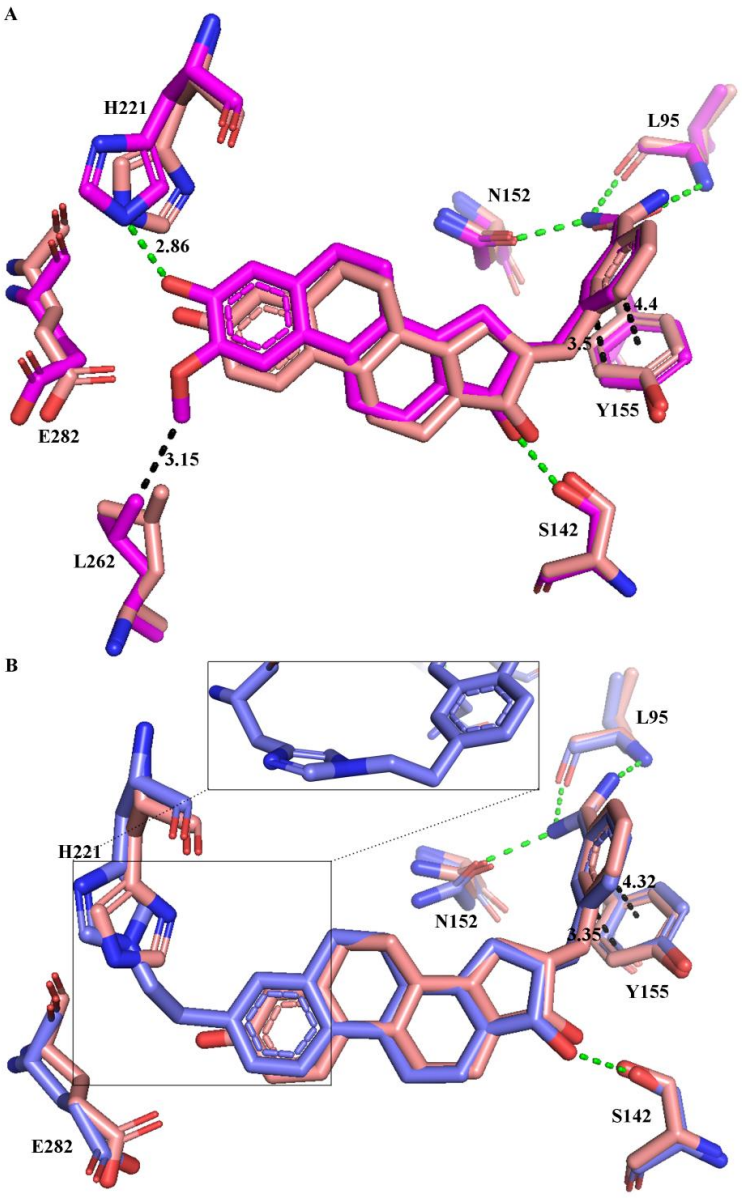

Figure 1.4. Superposition of A subunit of 2-MeO-CC-156 (magenta) and PBRM (blue) ternary complexes along with 17β-HSD1–CC-156–$NADP^+$ (pink) at the binding sites, showing the inhibitors and important residues. (A) Superposition of 2-MeO-CC-156 and CC-156 complexes at the steroid binding site. (B) Superposition of PBRM and CC-156 complexes at the steroid binding sites. Interacting residues are labeled and shown as sticks. Hydrogen bonds of inhibitor 2-MeO-CC-156 and PBRM with their surrounding residues are presented in green dashed lines. Several important distances are labeled and indicated with black dashed lines.

Tables

Table 1.1 Data collection and refinement statistics

	17β-HSD1-2-MeO-CC-156-NADP+	17β-HSD1-PBRM-NADP+
Data Collection		
Space group	$P2_12_12_1$	$P2_12_12_1$
Unit cell		
a,b,c (Å)	41.75, 107.98, 115.72	42.82, 108.94, 116.36
α,β,γ (°)	90, 90, 90	90, 90, 90
Resolution range (Å)	25-2.10 (2.21-2.10)[a]	25-2.2 (2.32-2.20)
Number of reflections	173088 (23506)	184811 (24512)
Unique reflections	28809 (3929)	28372 (4006)
Completeness (%)	91.9 (87.7)	99.5 (98.1)
I/σ(I)	7.4 (3.2)	11.0 (3.4)
R_{means}[b]	0.144 (0.456)	0.108 (0.521)
Multiplicity	6.0 (6.0)	6.5 (6.1)
Wilson B-factor (Å^2)	27.5	33.0
Refinement		
R-work[c]	0.21	0.23
R-free[d]	0.26	0.30
r.m.s.d		
Bond lengths (Å)	0.013	0.011
Bond angles (°)	1.79	1.68
Ramachandran plot[e] (%)		
Most favored regions	93.9	93.3
Additional allowed regions	6.1	6.5
Generously allowed regions	0.0	0.2
Disallowed regions	0.0	0.0
Average B, all atoms (Å^2)	39.0	47.0

[a] Data statistics for the outer shell are given in parentheses.

[b] The redundancy-independent R_{merge}/R_{sym}, $R_{means} = \sum_{hkl}\sqrt{\frac{n}{n-1}}\sum_{i=1}^{n}\left|I_{hkl,i} - \langle I_{hkl}\rangle\right| / \sum_{hkl}\sum_i I_{hkl,i}$

[c] $R_{work} = \sum_{hkl}\left||F_{obs}(hkl)| - |F_{calc}(hkl)|\right| / \sum_{hkl}|F_{obs}(hkl)|$

[d] R_{free} = the cross-validation R factor for 5% of reflections

[e] Calculated with *PROCHECK*.

Table 1.2. Hydrogen bonds between bound inhibitor and surrounding residues in 17β-HSD1 ternary complexes

Complexes	Donor	Acceptor	Length (Å)
17β-HSD1–2-MeO-CC-156–NADP+ (PDB ID: 6CGC)	Ser^{142}: Oγ	2-MeO-CC-156: O-19	2.73
	Leu^{95}: N	2-MeO-CC-156: O-29	2.55
	2-MeO-CC-156: N-30	Leu^{95}: O	2.94
	2-MeO-CC-156: N-30	Asn^{152}: Oδ	2.52
	2-MeO-CC-156: O-4	His^{221}: Nε	2.86
17β-HSD1–PBRM–NADP+ (PDB ID: 6CGE)	Ser^{142}: Oγ	PBRM: O-19	3.22
	Leu^{95}: N	PBRM: O-29	2.82
	PBRM: N-30	Leu^{95}: O	2.88
	PBRM: N-30	Asn^{152}: Oδ	2.61
17β-HSD1–CC-156–NADP+ (PDB ID: 3HB5)	CC-156: O-4	Glu^{282}: Oε	2.61
	Ser^{142}: Oγ	CC-156: O-19	2.72
	Leu^{95}: N	CC-156: N-30	2.77
	CC-156: O-29	Leu^{95}: O	3.06
	CC-156: O-29	Asn^{152}: Oδ	2.65

Chapitre 2 Crystal structures of human 17β-hydroxysteroid dehydrogenase type 1 complexed with the dual-site inhibitor EM-139

2.1 Résumé

La 17β-HSD1 catalyse la biosynthèse du 17β-estradiol (E2) à partir de l'œstrone (E1), jouant un rôle central dans la progression des maladies dépendantes des œstrogènes. Le *N*-*n*-Butyl-*N*-methyl-ll-(16'*α*-chloro-3',17'*β*-dihydroxyestra- 1',3',5'(10')-trien-7'*α*-yl)undecanamide (EM-139) a été précédemment décrit comme un inhibiteur à deux cibles pouvant inhiber le récepteur des œstrogènes ainsi que l'activité de la 17β-HSD1. Dans la présente étude, nous rapportons la structure cristalline du complexe binaire 17β-HSD1-EM-139. Il est intéressant de noter quel cristal du complexe binaire EM-139 développé dans des conditions similaires à celles du cristal natif a un groupe d'espace de I121 qui n'a jamais été observé auparavant dans d'autres cristaux de 17β-HSD1. La compréhension au niveau atomique du mécanisme inhibiteur de l'EM-139 fournit des informations importantes sur la conception de l'inhibiteur de la 17β-HSD1. Aussi, cette compréhension facilitera le développement futur d'inhibiteurs plus puissants et sélectifs de l'enzyme à des fins cliniques.

2.2 Abstract

Human 17β-hydroxysteroid dehydrogenase type 1 (17β-HSD1) catalyzes the biosynthesis of 17β-estradiol (E2) from estrone (E1), playing a pivotal role in the progression of estrogen-dependent diseases. N-n-Butyl-N-methyl-ll-(16'α-chloro-3',17'β-dihydroxyestra- 1',3',5'(10')-trien-7'α-yl)undecanamide (EM-139) was previously described as a dual-site inhibitor that can inhibit estrogen receptor as well as 17β-HSD1 activity. In the present study, we report the crystal structure of the 17β-HSD1-EM-139 binary complex. Interestingly, the EM-139 binary complex crystal grown under similar condition as native crystal has a space group of I121 never observed in other 17β-HSD1 crystals before. The structural analysis showed that the steroidal moiety of the bound EM-139 molecule has a binding pattern similar to E2 in the E2 binary complex, with the O-3 of the inhibitor interacts with residues His^{221} and Glu^{282}, and the O-17 of the inhibitor makes hydrogen bonds with Ser^{142} and Tyr^{155}. As for the long 7α-alkyl moiety of the inhibitor, which is essential for its anti-estrogenic activity, may compromise the inhibitory effect of the inhibitor to 17β-HSD1. Moreover, no obvious interaction is observed between the 16α-Cl atom and the surrounding residues. The atomic level understanding of the inhibitory mechanism of EM-139 provides important information for the inhibitor design of 17β-HSD1, which will facilitate future development of more potent and selective inhibitors of the enzyme for clinical purposes.

2.3 Introduction

Seventeen β-hydroxysteroid dehydrogenase type 1 (17β-HSD1, EC. 1.1.1.62) catalyzes the NAD(P)H dependent conversion of estrone (E1) to the most potent estrogen, 17β-estradiol (E2)[1]. E2 is well known to play a crucial role in the progression and development of several estrogen-dependent diseases (EDD). Increased E2 levels as well as up-regulated 17β-HSD1 expression indicate the involvement of the enzyme in EDDs, such as breast cancer[2-3], endometrial cancer[4-5], endometriosis[6-8], and ovarian cancer[9]. Moreover, patients with tumors that have high mRNA levels of 17β-HSD1 have significantly shortened disease-free and overall survival[10-12]. Therefore, blocking the production of E2 through the specific inhibition of 17β-HSD1 activity is considered to be of therapeutic benefit in the treatment of EDDs.

Over the past decades, major efforts from many different laboratories have been devoted to developing highly selective inhibitors of the key steroidogenic enzyme 17β-HSD1, yielding several lead compounds with significant inhibitory activity[13-14]. However, due to the lack of specificity, especially for the presence of undesired estrogenic activity, no inhibitor has yet reached the stage of clinical trials[15-18]. N-n-Butyl-N-methyl-ll-(16'α-chloro-3',17'β-dihydroxyes-tra-1',3',5'(10')-trien-7'α-yl) undecanamide (EM-139) is a 7α-alkyl, 16α-halo estradiol derivative which was first synthesized as a pure antiestrogen (**Figure 2.1**)[19]. Following experiments demonstrated its inhibitory effect on 17β-HSD1 activity with a K_i of 6 μM[20]. Thus the compound was defined as a dual-site inhibitor which possesses inhibitory effect on estrogen receptor and on the estrogen formation[21]. Although this compound was proven to be a non-selective inhibitor of the 17β-HSD family members[22], study of the EM-139/17β-HSD1 complex structure should help us to better understand the inhibitory mechanism of the dual-site inhibitor, thus facilitating further inhibitor design of the enzyme.

Previously, we have reported the crystallization of the 17β-HSD1/EM-139 complex using both co-crystallization and soaking methods[23]. The crystals obtained were isomorphous to the native crystals with a monoclinic space group C2[23]. After careful analysis of the structures, the inhibitor couldn't be identified at the binding site of the enzyme due to poor electron density. In the present study, we optimized the co-crystallization procedure and successfully obtained complex crystals with a unique space group never observed in 17β-HSD1 complexes before. The clear electron density at the binding site indicated the presence of the dual-site inhibitor in the enzyme complex.

2.4 Materials and Methods

Protein Preparation and Co-Crystallization

The 17β-HSD1 enzyme was expressed in Sf9 insect cells and purified as described previously[24]. After the measurement of specific activity[25], the purified enzyme was concentrated to a final concentration of 15 mg/ml

in the presence of 0.06% β-octyl glucoside (β-OG), and then subjected to a buffer change procedure[26] via centricon (Emdmillipore, USA) to saturate the enzyme with the inhibitor EM-139. The co-crystallization experiment was carried out using the vapor diffusion method at room temperature. Crystals were obtained under conditions containing 22% - 26% (w/v) polyethyleneglycol (PEG) 4000, 0.15 M magnesium chloride, and 0.1 M HEPES buffered to pH 7.5.

Data Collection and Structure Determination

The X-ray diffraction data of the 17β-HSD1-EM-139 crystals were collected at 100 K using synchrotron radiation at Advanced Photon Source (APS) beamline 31-LRL-CAT (Chicago, USA) equipped with a MAR CCD 165 mm detector at a wavelength of 0.9793 Å. The dataset was indexed and intergraded using *MOSFLM*[27], and scaled with *SCALA*[28] from the *CCP4* suite[29]. The structure was solved by molecular replacement with *Molrep*[30] using a reported 17β-HSD1 coordinate (PDB code 1JTV)[31] as search model. The initial model was subjected to multiple rounds of auto-refinement using *Refmac*[32] and manual rebuild using *Coot*[33]. Missing portions of the models, inhibitor EM-139, glycerol, polyethylene glycol, and water molecules were progressively added with great caution during the refinement procedure. The final model was verified with *PROCHECK*[34]. Molecular graphics were presented using the *Pymol* software (version 2.0 Schrödinger, LLC).

2.5 Results

Crystal utilized in this study belonged to space group I121 and each asymmetric unit contained a dimer, which is known to be the functional unit of the enzyme[25]. The complex structure was refined at 2 Å with good stereochemistries[35], and the quality of the final model can be assessed in **Table 2.1**. Similar to most previously reported 17β-HSD1 structures, the highly flexible βFαG'-loop (amino acids Phe^{192} to Leu^{197}) as well as the C-terminal end of the protein (amino acids 286 to 327) cannot be defined in the electron density (**Figure 2.2**) [36-39].

In the binary complex structure, EM-139 has definable electron density in the A subunit of the dimeric enzyme. However, the ligand density in the B subunit is poorly defined, similar to previously described complex with equilin[40]. Accordingly the ligand was not included in the B subunit of the final model. Even for the A subunit, only the steroid moiety of EM-139 can be defined but with a high average B-factor (97.5 $Å^2$), whereas the 7α-alkyl side chain of the inhibitor cannot be defined in the electron density (**Figure 2.3**). This high flexibility of the inhibitor is in accordance with its relatively low affinity for the enzyme[20].

2.6 Discussion

The space group of 17β-HSD1 crystals can be affected by the presence of cations in the crystallization conditions[41]. The space group of crystals obtained in the presence of Mg^{2+} and Mn^{2+} belong to C2, whereas crystals grown under conditions with Li^{+} and Na^{+} had a space group of $P2_12_12_1$[41]. Despite the presence of Mg^{2+}, the space group of the co-crystallized EM-139 complex crystals has been changed to I121, not observed in any other reported 17β-HSD1 structures. The change in space group may be due to the long alkyl side chain at the C7 of EM-139, which may affect the packing during crystal growth.

When the EM-139 binary and E2 binary (PDB ID 1IOL[37]) complexes as well as the apo structure of 17β-HSD1 (PDB ID 1BHS[42]) are superimposed, a similar conformation is observed at the steroid binding site of the enzyme (**Figure 2.4A**). The root-mean-square deviation (RMSD) for all paired Cα atoms obtained between EM-139 complex and apo structure is 0.456 Å, similar to the value obtained between EM-139 and E2 complexes (0.508 Å). It is worth mentioning that the position observed for the steroidal moiety of EM-139 has roughly 9° rotation around the axis at the C-3 atom and perpendicular to its β-face, when compared with the position of E2. This leads to the shifting of the O-17 by 1.4 Å as compared with the position of its counterpart in the E2 complex (**Figure 2.4B,C**). As a result, the bifurcated hydrogen bonds between the O-17 of EM-139 with Ser^{142} and Tyr^{155} (3.5 and 3.2 Å, respectively) are established, although the bond distances differ from their counterparts observed in the E2 complex (3.1 and 3.5 Å, respectively)[37]. Moreover, the bifurcated hydrogen bond between the 3-hydroxyl group of EM-139 with His^{221} and Glu^{282} (3.2 and 3.5 Å, respectively) at the recognition end of the steroid binding cleft is conserved. Although much weaker as compared to their counterparts in the E2 complex (3.1 and 2.7 Å, respectively)[37], these hydrogen bonds are essential for stabilizing the inhibitor in the steroid binding cavity together with the hydrogen bonds at the O-3 of EM-139.

The 7α-alkyl moiety of EM-139 is facing toward the outside of the steroid binding cavity which is apparently accommodated by the βFαG'-loop. However, both the 7α-alkyl side chain of the inhibitor and the βFαG'-loop of the enzyme are unable to be defined by electron density due to their high degree of flexibility. This bulky 7α-alkyl side chain is essential for the inhibitor to possess anti-estrogenic activity[43]. It is also safe to conclude that the α conformation of the C-7 is essential for this compound to be able to bind with 17β-HSD1. Similar results can also be observed at the C-16 of the inhibitor where a 16β halogen atom may have steric hindrance with Tyr^{155}. However, no obvious interaction is observed between the 16α-Cl atom and surrounding residues (**Figure 2.4B,C**).

2.7 Conclusion

The present work was aimed at investigating the molecular basis of the inhibitory mechanism of the dual-site inhibitor EM-139 in 17β-HSD1. We successfully co-crystallized and solved the crystal structure of 17β-HSD1 in

complex with the inhibitor. Through comparative analyses of EM-139 binary complexes and previously reported E2 binary complex as well as the apo structure, we observed a similar binding pattern of the inhibitor to the enzyme. The bifurcated hydrogen bonds between the O-3 of the inhibitor and the recognition end (His^{221} and Glu^{282}) of the binding site as well as the O-17 of the inhibitor and the catalytic end (Ser^{142} and Tyr^{155}) of the binding site are critical in stabilizing the bound inhibitor molecule. However, the introduction of a bulky side chain at the C-7 of the steroid core, which contributes to the anti-estrogenic activity of the dual-site inhibitor, may negatively affect the binding of inhibitor to 17β-HSD1. These results will contribute to the design of more potent and selective inhibitors of 17β-HSD1 for clinical purposes.

Acknowledgements

We thank Dre. M. Zhou for her technical support in enzyme purification and crystal growth. We acknowledge the use of beamline 31-LRL-CAT at the Advanced Photon Source, Argonne National Laboratory, USA.

Conflicts of Interest

The authors declare no conflicts of interest regarding the publication of this paper.

2.8 Reference

1. Luu-The, V.; Labrie, C.; Zhao, H. F.; Couët, J.; Lachance, Y.; Simard, J.; Leblanc, G.; Côté, J.; Bérubé, D.; Gagné, R., Characterization of cDNAs for human estradiol 17 beta-dehydrogenase and assignment of the gene to chromosome 17: evidence of two mRNA species with distinct 5'-termini in human placenta. *Mol Endocrinol* 1989, *3* (8), 1301-9.

2. Miyoshi, Y.; Ando, A.; Shiba, E.; Taguchi, T.; Tamaki, Y.; Noguchi, S., Involvement of up-regulation of 17beta-hydroxysteroid dehydrogenase type 1 in maintenance of intratumoral high estradiol levels in postmenopausal breast cancers. *Int J Cancer* **2001,** *94* (5), 685-9.

3. Lin, S. X.; Chen, J.; Mazumdar, M.; Poirier, D.; Wang, C.; Azzi, A.; Zhou, M., Molecular Therapy of Breast Cancer: Progress and Future Directions. *Nat. Rev. Endocrinol.* **2010,** *6* (9), 485-493.

4. Cornel, K. M.; Kruitwagen, R. F.; Delvoux, B.; Visconti, L.; Van de Vijver, K. K.; Day, J. M.; Van Gorp, T.; Hermans, R. J.; Dunselman, G. A.; Romano, A., Overexpression of 17beta-hydroxysteroid dehydrogenase type 1 increases the exposure of endometrial cancer to 17beta-estradiol. *J Clin Endocrinol Metab* **2012,** *97* (4), E591-601.

5. Konings, G. F.; Cornel, K. M.; Xanthoulea, S.; Delvoux, B.; Skowron, M. A.; Kooreman, L.; Koskimies, P.; Krakstad, C.; Salvesen, H. B.; van Kuijk, K.; Schrooders, Y. J.; Vooijs, M.; Groot, A. J.; Bongers, M. Y.; Kruitwagen, R. F.; Enitec; Romano, A., Blocking 17beta-hydroxysteroid dehydrogenase type 1 in endometrial cancer: a potential novel endocrine therapeutic approach. *J Pathol* **2018,** *244* (2), 203-214.

6. Delvoux, B.; D'Hooghe, T.; Kyama, C.; Koskimies, P.; Hermans, R. J.; Dunselman, G. A.; Romano, A., Inhibition of type 1 17beta-hydroxysteroid dehydrogenase impairs the synthesis of 17beta-estradiol in endometriosis lesions. *J Clin Endocrinol Metab* **2014,** *99* (1), 276-84.

7. Mori, T.; Ito, F.; Matsushima, H.; Takaoka, O.; Koshiba, A.; Tanaka, Y.; Kusuki, I.; Kitawaki, J., Dienogest reduces HSD17beta1 expression and activity in endometriosis. *J Endocrinol* **2015,** *225* (2), 69-76.

8. Šmuc, T.; Pucelj, M. R.; Šinkovec, J.; Husen, B.; Thole, H.; Rižner, T. L., Expression analysis of the genes involved in estradiol and progesterone action in human ovarian endometriosis. *Gynecological Endocrinology* **2009,** *23* (2), 105-111.

9. Blomquist, C. H.; Bonenfant, M.; McGinley, D. M.; Posalaky, Z.; Lakatua, D. J.; Tuli-Puri, S.; Bealka, D. G.; Tremblay, Y., Androgenic and estrogenic 17β-hydroxysteroid dehydrogenase/17-ketosteroid reductase

in human ovarian epithelial tumors: evidence for the type 1, 2 and 5 isoforms. *The Journal of Steroid Biochemistry and Molecular Biology* **2002,** *81* (4), 343-351.

10. Gunnarsson, C.; Olsson, B. M.; Stål, O.; Group, S. S. B. C., Abnormal expression of 17beta-hydroxysteroid dehydrogenases in breast cancer predicts late recurrence. *Cancer Res* **2001,** *61* (23), 8448-51.

11. Vihko, P.; Harkonen, P.; Soronen, P.; Torn, S.; Herrala, A.; Kurkela, R.; Pulkka, A.; Oduwole, O.; Isomaa, V., 17 beta-hydroxysteroid dehydrogenases--their role in pathophysiology. *Mol Cell Endocrinol* **2004,** *215* (1-2), 83-8.

12. Salhab, M.; Reed, M. J.; Al Sarakbi, W.; Jiang, W. G.; Mokbel, K., The role of aromatase and 17-beta-hydroxysteroid dehydrogenase type 1 mRNA expression in predicting the clinical outcome of human breast cancer. *Breast Cancer Res Treat* **2006,** *99* (2), 155-62.

13. Poirier, D., 17β-Hydroxysteroid Dehydrogenase Inhibitors: A Patent Review. *Expert. Opin. Ther. Pat.* **2010,** *20* (9), 1123-1145.

14. Lin, S. X.; Poirier, D.; Adamski, J., A Challenge for Medicinal Chemistry by the 17β-Hydroxysteroid Dehydrogenase Superfamily: An Integrated Biological Function and Inhibition Study. *Curr. Top. Med. Chem.* **2013,** *13* (10), 1164-1171.

15. Trottier, A.; Maltais, R.; Ayan, D.; Barbeau, X.; Roy, J.; Perreault, M.; Poulin, R.; Lague, P.; Poirier, D., Insight into the Mode of Action and Selectivity of PBRM, a Covalent Steroidal Inhibitor of 17beta-Hydroxysteroid Dehydrogenase Type 1. *Biochem. Pharmacol.* **2017,** *144*, 149-161.

16. Day, J. M.; Tutill, H. J.; Purohit, A.; Reed, M. J., Design and validation of specific inhibitors of 17beta-hydroxysteroid dehydrogenases for therapeutic application in breast and prostate cancer, and in endometriosis. *Endocr Relat Cancer* **2008,** *15* (3), 665-92.

17. Poirier, D., Contribution to the development of inhibitors of 17beta-hydroxysteroid dehydrogenase types 1 and 7: key tools for studying and treating estrogen-dependent diseases. *J Steroid Biochem Mol Biol* **2011,** *125* (1-2), 83-94.

18. Brozic, P.; Lanisnik Risner, T.; Gobec, S., Inhibitors of 17beta-hydroxysteroid dehydrogenase type 1. *Curr Med Chem* **2008,** *15* (2), 137-50.

19. Levesque, C.; Merand, Y.; Dufour, J. M.; Labrie, C.; Labrie, F., Synthesis and biological activity of new halo-steroidal antiestrogens. *J Med Chem* **1991,** *34* (5), 1624-30.

20. Lin, S. X.; Han, Q.; Azzi, A.; Zhu, D. W.; Gangloff, A.; Campbell, R. L., 3D-structure of human estrogenic 17β-HSD1: binding with various steroids. *J Steroid Biochem Mol Biol* **1999,** *69*, 425-29.

21. Labrie, C.; Martel, C.; Dufour, J. M.; Lévesque, C.; Mérand, Y.; Labrie, F., Novel compounds inhibit estrogen formation and action. *Cancer Res* **1992,** *52* (3), 610-5.

22. Poirier, D., Inhibitors of 17β-Hydroxysteroid Dehydrogenases. *Current Medicinal Chemistry* **2003,** *10* (6), 453-77.

23. Zhu, D. W.; Campbell, R.; Labrie, F.; Lin, S. X., Crystallization and preliminary crystal structure of the complex of 17β-hydroxysteroid dehydrogenase with a dual-site inhibitor. *J Steroid Biochem Mol Biol* **1999,** *70*, 229-35.

24. Breton, R.; Yang, F.; Jin, J. Z.; Li, B.; Labrie, F.; Lin, S. X., Human 17β-Hydroxysteroid Dehydrogenase: Overproduction Using a Baculovirus Expression System and Characterization. *J. Steroid Biochem. Mol. Biol.* **1994,** *50*, 275-282.

25. Lin, S. X.; Yang, F.; Jin, J. Z.; Breton, R.; Zhu, D. W.; Luu-The, V.; Labrie, F., Subunit Identity of the Dimeric 17β-Hydroxysteroid Dehydrogenase from Human Placenta. *J. Biol. Chem.* **1992,** *267*, 16182-16187.

26. Zhu, D. W.; Azzi, A.; Rehse, P.; Lin, S. X., The Crystallogenesis of a Human Estradiol Dehydrogenase-Substrate Complex. *J. Cryst. Growth* **1996,** *168*, 275-279.

27. Leslie, A. G. W.; Powell, H. R., *Processing Diffraction Data with Mosflm*. Springer Netherlands: 2007.

28. Evans, P., Scaling and Assessment of Data Quality. *Acta Crystallogr. D Biol. Crystallogr.* **2006,** *62* (Pt 1), 72-82.

29. Winn, M. D.; Ballard, C. C.; Cowtan, K. D.; Dodson, E. J.; Emsley, P.; Evans, P. R.; Keegan, R. M.; Krissinel, E. B.; Leslie, A. G.; McCoy, A.; McNicholas, S. J.; Murshudov, G. N.; Pannu, N. S.; Potterton, E. A.; Powell, H. R.; Read, R. J.; Vagin, A.; Wilson, K. S., Overview of the CCP4 Suite and Current Developments. *Acta Crystallogr. D Biol. Crystallogr.* **2011,** *67* (Pt 4), 235-242.

30. Vagin, A.; Teplyakov, A., Molecular Replacement with MOLREP. *Acta Crystallogr. D Biol. Crystallogr.* **2010,** *66* (Pt 1), 22-25.

31. Gangloff, A.; Shi, R.; Nahoum, V.; Lin, S. X., Pseudo-Symmetry of C19 Steroids, Alternative Binding Orientations, and Multispecificity in Human Estrogenic 17beta-Hydroxysteroid Dehydrogenase. *FASEB J.* **2003,** *17* (2), 274-276.

32. Murshudov, G. N.; Vagin, A. A.; Lebedev, A.; Wilson, K. S.; Dodson, E. J., Efficient anisotropic refinement of macromolecular structures using FFT. *Acta Crystallogr D Biol Crystallogr* **1999,** *55*, 247-55.

33. Emsley, P.; Lohkamp, B.; Scott, W. G.; Cowtan, K., Features and Development of Coot. *Acta Crystallogr. D Biol. Crystallogr.* **2010,** *66* (Pt 4), 486-501.

34. Laskowski, R. A.; MacArthur, M. W.; Moss, D. S.; Thornton, J. M., PROCHECK: A Program to Check the Stereochemical Quality of Protein Structures. *J. Appl. Crystallogr.* **1993,** *26* (2), 283-291.

35. Kleywegt, G. J.; Jones, T. A., Phi/Psi-Chology: Ramachandran Revisited. *Structure* **1996,** *4* (12), 1395-1400.

36. Aka, J. A.; Mazumdar, M.; Chen, C. Q.; Poirier, D.; Lin, S. X., 17beta-Hydroxysteroid Dehydrogenase Type 1 Stimulates Breast Cancer by Dihydrotestosterone Inactivation in Addition to Estradiol Production. *Mol. Endocrinol.* **2010,** *24* (4), 832-845.

37. Azzi, A.; Rehse, P. H.; Zhu, D. W.; Campbell, R. L.; Labrie, F.; Lin, S. X., Crystal Structure of Human Estrogenic 17β-Hydroxysteroid Dehydrogenase Complexed with 17β-Estradiol. *Nat. Struct. Biol.* **1996,** *3*, 665-668.

38. Breton, R.; Housset, D.; Mazza, C.; Fontecilla-Camps, J. C., The Structure of a Complex of Human 17β-Hydroxysteroid Dehydrogenase with Estradiol and NADP+ Identifies Two Principal Targets for the Design of Inhibitors. *Structure* **1996,** *4*, 905-915.

39. Shi, R.; Lin, S. X., Cofactor Hydrogen Bonding onto the Protein Main Chain is Conserved in the Short Chain Dehydrogenase/Reductase Family and Contributes to Nicotinamide Orientation. *J. Biol. Chem.* **2004,** *279* (16), 16778-16785.

40. Sawicki, M. W.; Erman, M.; Puranen, T.; Vihko, P.; Ghosh, D., Structure of the Ternary Complex of Human 17beta-Hydroxysteroid Dehydrogenase Type 1 with 3-hydroxyestra-1,3,5,7-tetraen-17-one (Equilin) and NADP+. *Proc. Natl. Acad. Sci. USA* **1999,** *96* (3), 840-845.

41. Zhu, D. W.; Han, Q.; Qiu, W.; Campbell, R.; Xie, B. X.; Azzi, A.; Lin, S. X., Human 17β-hydroxysteroid dehydrogenase-ligand complexes: crystals of different space groups with various cations and combined seeding and co-crystallization. *Journal of Crystal Growth* **1999,** *196*, 356-64.

42. Ghosh, D.; Pletnev, V. Z.; Zhu, D. W.; Wawrzak, Z.; Duax, W. L.; Pangborn, W.; Labrie, F.; Lin, S. X., Structure of human estrogenic 17 beta-hydroxysteroid dehydrogenase at 2.20 A resolution. *Structure* **1995,** *3* (5), 503-13.

43. Wakeling, A. E.; Bowler, J., Biology and mode of action of pure antioestrogens. *Journal of chemotherapy* **1989,** *1* (4 Suppl), 1140-1.

Figures and Legends

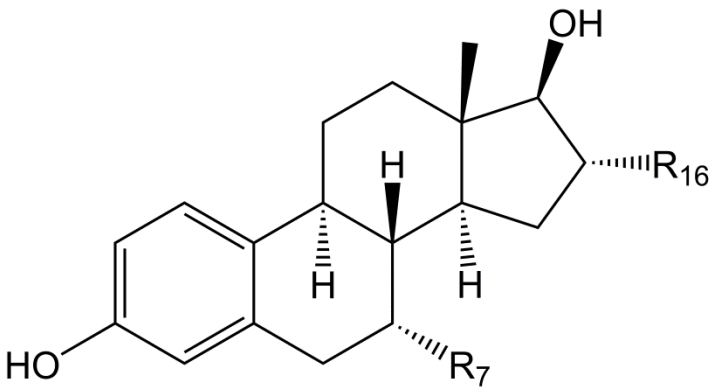

E_2 (estradiol): R_7=H, R_{16}=H
EM-139: R_7=$(CH_2)_{10}$CONBuMe, R_{16}=Cl

Figure 2.1. Structure of dual-site inhibitor N-n-Butyl-N-methyl-ll-(16'α-chloro-3',17'β-dihydroxyestra-1',3',5'(10')-trien-7'α-yl)undecanamide (EM-139).

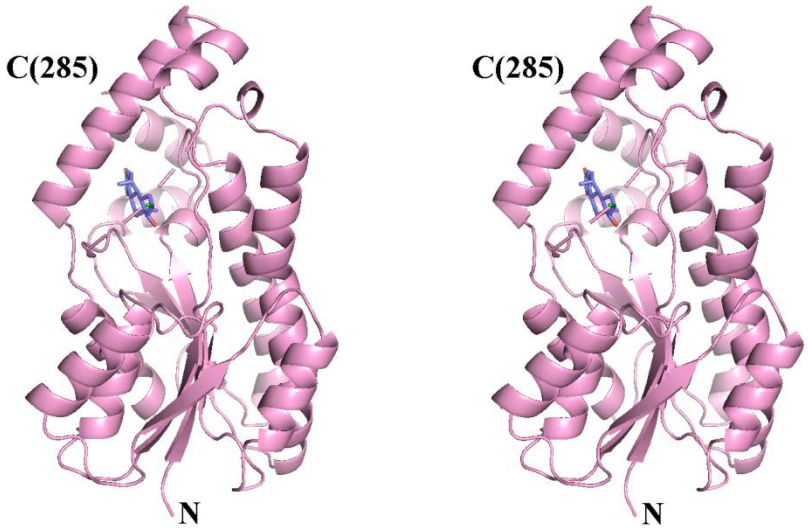

Figure 2.2. Stereo representation of the overall structure of A subunit of 17β-HSD1-EM-139 complex. The protein molecule is shown in cartoon and colored in pink. The bound EM-139 molecule is depicted as stick and colored in blue. The N-terminus and the C-terminus of the protein molecule are indicated. Segment of residues 190-197, which unable to be defined in the electron density, is represented as dash line.

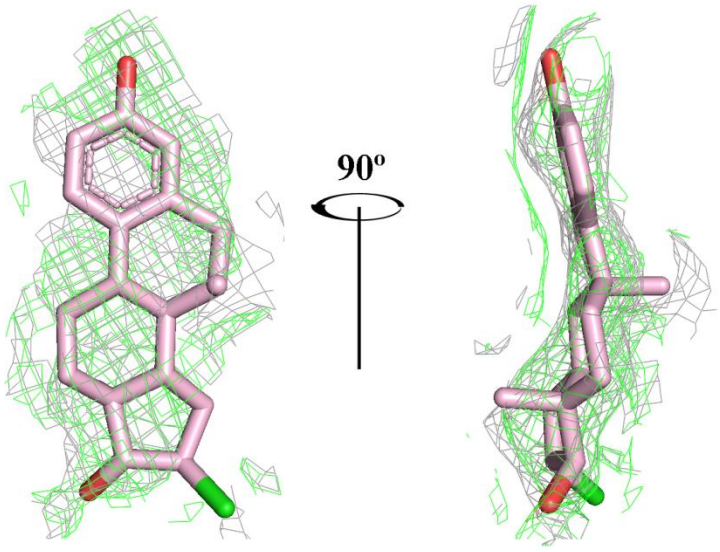

Figure 2.3. Front and side views of the electron density of EM-139 in the 17β-HSD1-EM-139 complex structure. EM-139 (ligand ID EM9) was shown in the omit Fo-Fc and 2Fo-Fc electron density. 2Fo-Fc map draw in gray and contoured at 0.8σ; Fo-Fc map draw in green and contoured at 1.5σ. The occupancy of the inhibitor was refined to 1. No significant negative density features were present in the region of binding site.

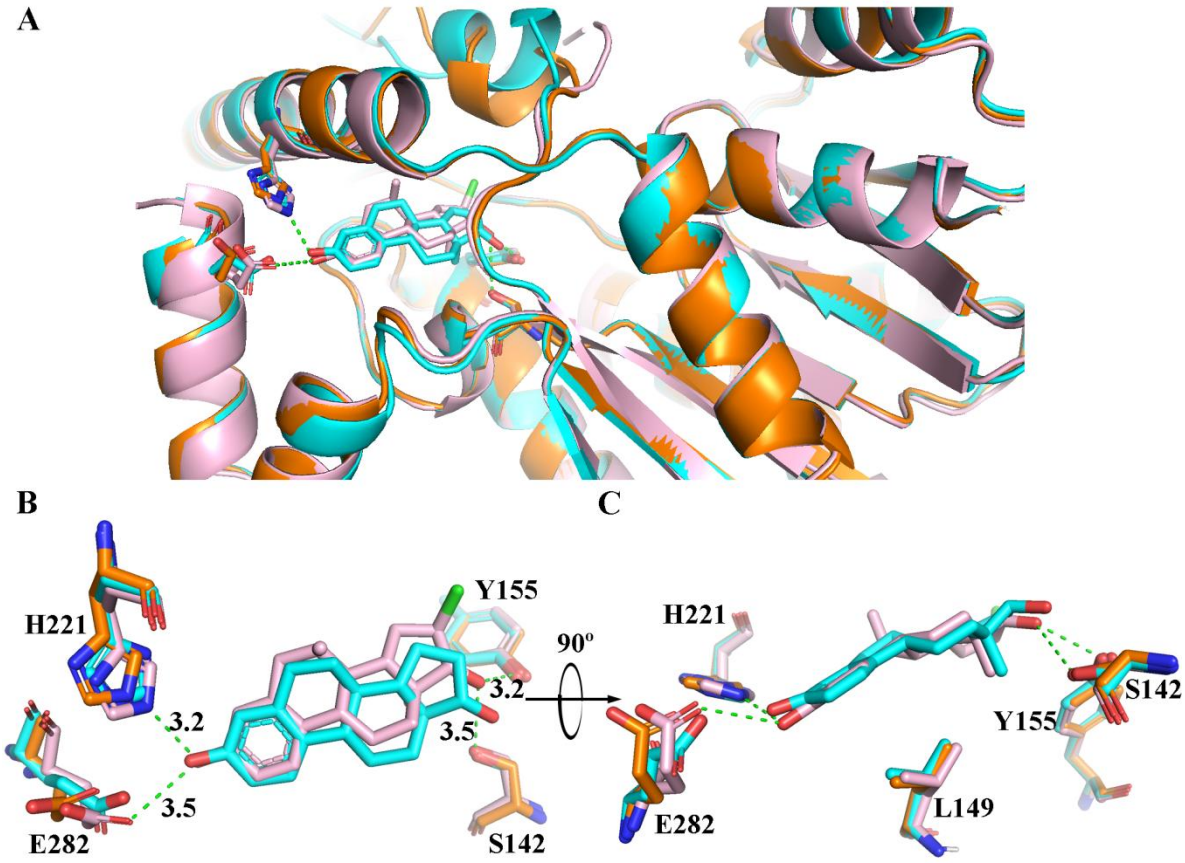

Figure 2.4. Superposition of A subunit of EM-139 (EM9) binary complex (pink) and E2 binary complex (cyan) along with 17β-HSD1 apo structure (orange), showing the steroid ligand binding sites. (a) General view of the active sites within the A subunit of EM-139 and E2 complex structures as well as the apo structure; (b) Top and (c) side view of the steroid binding sites in the superposed structures. Residues Ser^{142}, Leu^{149}, Tyr^{155}, His^{221}, and Glu^{282} are labeled and shown in sticks. Hydrogen bonds between EM-139 and surrounding residues are drawn in green dash lines and labeled. Chloride atom is colored in green.

Tables

Table 2.1. Data collection and refinement statistics

Parameter	17β-HSD1-EM-139
Data Collection	
Space group	I121
Unit cell	
a,b,c (Å)	120.76, 42.19, 122.67
α,β,γ (°)	90, 102.07, 90
Resolution range (Å)	35.67-2.00 (2.11-2.00)[a]
Number of reflections	138222 (20278)
Unique reflections	38108 (5536)
Completeness (%)	92.7 (92.5)
I/σ(I)	8.5 (2.8)
Rmeans[b]	0.086 (0.315)
Multiplicity	3.6 (3.7)
Wilson B-factor (Å^2)	30.5
Refinement	
R-work[c]	0.20
R-free[d]	0.24
r.m.s.d	
Bond lengths (Å)	0.010
Bond angles (°)	1.483
Ramachandran plot[e] (%)	
Most favored regions	94.4
Additional allowed regions	5.6
Generously allowed regions	0.0
Disallowed regions	0.0
Average B, all atoms (Å^2)	42.0
PDB ID	6DTP

[a]. Data statistics for the outer shell are given in parentheses.

[b]. The redundancy-independent R_{merge}/R_{sym}, $R_{means} = \sum_{hkl}\sqrt{\frac{n}{n-1}}\sum_{i=1}^{n}\left|I_{hkl,i} - \langle I_{hkl}\rangle\right| / \sum_{hkl}\sum_{i} I_{hkl,i}$

[c]. $R_{work} = \sum_{hkl}\left||F_{obs}(hkl)| - |F_{calc}(hkl)|\right| / \sum_{hkl}|F_{obs}(hkl)|$

[d]. R_{free} = the cross-validation R factor for 5% of reflections against which the model was not refined.

[e]. Calculated with *PROCHECK.*

Chapitre 3 Crystal structures of human 17β-hydroxysteroid dehydrogenase type 1 complexed with estrone and cofactor reveal the mechanism of substrate inhibition

3.1 Résumé

La 17β-HSD1 catalyse la dernière étape de la bioactivation de l'estradiol, l`œstrogène le plus puissant et est également capable de convertir la dihydrotestostérone en 3β, 17β-androstanediol par le biais de son activité 3β-hydroxystéroïde déshydrogénase. À la différence des autres membres des 17β-HSDs, la 17β-HSD1 subit une inhibition induite par le substrat que nous avons récemment rapportée. Afin d'élucider les bases moléculaires de l'inhibition du substrat, on a résolu les structures cristallines binaires et ternaires de la 17β-HSD1 en complexe avec l'estrone et l'analoque du cofacteur, le NADP+, qui fournissent une image complète des interactions enzyme-substrat-cofacteur. Ces structures complexes ont révélé un mode de liaison inversé de l'œstrone dans la 17β-HSD1 jamais trouvé dans les complexes d'estradiol. Cela conduit à la formation d'un complexe sans issue, similaire au mécanisme d'inhibition du substrat décrit dans la 5β-réductase, l'aldéhyde déshydrogénase et la déhydroépiandrostérone sulfotransférase.

3.2 Abstract

Human type 1 17β-hydroxysteroid dehydrogenase (17β-HSD1) catalyzes the last step in the bioactivation of the most potent estrogen estradiol, and is also able to convert dihydrotestosterone into 3β,17β-androstanediol through its 3β-hydroxysteroid dehydrogenase activity. Unlike in other member of 17β-HSDs, 17β-HSD1 undergoes a substrate induced inhibition that we have recently reported. In order to elucidate the molecular basis of the substrate inhibition, here we solved the binary and ternary crystal structures of 17β-HSD1 in complex with estrone and cofactor analog NADP+ that provide a complete picture of enzyme-substrate-cofactor interactions. These complex structures revealed a reversely orientated binding mode of estrone in 17β-HSD1, never found in estradiol complexes. This leads to the formation of a dead-end complex, similar as the substrate inhibition mechanism described in 5β-reductase, aldehyde dehydrogenase, and dehydroepiandrosterone sulfotransferase. Structural comparison with 17β-HSD1-estradiol/testosterone binary complexes confirmed that residue His^{221} is responsible for the recognizing and stabilizing the reversely bound estrone, leading to the formation of dead-end complex. Thus, the overall catalytic activity of 17β-HSD1 is modulated through its substrate inhibition, indicating a simple mechanism for regulation of enzyme activity in physiological background, which may be used more widely across this family of enzymes.

3.3 Introduction

Estradiol (E2) is well known to play an important role in promoting the genesis and development of estrogen-dependent diseases such as breast cancer, endometrial cancer, endometriosis and ovarian cancer [1-4]. Under normal circumstances E2 is acquired from the circulating plasma. However, for postmenopausal women, ovarian-derived estrogens are withdrawn and replaced by estrogens synthesized in an intracrine manner[5]. The E2 concentration is significantly higher in malignant breast tissues than in plasma levels in postmenopausal women[6]. Human 17β-hydroxysteroid dehydrogenase type 1 (17β-HSD1, EC. 1.1.1.62) catalyzes the conversion of an inactive estrogen, estrone (E1), into the biologically active estrogen, E2, in living cells [7-8]. It is also involved in the reduction of dehydroepiandrosterone (DHEA) into 5-androstene-3β,17β-diol (A-diol), and dihydrotestosterone (DHT) into 5α-androstane-3β,17β-diol (3β-diol) [9-10]. A-diol has been proposed to be the major estrogens present after menopause [11-12], whereas 3β-diol was able to induce estrogen receptor (ER) α activation and proliferation [13]. Therefore, inhibiting the 17β-HSD1 activity is a promising approach for the treatment of estrogen-dependent diseases.

17β-HSD1 is a membrane-associated protein whose first structure was solved in this laboratory [14-15]. It requires the presence of a dinucleotide cofactor ($NADP^+$/NADPH or NAD+/NADH) during the conversion of estrogens. It uses NAD(H) and NADP(H) as cofactors *in vitro*[16]; however, only NADPH was subsequently confirmed to be used by the enzyme as a cofactor during the reduction of E1 in cells and *in vivo* [17]. The cofactor binding site of the enzyme molecule involves βA to βF and forms a typical Rossmann fold, while the substrate binding site involving βD to βG only partially belongs to the Rossmann fold [18-19]. The mechanism for estrogen recognition as well as androgen discrimination by 17β-HSD1 was previously studied using the crystallographic structure of the enzyme in complex with E2, DHT and testosterone (T) [20-21]. The E2 complex showed that the hydrogen bonds and van der Waals interactions were major contributors to the binding energy, indicating that these non-bond interactions help to orientate and stabilize E1 in such a way that the carbonyl group is close to the catalytic triad (Ser142, Tyr155 and Lys159) of the enzyme and undergoes reduction to a 17β-hydroxyl group[20]. The 17β-HSD1-C19-steroid complexes further demonstrated the role of residue Leu[149] in discriminating the binding of C19-steroids to the enzyme [10, 21].

Substrate inhibition has previously been reported in many enzymes, such as 5β-reductase (AKR1D1) [22-23], aldehyde dehydrogenase (ALDH) [24], dehydroepiandrosterone sulfotransferase (SULT2A1) [25], indoleamine 2,3-dioxygenase (IDO) [26], lactate dehydrogenase [27], trimethylamine dehydrogenase [28], etc. Their enzymatic activities can be inhibited by their own substrate, which causes the reaction velocity curve to rise to the maximum as substrate concentration increases and then decreases to zero or to a non-zero asymptote [29]. The substrate inhibition mechanism of an enzyme which has a coenzyme can generally be divided into three major groups: one is the formation of a dead-end complex resulted from the nonproductive binding of the substrate

molecule [22, 24-25]; another is a reversed binding order of substrates which leads to a slowing down of the reaction [26]; the third is a limited dissociation rate of cofactor [27, 30]. Substrate inhibition resulting in a dead-end complex of 17β-HSD1-E1 was first proposed by our group [31], illustrating its important role in enzyme activity regulation in cells [32]. In order to better understand the peculiarities of 17β-HSD1 in terms of substrate binding and stabilization as well as the molecular basis of substrate inhibition, we crystallized this enzyme in complex with E1 and $NADP^+$. The dead-end complex of reversely bound E1 inside the substrate-binding site of the 17β-HSD1 revealed the crucial information on the mechanism by which steroid substrate can influence the activity of this enzyme. Moreover, these complex structures confirmed the role of His^{221} in the substrate inhibition mechanism of the enzyme.

3.4 Materials and Methods

Protein preparation and co-crystallization.

The 17β-HSD1 enzyme was expressed in Sf9 insect cells and purified by a procedure comprising three chromatographic steps: Q-Sepharose anion exchange, Blue-Sepharose affinity, and phenyl-Superose hydrophobic interaction columns, as described by Zhu *et al*[33]. The purified enzyme was then subjected to a buffer change procedure via centricon (Emdmillipore, USA) to saturate the enzyme with E1[34] for binary complex, and NADP+ was added to a final concentration of 1 mM to generate ternary complexes. These binary and ternary complexes were then concentrated to 18~20 mg/ml and used for crystal growth. Crystals were obtained at 27°C using the hanging-drop vapor diffusion method. The 17β-HSD1-E1 binary crystals were grown under conditions containing 26% (w/v) PEG 3350, 150 mM magnesium chloride, 20% glycerol and 100 mM HEPES; while the ternary complex crystals were grown under conditions of 24–29% (w/v) PEG 8K, 100 mM Tris buffer (pH 7.5–7.8) and 50 mM KH_2PO_4.

Data collection and structure determination.

Diffraction data of the 17β-HSD1-E1 binary crystal were collected using an R-AXIS IIc image plate area detector and Rigarku RU300 rotating anode generator at 298 K with a wavelength of 1.5418 Å. The 17β-HSD1-E1-$NADP^+$ ternary crystal diffraction data were collected using synchrotron radiation at Canadian Light Source (CLS) beamline 08B1-1(Saskatoon, Canada) equipped with a RAYONIX MX300HE CCD detector at 100 K using a wavelength of 0.9795 Å. Mineral oil was used as the cryoprotectant for all crystals. The datasets were intergraded using *MOSFLM* [35] and scaled with *SCALA* [36] from the *CCP4* suite [37]. The structures were solved by molecular replacement with *Molrep* [38] using the coordinates of 17β-HSD1, with the highest resolution (PDB ID: 1JTV) [21], as search model. The initial models issued from rigid body refinements were subjected to multiple rounds of refinement using *Refmac* [39] and manual rebuild using *Coot* [40]. After the E1 and $NADP^+$

being added, models were further refined by isotropic B-factor refinement (restrained, individual B-factor refinement) and corrected by manual rebuilding. Missing portions of the models, glycerol, polyethylene glycol, and water molecules were progressively added during the refinement procedure. The final model was verified with *PROCHECK* [41]. Final statistics for all the refined structures are summarized in **Table 3.1**. Molecular graphics were derived using the *Pymol* (version 2.0 Schrödinger, LLC). A plot showing the interaction between $NADP^+$ and surrounding residues was prepared using the *LigPlot+* version 1.4 program [42].

***In silico* studies.**

The manual compound edition was performed using *SeeSAR*[43] software. The pseudo E1 complex was build based on E2 in E2 complex (PDB ID 1IOL[20]). Whereas the new compound designed in light of substrate inhibition mechanism was built from reversely bound E1 in the E1 ternary complex (PDB ID 6BBC). Ten binding poses of steroid ligands were generated with *SeeSAR*, whose geometry were optimized by the Hydrogen bond and Dehydration (HYDE)[44] as implemented in *SeeSAR*, and ranked according to their estimated affinity according to the HYDE affinity assessment.

The docking studies were carried out using *Gold* software[45]. The 3D structure of proteins (6BBC for 17βHSD1 and 1ERE for estrogen receptor α ligand binding domain) were taken from PDB. The ligands for docking studies were prepared in *OpenBabel* (http://openbabel.org/wiki/Main_Page) and the energy minimization was carried out in *Avogadro*[46]. Genetic algorithm *Gold*[47] was used in docking studies and the ChemPLP scoring was used for ranking the binding poses.

3.5 Results

Previously reported substrate inhibition in 5β-reductase, aldehyde dehydrogenase and dehydroepiandrosterone sulfotransferase revealed an alternative binding mode of the substrate, which resulted in the formation of dead-end complex [22, 24-25]. Particularly, a possibility for E1 to adopt an alternative conformation in the binding site was observed in several 17β-HSD1-C-19 steroid complexes [10, 21, 48]. Thus, we have employed molecular docking to investigate the different binding modes of E1 in 17β-HSD1. We manually built the pseudo E1 complex structure from the previous reported E2 complex (PDB ID 1IOL [20]) using the *SeeSAR* [43] software. The top two poses of E1 having similar calculated binding affinities in the Hydrogen bond and Dehydration (HYDE) [44] assessment are presented in **Figure 3.1.** Interestingly, the two poses have very different steroid orientations. The first pose of E1 has a normal oriented conformation with its 17-ketone group close to the catalytic triad. The hydrogen bonds between the 17-ketone group and residues Tyr^{155} and Ser^{142} were maintained (**Figure 3.1A**). The second pose of E1 is almost reversely oriented with the 17-ketone group close to His^{221} whereas the O-3 hydroxyl group facing toward residues Ser^{142} and Cys^{185}, which were stabilized

by the hydrogen bonds between them (**Figure 3.1B**). This *in silico* analysis urged us to engage co-crystallization experiment for 17β-HSD1-E1 to further clarify the mechanism.

Overall Structure and Model Quality

Crystals utilized in this study belonged to the space group $P2_12_12_1$ and contained a dimer per asymmetric unit, similar to previously described ternary complexes with equilin [49]. The 17β-HSD1-E1-$NADP^+$ ternary complex was refined at 1.86 Å, whereas the 17β-HSD1-E1 binary complex was refined at 2.4 Å. The two models show good stereochemistry [50] and the quality of the final models is demonstrated in **Table 3.1**. Similar to the most previously reported 17β-HSD1 complex structures, no clear electron density was present either for the highly flexible βFαG'-loop (amino acids Ala^{191} to Gly^{198}) or for the C-terminal end of the protein (amino acids 286 to 327) [10, 18, 20, 48].

Crystal structure of 17β-HSD1 in complex with E1

In order to understand the interactions between 17β-HSD1 and E1, and also the mechanism of the substrate inhibition, we first solved the crystal structure of 17β-HSD1 in complex with E1. In this binary complex, E1 has a well-defined electron density in the B subunit of the dimer (**Figure 3.2A**), whereas the ligand density in the A subunit is poorly defined. The presence of only a few disconnected density peaks in this region led to the conclusion that the ligand is disordered in this subunit in the crystal. Thus, the ligand was not included in the A subunit. The protein portions of the two subunits are almost identical, with a root mean-square deviation (RMSD) of 0.59 Å for the Cα of 276 amino acids. However, it is worth mentioning that residues Phe^{226} and Phe^{259} in the ligand-binding pocket of the two subunits exhibit significant differences (**Figure 3.3A**). The side chains of residues Phe^{226} and Phe^{259} in B subunit face toward E1, forming a "closed" conformation to favor the van der Waals contacts with the ligand. In contrast, Phe^{226} and Phe^{259} in the A subunit adopt an "opened" conformation with their side chains rotating about 60º and 100º respectively.

Interestingly, we found that E1 is bound in a very different manner to 17β-HSD1 compared with the binding mode previously described for E2 and other steroids [18, 20, 49, 51], but is similar to the mode described for C19-steroid complexes [10, 21, 48]. It is reverse-orientated in the substrate binding site with its A-ring facing toward the catalytic site while its D-ring faces the recognition end (His^{221}, Glu^{282}) of the binding site (**Figure 3.3A**). This is similar to the second pose of E1 in the pseudo E1 complex described above with a roughly 32º rotation around the axis perpendicular to its β-face. Obviously, the reverse-orientated E1 cannot be catalyzed by 17β-HSD1, suggesting that a potential dead-end complex likely accounts for its substrate inhibition. Moreover, the residue Leu^{149}, which is responsible for the reverse binding of C19-steroids [21, 48], is not likely to be involved in the reverse binding of E1 since the closest distance between the Cδ of Leu^{149} and C18 of E1 is more than 4 Å.

However, the presence of NADP(H) may have significant influence on the binding mode of E1 considering that $NADP^+$ can significantly increase the affinity of 17β-HSD1 to E1 with a K_D of 1.6 ± 0.2 μM [52]. Thus we further co-crystallized E1 ternary complex with $NADP^+$, the product of cofactor NADPH, used as an analogue of the cofactor.

Crystal structure of 17β-HSD1 in the presence of $NADP^+$ and E1

The electron density in the substrate binding pocket of 17β-HSD1-E1-$NADP^+$ ternary complex clearly indicates the presence of E1 in both subunit of the dimeric protein (**Figure 3.2B**). However, similar to previously reported 17β-HSD1-A-dione-NADP and 17β-HSD1-4-dione-NADP complex structures [48], only the ADP moiety and the 2'-phosphate group of the adenine ribose can be unambiguously defined for the bound $NADP^+$ molecule (**Figure 3.2C**). The nicotinamide and the attached ribose of the $NADP^+$ molecules are poorly defined in the electron densities in both subunits and thus omitted from the final model. It indicates that the major interactions between $NADP^+$ and the enzyme happen at the ADP part in agreement with previous structure-function study [53]. The overall conformations of ADP moiety and surrounding residues are almost identical in the two subunits of the ternary complex and similar to those in the previously described 17β-HSD1 complexes [19, 48]. The adenine ring adopts an *anti* conformation [18], stabilized through the hydrogen bonds established with Asp^{65} and Val^{66}. The important hydrogen bond interactions between the ribose and pyrophosphate groups and the residues Ser^{11}, Ser^{12}, and Ile^{14} are conserved (**Figure 3.4**). However, it is worth mentioning that noticeable difference exists at the binding of the 2'-phosphate group of $NADP^+$ in the A and B subunits. In the B subunit, the 2'-phosphate of $NADP^+$ is stabilized by a salt bridge formed with side chain of Arg^{37} (**Figure 3.4B**), similar to what was seen in several $NADP^+$ complexes reported previously [19, 48-49, 54]. Despite an identical 2'-phosphate in the A and B subunits, there is no direct interaction between the Arg^{37} and the 2'-phosphate group (**Figure 3.4A**) in subunit A, a phenomenon observed in the complexes of 17β-HSD1 with C19-steroids such as 5α-Androstane-3,17-dione and 4-Androstene-3,17-dione [48].

As for the bound substrate, E1 in both subunits adopts the same reverse binding mode similar as described in the E1 binary complex (**Figure 3.3B**). Although E1 in the A subunit of the ternary complex can be unambiguously defined in the electron density, it shows higher mobility (average B-factor 61.9 $Å^2$) compared to its counterpart (average B-factor 41.2 $Å^2$) in the B subunit. Some residues in the substrate binding site are differently oriented in these two subunits (**Figure 3.3B**). Phe^{226} in the B subunit adopts a "closed" conformation, whereas it has an "opened" conformation in the A subunit, similar to what is seen in the E1 binary complex. As a result, the space around the A-ring of E1 is less compact in the A subunit, and E1 shifts away from Tyr^{155}. Thus, no hydrogen bonds can form with surrounding residues at the O3 end of E1 (**Figure 3.3B**).

17β-HSD1 inhibitor design based on substrate inhibition mechanism

An inhibitor design, in the light of reversible binding of E1, was conducted by manual editing using *SeeSAR* [43]. The complex structures of 17β-HSD1 with inhibitor CC-156 [55], 2-MeO-CC-156 and PBRM [56] have showed a space in the active site which was not occupied by the native substrates and suitable to accommodate an extra benzylamide ring [55]. Thus we added a benzylamide ring moiety at the O-3 of E1 to form a novel compound 3-(((8*R*,9*S*,13*S*,14*S*)-13-methyl-17-oxo-7,8,9,11,12,13,14,15,16,17-decahydro-6*H*-cyclopenta[*a*]phenanthren-3-yl)oxy) benzamide (SX7) (**Figure 3.5**). After structure optimization and poses generation, the pose with the highest estimated binding affinity (43nM) by HYDE is presented below (**Figure 3.6**). As a comparison, the estimated affinity of the best pose of CC-156 in CC-156 ternary complex [55] calculated by HYDE is 31 nM, whereas its IC_{50} obtained by experiments is 44 nM [57]. The added benzylamide ring moiety established a hydrogen bond network with residues Leu^{95} and Gln^{152}, similar to that observed in the CC-156 ternary complex [55]. The energetically favorable edge-to-face π-π interaction [58] between the benzylamide ring of the inhibitor and the phenol ring of Tyr^{155} was also formed with a distance of 4.4 Å, similar to that in the CC-156 binary complex (4.3 Å) but longer than in the CC-156 ternary complex (3.8 Å) [55]. Moreover, a π-donor hydrogen bond contributing to the stabilization of the local 3D structures [59] was also observed between the benzylamide ring of the inhibitor and the OH group of Tyr^{155} with a distance of 3.5 Å. As for the recognition end of the binding site, a hydrogen bond was formed between the inhibitor and His^{221}, similar to that observed in the E1 binary and ternary complexes.

3.6 Discussion

The present work was carried out to investigate the molecular basis of the substrate inhibition observed in 17β-HSD1. We solved the crystal structures of 17β-HSD1 in complex with E1 as well as the ternary complexes with $NADP^+$. Interestingly, E1 in both binary and ternary complexes adopt the same reverse binding mode. This binding orientation is judged to be nonproductive. The reversely oriented E1 acts as a competitive inhibitor and the presence of a phenolic hydroxyl group of E1 at the catalytic triad of the enzyme can be the key for the formation of a non-catalytic dead-end complex. The substrate binding pocket in 17β-HSD1 is narrow and deep (**Figure 3.7**), which is similar to that of dehydroepiandrosterone sulfotransferase [25, 60] but differs from 5β-reductase [22] which has a relatively large steroid binding pocket. Besides, in both the 17β-HSD1-E1 binary and ternary complexes, the bound E1 adopted a reverse orientation. The well-defined electron density for the reversely bound E1 and the resulted B factors after refinement indicate almost no normally bound E1 existed in the crystal structures. This may be due to the relatively high concentration of E1 (>600μM) with multiple cycles of buffer exchange via centricon to saturate the enzyme with E1 used in co-crystallization experiments [34]. Moreover, the K_i (1.3 μM) [31] of E1 to 17β-HSD1 is similar to the apparent K_D (1.6 μM) [52] of the steroid to the enzyme, suggested that the affinity between 17β-HSD1 and normally oriented E1 is lower than that of the

reversely oriented one. The reverse binding mode is relatively energy favourable compared to the normal oriented one in the steroid binding pocket, which is strengthened by the presence of $NADP^+$.

Further superposing E1, E2 [20] and T [21] in the 17β-HSD1 complex crystal structures, varying conformations are observed (**Figure 3.8**). In general, the position observed for E1 is roughly in 180º rotation around the axis perpendicular to its β-face as compared with the position of E2. The orientation of T is similar to that of E1 with an approximate 26º rotation around the axis perpendicular to its β-face and a rotation of 20º around its long axis (O3–O17). At the catalytic end of the substrate binding pocket in 17β-HSD1, the phenolic hydroxyl of E1 establishes a hydrogen bond with the OH group of Tyr^{155} (3.3 Å), similar to the E2 complex structure (**Figure 3.8B**). However, the hydrogen bond between E1 and Tyr^{155} is not presented in the chain A of the E1 ternary complex (**Figure 3.3B**), indicating that this residue does not play a critical role in the binding mode of E1. Meanwhile, at the recognition end of the substrate binding pocket, the 17-carbonyl group of E1 faces toward His^{221}, forming a strong hydrogen bond (2.9 Å) with the side chain of His^{221} (**Figure 3.8**). As for the nearby Glu^{282} residue, it does not form hydrogen bond with E1, indicating that it does not significantly contribute to the binding of the reversely oriented steroid. In contrast, the residues His^{221} and Glu^{282} are both involved in hydrogen bond formation with the O17 of T and O3 of E2 in their complexes (**Figure 3.8**). Furthermore, the mutation of His^{221} indeed diminished the substrate inhibition of 17β-HSD1 in intact cells [53]. Thus it further substantiates that the His^{221} is a key residue, responsible for the substrate inhibition of 17β-HSD1 through its binding to the reversely oriented E1 and the formation of a dead-end complex.

Moreover, the residue at position 36 plays an essential role in the discrimination of cofactor NADP(H)/NAD(H) in the SDR family [53]. A negatively charged residue at this position will serve to repel the 2'-phosphate of NADP(H) and accept hydrogen bonds from the 2' and 3' ribose hydroxyls [61], typically found in NAD(H)-preferring enzyme. Mutagenesis study demonstrated that the sole mutation of the Leu^{36} into aspartic acid residue indeed changed the cofactor preference of 17β-HSD1 from NADP(H) to NAD(H) [53], and eliminated the substrate inhibition of the enzyme in the presence of NADPH[31]. Although the (phosphor-)adenosine moiety of NADP is distal from the catalytic site of the enzyme, subtle perturbations to the (phosphor-) adenosine binding pocket was proved to have a dramatic effect on activity [62] and mutations at the 2'-phosphate binding site was demonstrated to affect substrate specificity [63]. Thus the stabilization of the 2'-phosphate group of NADPH is essential for maintaining the substrate inhibition in 17β-HSD1.

3.7 Conclusion

Taking together, the stabilization of the reversely oriented E1 requires the presence of His^{221} at the recognition end of the substrate binding site, and the mutation of His^{221} is sufficient to destabilize the reversely bound E1, and prevent the formation of a dead-end complex. Meanwhile, the presence of $NADP^+$ may strengthen the

reverse binding mode of E1. Besides, this mechanism may play a protective role under physiological background by limiting the E2 levels upon an increase in intracellular E1 levels. Moreover, 17β-HSD1 is primarily expressed in the placenta and ovarian granulose cells [64], and the physiological E1 level in human placenta was measured to reach 1.5 μM [65], while the threshold concentrations required to exhibit substrate inhibition in both molecular level (0.2 μM) [31] and cell level (0.65 μM) [32]. Therefore, it is likely that the substrate inhibition of 17β-HSD1 takes place in living cells. Furthermore, based on this dead-end complex, we employed the *in silico* method to design 17β-HSD1 inhibitor, yielding a novel compound with a high estimated binding affinity. This substrate inhibition mechanism described in 17β-HSD1 may widely exist in NADP(H)-preferred enzymes for regulation of their enzymatic activity. These results will contribute to advance the knowledge of enzyme inhibition and encourage the development of inhibitors for clinical purposes.

Notes

The authors declare no competing financial interests.

The PDB ID of 17β-HSD1-E1 and 17β-HSD1-E1-$NADP^+$ are 6MNC and 6MNE, respectively.

Acknowledgements

We thank Dr. D. W. Zhu and Dre. M. Zhou for their technical support in enzyme purification. We would also like to thank Dr. Muriel Steel for her editing of the manuscript. We acknowledge the use of beamline 08B1-1 at the Canadian Light Source, Brookhaven National Laboratory.

3.8 Reference

1. Lippman, M. E.; Dickson, R. B.; Bates, S.; Knabbe, C.; Huff, K.; Swain, S.; McManaway, M.; Bronzert, D.; Kasid, A.; Gelmann, E. P., Autocrine and paracrine growth regulation of human breast cancer. *Breast Cancer Research and Treatment* **1986,** *7* (2), 59-70.

2. Rizner, T. L., Estrogen biosynthesis, phase I and phase II metabolism, and action in endometrial cancer. *Mol Cell Endocrinol* **2013,** *381* (1-2), 124-39.

3. Šmuc, T.; Pucelj, M. R.; Šinkovec, J.; Husen, B.; Thole, H.; Rižner, T. L., Expression analysis of the genes involved in estradiol and progesterone action in human ovarian endometriosis. *Gynecological Endocrinology* **2009,** *23* (2), 105-111.

4. Ho, S. M., Estrogen, Progesterone and Epithelial Ovarian Cancer. *Reprod Biol Endocrinol* **2003,** *1*, 73.

5. Labrie, F., All sex steroids are made intracellularly in peripheral tissues by the mechanisms of intracrinology after menopause. *J Steroid Biochem Mol Biol* **2015,** *145*, 133-8.

6. Jefcoate, C. R.; Liehr, J. G.; Santen, R. J.; Sutter, T. R.; Yager, J. D.; Yue, W.; Santner, S. J.; Tekmal, R.; Demers, L.; Pauley, R.; Naftolin, F.; Mor, G.; Berstein, L., Tissue-specific synthesis and oxidative metabolism of estrogens. *J Natl Cancer Inst Monogr* **2000,** *2000* (27), 95-112.

7. Luu-The, V.; Labrie, C.; Zhao, H. F.; Couët, J.; Lachance, Y.; Simard, J.; Leblanc, G.; Côté, J.; Bérubé, D.; Gagné, R., Characterization of cDNAs for human estradiol 17 beta-dehydrogenase and assignment of the gene to chromosome 17: evidence of two mRNA species with distinct 5'-termini in human placenta. *Mol Endocrinol* **1989,** *3* (8), 1301-9.

8. Dumont, M.; Luu-The, V.; de Launoit, Y.; Labrie, F., Expression of human 17β-hydroxysteroid dehydrogenase in mammalian cells. *The Journal of Steroid Biochemistry and Molecular Biology* **1992,** *41*, 605-608.

9. Lin, S. X.; Chen, J.; Mazumdar, M.; Poirier, D.; Wang, C.; Azzi, A.; Zhou, M., Molecular Therapy of Breast Cancer: Progress and Future Directions. *Nat. Rev. Endocrinol.* **2010,** *6* (9), 485-493.

10. Aka, J. A.; Mazumdar, M.; Chen, C. Q.; Poirier, D.; Lin, S. X., 17beta-Hydroxysteroid Dehydrogenase Type 1 Stimulates Breast Cancer by Dihydrotestosterone Inactivation in Addition to Estradiol Production. *Mol. Endocrinol.* **2010,** *24* (4), 832-845.

11. Simard, J.; Vincent, A.; Duchesne, R.; Labrie, F., Full Oestrogenic Activity of C19-Δ5 Adrenal Steroids in Rat Pituitary Lactotrophs and Somatotrophs. *Mol. Cell Endocrinol.* **1988,** *55*, 233-242.

12. Trottier, A.; Maltais, R.; Ayan, D.; Barbeau, X.; Roy, J.; Perreault, M.; Poulin, R.; Lague, P.; Poirier, D., Insight into the Mode of Action and Selectivity of PBRM, a Covalent Steroidal Inhibitor of 17beta-Hydroxysteroid Dehydrogenase Type 1. *Biochem. Pharmacol.* **2017,** *144*, 149-161.

13. Hanamura, T.; Niwa, T.; Gohno, T.; Kurosumi, M.; Takei, H.; Yamaguchi, Y.; Ito, K.; Hayashi, S., Possible Role of the Aromatase-Independent Steroid Metabolism Pathways in Hormone Responsive Primary Breast Cancers. *Breast Cancer Res. Treat.* **2014,** *143* (1), 69-80.

14. Ghosh, D.; Pletnev, V. Z.; Zhu, D. W.; Wawrzak, Z.; Duax, W. L.; Pangborn, W.; Labrie, F.; Lin, S. X., Structure of human estrogenic 17 beta-hydroxysteroid dehydrogenase at 2.20 A resolution. *Structure* **1995,** *3* (5), 503-13.

15. Lin, S. X.; Yang, F.; Jin, J. Z.; Breton, R.; Zhu, D. W.; Luu-The, V.; Labrie, F., Subunit Identity of the Dimeric 17β-Hydroxysteroid Dehydrogenase from Human Placenta. *J. Biol. Chem.* **1992,** *267*, 16182-16187.

16. Blomquist, C. H.; Lindemann, N. J.; Hakanson, E. Y., Steroid Modulation of 17β-Hydroxysteroid Oxidoreductase Activities in Human Placental Villi in Vitro. *The Journal of Clinical Endocrinology & Metabolism* **1987,** *65*, 647-652.

17. Luu-The, V.; Zhang, Y.; Poirier, D.; Labrie, F., Characteristics of human types 1, 2 and 3 17β-hydroxysteroid dehydrogenase activities: Oxidation/reduction and inhibition. *Journal of Steroid Biochemistry and Molecular Biology* **1995,** *55*, 581-587.

18. Breton, R.; Housset, D.; Mazza, C.; Fontecilla-Camps, J. C., The Structure of a Complex of Human 17β-Hydroxysteroid Dehydrogenase with Estradiol and NADP+ Identifies Two Principal Targets for the Design of Inhibitors. *Structure* **1996,** *4*, 905-915.

19. Mazza, C.; Breton, R.; Housset, D.; Fontecilla-Camps, J. C., Unusual charge stabilization of NADP+ in 17beta-hydroxysteroid dehydrogenase. *Journal of Biological Chemistry* **1998,** *273* (14), 8145-52.

20. Azzi, A.; Rehse, P. H.; Zhu, D. W.; Campbell, R. L.; Labrie, F.; Lin, S. X., Crystal Structure of Human Estrogenic 17β-Hydroxysteroid Dehydrogenase Complexed with 17β-Estradiol. *Nat. Struct. Biol.* **1996,** *3*, 665-668.

21. Gangloff, A.; Shi, R.; Nahoum, V.; Lin, S. X., Pseudo-Symmetry of C19 Steroids, Alternative Binding Orientations, and Multispecificity in Human Estrogenic 17beta-Hydroxysteroid Dehydrogenase. *FASEB J.* **2003,** *17* (2), 274-276.

22. Di Costanzo, L.; Drury, J. E.; Penning, T. M.; Christianson, D. W., Crystal Structure of Human Liver Δ4-3-Ketosteroid 5β-Reductase (AKR1D1) and Implications for Substrate Binding and Catalysis. *Journal of Biological Chemistry* **2008,** *283* (24), 16830-16839.

23. Faucher, F.; Cantin, L.; Luu-The, V.; Labrie, F.; Breton, R., Crystal Structures of Human Δ4-3-Ketosteroid 5β-Reductase (AKR1D1) Reveal the Presence of an Alternative Binding Site Responsible for Substrate Inhibition. *Biochemistry* **2008,** *47* (51), 13537–13546.

24. Chen, C.; Joo, J. C.; Brown, G.; Stolnikova, E.; Halavaty, A. S.; Savchenko, A.; Anderson, W. F.; Yakunin, A. F., Structure-based mutational studies of substrate inhibition of betaine aldehyde dehydrogenase BetB from Staphylococcus aureus. *Appl Environ Microbiol* **2014,** *80* (13), 3992-4002.

25. Lu, L. Y.; Hsieh, Y. C.; Liu, M. Y.; Lin, Y. H.; Chen, C. J.; Yang, Y. S., Identification and characterization of two amino acids critical for the substrate inhibition of human dehydroepiandrosterone sulfotransferase (SULT2A1). *Mol Pharmacol* **2008,** *73* (3), 660-8.

26. Efimov, I.; Basran, J.; Sun, X.; Chauhan, N.; Chapman, S. K.; Mowat, C. G.; Raven, E. L., The mechanism of substrate inhibition in human indoleamine 2,3-dioxygenase. *J Am Chem Soc* **2012,** *134* (6), 3034-41.

27. Eszes, C. M.; Sessions, R. B.; Clarke, A. R.; Moreton, K. M.; Holbrook, J. J., Removal of substrate inhibition in a lactate dehydrogenase from human muscle by a single residue change. *FEBS Lett* **1996,** *399* (3), 193-197.

28. Roberts, P.; Basran, J.; Wilson, E. K.; Hille, R.; Scrutton, N. S., Redox Cycles in Trimethylamine Dehydrogenase and Mechanism of Substrate Inhibition. *Biochemistry* **1999,** *38* (45), 14927-40.

29. Reed, M. C.; Lieb, A.; Nijhout, H. F., The biological significance of substrate inhibition: a mechanism with diverse functions. *Bioessays* **2010,** *32* (5), 422-9.

30. Fujioka, M., Saccharopine dehydrogenase. Substrate inhibition studies. *J Biol Chem* **1975,** *250* (23), 8986-9.

31. Gangloff, A.; Garneau, A.; Huang, Y. W.; Yang, F.; Lin, S. X., Human oestrogenic 17β-hydroxysteroid dehydrogenase specificity: Enzyme regulation through an NADPH-dependent substrate inhibition towards the highly specific oestrone reduction. *Biochem J* **2001,** *356*, 269-276.

32. Han, H.; Thériault, J. F.; Chen, G.; Lin, S. X., Substrate Inhibition of 17beta-HSD1 in living cells and regulation of 17beta-HSD7 by 17beta-HSD1 knockdown. *J Steroid Biochem Mol Biol* **2017,** *S0960-0760* (17), 10.1016/j.jsbmb.2017.05.011.

33. Zhu, D. W.; Lee, X.; Labrie, F.; Lin, S. X., Crystal Growth of Human Estrogenic 17β-Hydroxysteroid Dehydrogenase. *Acta Crystallogr. D Biol. Crystallogr.* **1994,** *50* (4), 550-555.

34. Zhu, D. W.; Azzi, A.; Rehse, P.; Lin, S. X., The Crystallogenesis of a Human Estradiol Dehydrogenase-Substrate Complex. *J. Cryst. Growth* **1996,** *168*, 275-279.

35. Leslie, A. G. W.; Powell, H. R., *Processing Diffraction Data with Mosflm*. Springer Netherlands: 2007.

36. Evans, P., Scaling and Assessment of Data Quality. *Acta Crystallogr. D Biol. Crystallogr.* **2006,** *62* (Pt 1), 72-82.

37. Winn, M. D.; Ballard, C. C.; Cowtan, K. D.; Dodson, E. J.; Emsley, P.; Evans, P. R.; Keegan, R. M.; Krissinel, E. B.; Leslie, A. G.; McCoy, A.; McNicholas, S. J.; Murshudov, G. N.; Pannu, N. S.; Potterton, E. A.; Powell, H. R.; Read, R. J.; Vagin, A.; Wilson, K. S., Overview of the CCP4 Suite and Current Developments. *Acta Crystallogr. D Biol. Crystallogr.* **2011,** *67* (Pt 4), 235-242.

38. Vagin, A.; Teplyakov, A., Molecular Replacement with MOLREP. *Acta Crystallogr. D Biol. Crystallogr.* **2010,** *66* (Pt 1), 22-25.

39. Murshudov, G. N.; Vagin, A. A.; Lebedev, A.; Wilson, K. S.; Dodson, E. J., Efficient anisotropic refinement of macromolecular structures using FFT. *Acta Crystallogr D Biol Crystallogr* **1999,** *55*, 247-55.

40. Emsley, P.; Lohkamp, B.; Scott, W. G.; Cowtan, K., Features and Development of Coot. *Acta Crystallogr. D Biol. Crystallogr.* **2010,** *66* (Pt 4), 486-501.

41. Laskowski, R. A.; MacArthur, M. W.; Moss, D. S.; Thornton, J. M., PROCHECK: A Program to Check the Stereochemical Quality of Protein Structures. *J. Appl. Crystallogr.* **1993,** *26* (2), 283-291.

42. Laskowski, R. A.; Swindells, M. B., LigPlot+: multiple ligand-protein interaction diagrams for drug discovery. *J Chem Inf Model* **2011,** *51* (10), 2778-86.

43. *SeeSAR version 7.3; BioSolveIT GmbH, Sankt Augustin, Germany, 2018*.

44. Schneider, N.; Lange, G.; Hindle, S.; Klein, R.; Rarey, M., A Consistent Description of Hydrogen Bond and Dehydration Energies in Protein-Ligand Complexes: Methods Behind the HYDE Scoring Function. *J. Comput. Aided. Mol. Des.* **2013,** *27* (1), 15-29.

45. Cole, J.; Willem, M.; Nissink, J.; Taylor, R., Protein-Ligand Docking and Virtual Screening with GOLD. In *Virtual Screening in Drug Discovery*, Alvarez, J.; Shoichet, B., Eds. CRC Press: 2005.

46. Hanwell, M. D.; Curtis, D. E.; Lonie, D. C.; Vandermeersch, T.; Zurek, E.; Hutchison, G. R., Avogadro: an advanced semantic chemical editor, visualization, and analysis platform. *J Cheminform* **2012,** *4* (1), 17.

47. Hartshorn, M. J.; Verdonk, M. L.; Chessari, G.; Brewerton, S. C.; Mooij, W. T. M.; Mortenson, P. N.; Murray, C. W., Diverse, High-Quality Test Set for the Validation of Protein−Ligand Docking Performance. *J Med Chem* **2007,** *50* (4), 726-741.

48. Shi, R.; Lin, S. X., Cofactor Hydrogen Bonding onto the Protein Main Chain is Conserved in the Short Chain Dehydrogenase/Reductase Family and Contributes to Nicotinamide Orientation. *J. Biol. Chem.* **2004,** *279* (16), 16778-16785.

49. Sawicki, M. W.; Erman, M.; Puranen, T.; Vihko, P.; Ghosh, D., Structure of the Ternary Complex of Human 17beta-Hydroxysteroid Dehydrogenase Type 1 with 3-hydroxyestra-1,3,5,7-tetraen-17-one (Equilin) and NADP+. *Proc. Natl. Acad. Sci. USA* **1999,** *96* (3), 840-845.

50. Kleywegt, G. J.; Jones, T. A., Phi/Psi-Chology: Ramachandran Revisited. *Structure* **1996,** *4* (12), 1395-1400.

51. Han, Q.; Campbell, R. L.; Gangloff, A.; Huang, Y. W.; Lin, S. X., Dehydroepiandrosterone and Dihydrotestosterone Recognition by Human Estrogenic 17β-Hydroxysteroid Dehydrogenase. *J. Biol. Chem.* **2000,** *275*, 1105-1111.

52. Jin, J. Z.; Lin, S. X., Human estrogenic 17beta-hydroxysteroid dehydrogenase: predominance of estrone reduction and its induction by NADPH. *Biochem Biophys Res Commun* **1999,** *259* (2), 489-93.

53. Huang, Y. W.; Pineau, I.; Chang, H. J.; Azzi, A.; Bellemare, V.; Laberge, S.; Lin, S. X., Critical Residues for the Specificity of Cofactors and Substrates in Human Estrogenic 17β-Hydroxysteroid Dehydrogenase 1: Variants Designed from the Three-Dimensional Structure of the Enzyme. *Mol. Endocrinol.* **2001,** *15* (11), 2010-2020.

54. Mazza, C. Human Type I 17Beta-Hydroxysteroid Dehydrogenase: Site Directed Mutagenesis and X-Ray Crystallography Structure-Function Analysis. Universite Joseph Fourier, 1997.

55. Mazumdar, M.; Fournier, D.; Zhu, D. W.; Cadot, C.; Poirier, D.; Lin, S. X., Binary and Ternary Crystal Structure Analyses of a Novel Inhibitor with 17beta-HSD type 1: A Lead Compound for Breast Cancer Therapy. *Biochem. J.* **2009,** *424* (3), 357-366.

56. Li, T.; Maltais, R.; Poirier, D.; Lin, S. X., Combined Biophysical Chemistry Reveals a New Covalent Inhibitor with a Low-Reactivity Alkyl Halide. *J Phys Chem Lett* **2018**, 5275-5280.

57. Laplante, Y.; Cadot, C.; Fournier, M. A.; Poirier, D., Estradiol and estrone C-16 derivatives as inhibitors of type 1 17beta-hydroxysteroid dehydrogenase: blocking of ER+ breast cancer cell proliferation induced by estrone. *Bioorganic & medicinal chemistry* **2008,** *16* (4), 1849-60.

58. Hunter, C. A.; Singh, J.; Thornton, J. M., Pi-pi interactions: the geometry and energetics of phenylalanine-phenylalanine interactions in proteins. *J Mol Biol* **1991,** *218* (4), 837-46.

59. Steiner, T.; Koellner, G., Hydrogen bonds with pi-acceptors in proteins: frequencies and role in stabilizing local 3D structures. *J Mol Biol* **2001,** *305* (3), 535-57.

60. Rehse, P. H.; Zhou, M.; Lin, S. X., Crystal structure of human dehydroepiandrosterone sulphotransferase in complex with substrate. *Biochem. J.* **2002,** *364*, 165-171.

61. Cahn, J. K.; Werlang, C. A.; Baumschlager, A.; Brinkmann-Chen, S.; Mayo, S. L.; Arnold, F. H., A General Tool for Engineering the NAD/NADP Cofactor Preference of Oxidoreductases. *ACS Synth Biol* **2017,** *6* (2), 326-333.

62. Mesecar, A. D., Orbital Steering in the Catalytic Power of Enzymes: Small Structural Changes with Large Catalytic Consequences. *Science* **1997,** *277* (5323), 202-206.

63. Maddock, D. J.; Patrick, W. M.; Gerth, M. L., Substitutions at the cofactor phosphate-binding site of a clostridial alcohol dehydrogenase lead to unexpected changes in substrate specificity. *Protein Eng Des Sel* **2015,** *28* (8), 251-8.

64. He, W.; Gauri, M.; Li, T.; Wang, R.; Lin, S. X., Current knowledge of the multifunctional 17beta-hydroxysteroid dehydrogenase type 1 (HSD17B1). *Gene* **2016,** *588* (1), 54-61.

65. Ferre, F.; Breuiller, M.; Tanguy, G.; Janssens, Y.; Cedard, L., Steroid concentrations and delta 5, 3 beta-hydroxysteroid dehydrogenase activity in human placenta. Comparison between elective cesarean section and spontaneous vaginal delivery. *Am J Obstet Gynecol* **1980,** *138* (5), 500-3.

Figures and Legends

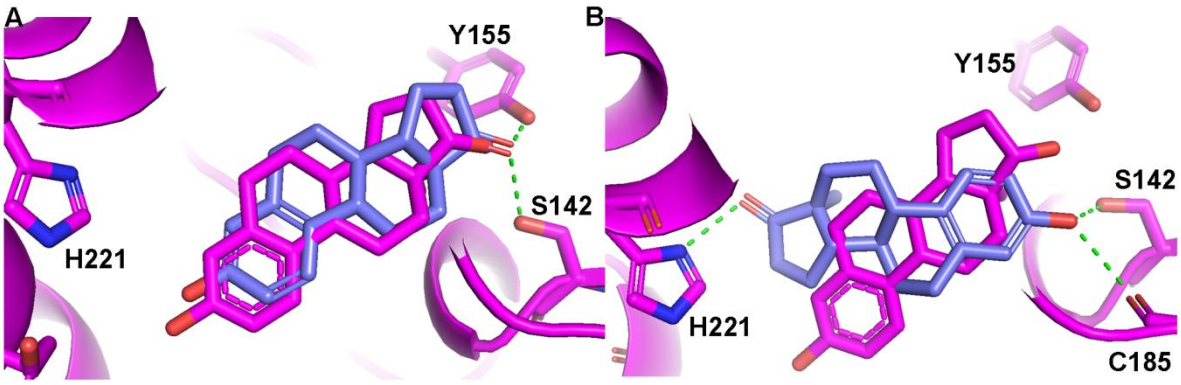

Figure 3.1. Results from the *in silico* building of E1 at the binding site of 17β-HSD1. The normal (A) and reverse (B) binding poses of E1, derived in *SeeSAR* analysis are shown as sticks and colored in blue. The binding site conformation of E2 complex structure (PDB ID IIOL) is represented (magenta). Residues Tyr^{155}, Ser^{142}, Cys^{185} and His^{221} are labeled and shown in sticks. Hydrogen bonds between E1 and surrounding residues are drawn in green dash lines.

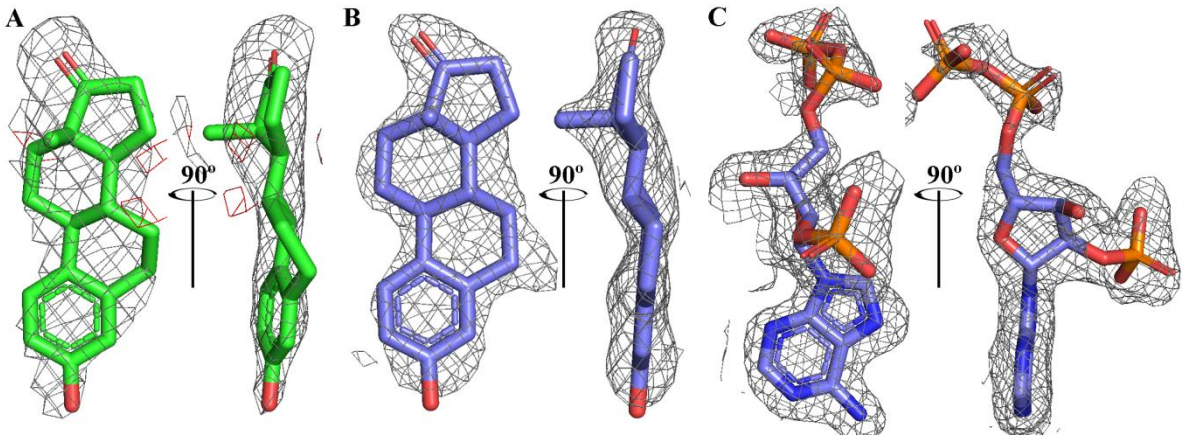

Figure 3.2. Front and side views of the electron density in E1 and NADP+ of the B subunit of E1 binary (A, green) and ternary (B and C, blue) complexes. E1 and the ADP moiety of NADP+ are shown in the omit *Fo-Fc* electron density contoured at 2.5σ level. The positive and negative densities are drawn in gray and red, respectively.

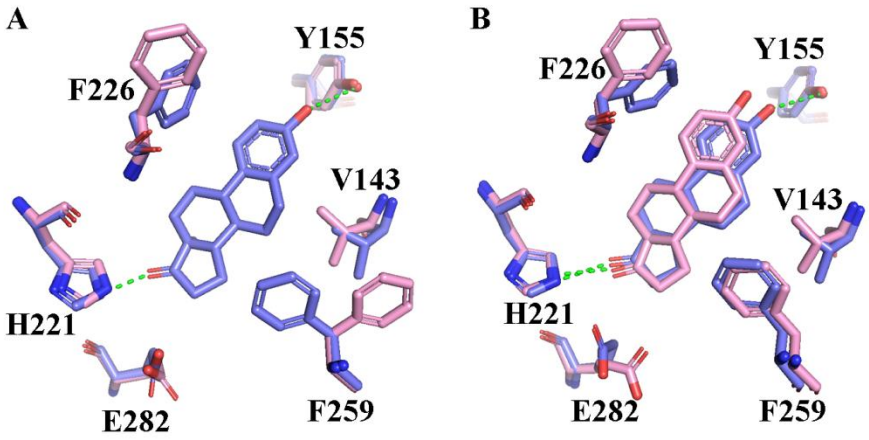

Figure 3.3. Superimposition of the steroid binding site in chain-A (pink) and chain-B (blue) in 17β-HSD1-E1 (A) and 17β-HSD1-E1-NADP+ (B) complexes. Residues Val^{143}, Tyr^{155}, His^{221}, Phe^{226}, Phe^{259}, and Glu^{282} are labeled and shown in sticks. Hydrogen bonds between E1 and surrounding residues are drawn in green dash lines.

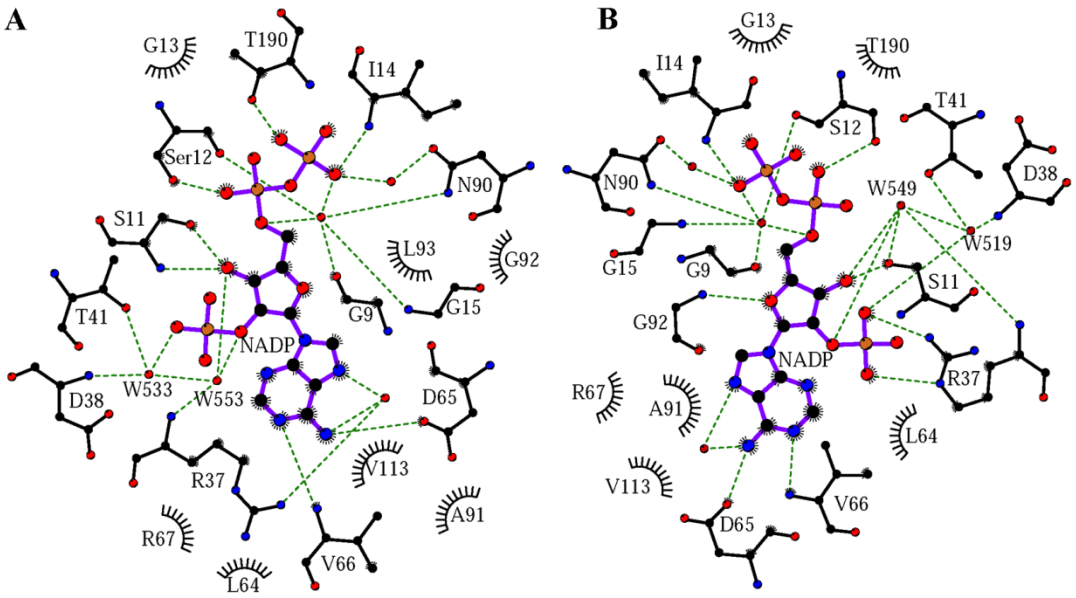

Figure 3.4. Plot of interactions between NADP+ and surrounding residues in A (A) and B (B) subunit. The 2'-phosphate of NADP in A subunit is stabilized through water (W533) bridged hydrogen bond with residues Thr[41] and Asp[38], whereas that in B subunit is stabilized by salt bridge with Arg[37] and water bridged hydrogen bond with residues Thr[41] and Asp[38]. The NADP+ and protein side chains are shown in ball-and-stick representation, with the NADP+ bonds colored in purple. Hydrogen bonds are shown as green dotted lines, while the spoked arcs represent protein residues making nonbonded contacts with the NADP+. Figure is prepared using the *LigPlot+* version 1.4 program.

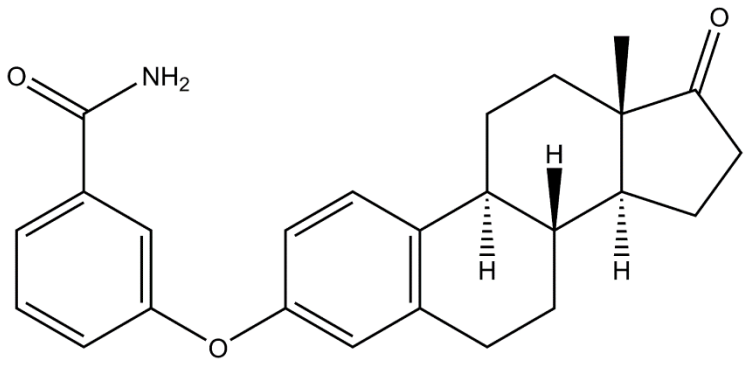

3-(((8*R*,9*S*,13*S*,14*S*)-13-methyl-17-oxo-7,8,9,11,12,13,14,15,16,17-decahydro-6*H*-cyclopenta[*a*]phenanthren-3-yl)oxy)benzamide

Figure 3.5. The 2D structure of modeled 17β-HSD1 inhibitor 3-(((8*R*,9*S*,13*S*,14*S*)-13-methyl-17-oxo-7,8,9,11,12,13,14,15,16,17-decahydro-6*H*-cyclopenta[*a*]phenanthren-3-yl)oxy)benzamide (SX7).

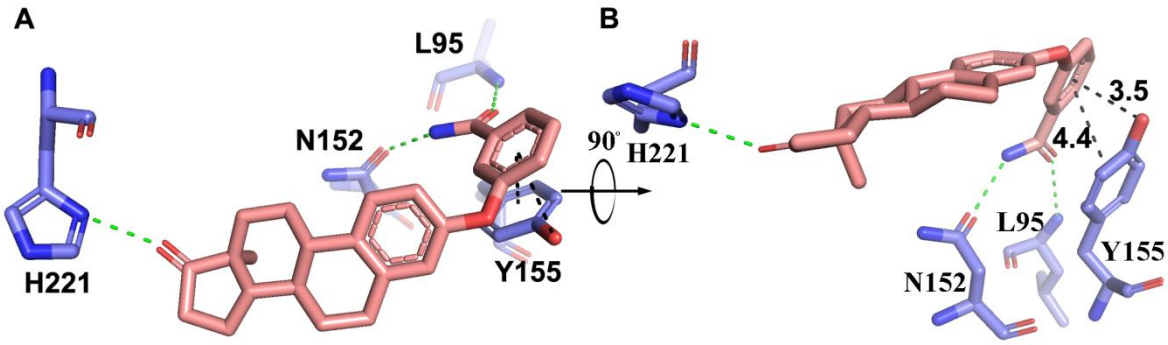

Figure 3.6. Top (A) and side (B) view of binding residues (blue sticks) and the best pose of the SX7 (pink stick) in 17β-HSD1. Hydrogen bonds between inhibitor and surrounding residues are drawn in green dash lines. Several important distances are labeled and shown in black dash line.

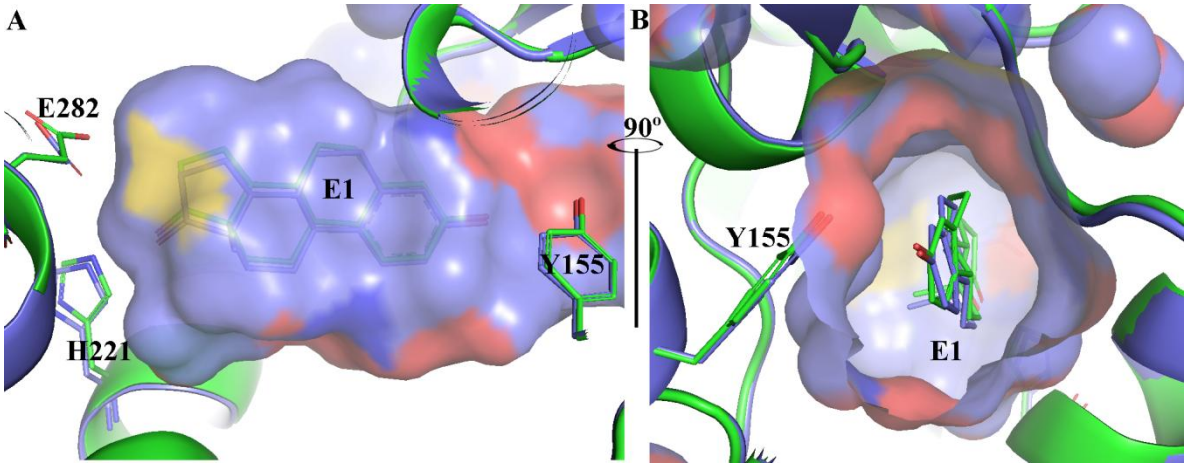

Figure 3.7. Surface representation of the substrate binding pocket of 17β-HSD1. The chain B of E1 binary (green) and ternary (blue) complexes are superimposed and shown in cartoon. The surface of the steroid binding pocket in E1 ternary complex is presented in side view (A) and top view (B) and colored by elements. Residues Tyr^{155}, His^{221}, and Glu^{282} are labeled and shown in sticks.

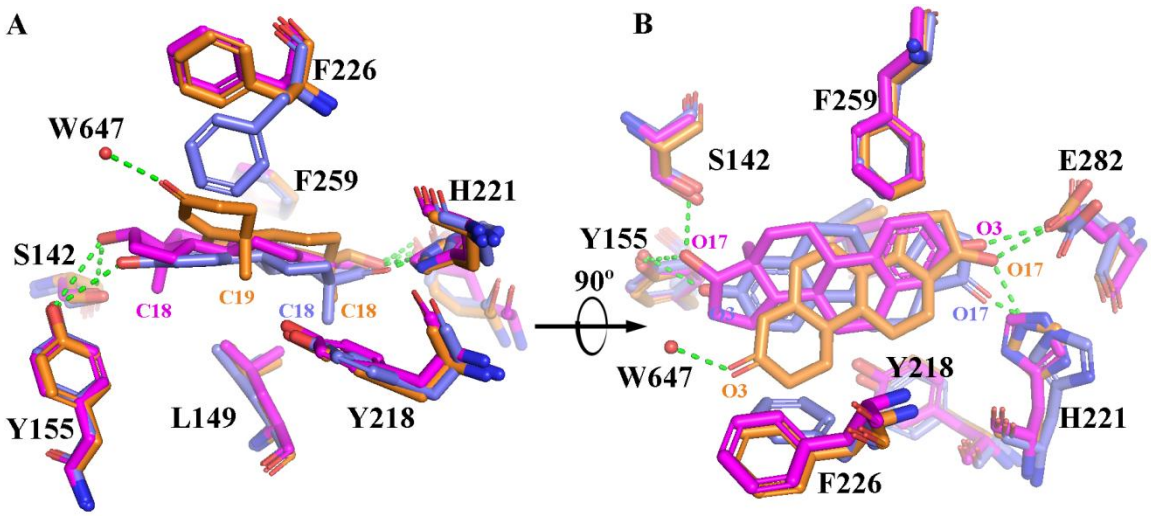

Figure 3.8. Superimposition of estrone, estradiol and testosterone binding in 17β-HSD1. Side view (A) and top view (B) of the active site residues of the 17β-HSD1-E2 (magenta, PDB ID 1IOL), 17β-HSD1-T (orange, PDB ID 1JTV), and the B subunit of 17β-HSD1-E1-NADP+ (blue) complexes. The steroid molecules are colored the same as their binding residues. Hydrogen bonding interactions between steroid molecules and the enzyme residues are represented by green dash lines. Water molecule (W647 from 17β-HSD1-T) is shown as red spheres.

Tables

Table 3.1. Data collection and refinement statistics

Parameter	17β-HSD1-E1	17β-HSD1-E1-NADP+
Data Collection		
Space group	$P2_12_12_1$	$P2_12_12_1$
Unit cell		
a,b,c (Å)	43.56, 110.02, 117.14	43.78, 108.24, 117.67
α,β,γ (°)	90, 90, 90	90, 90, 90
Resolution range (Å)	50-2.4 (2.53-2.4)[a]	50-1.86 (1.96-1.86)
Number of reflections	77771 (9146)	353641 (51177)
Unique reflections	21966 (2955)	47986 (6911)
Completeness (%)	96.6 (91.7)	100.0 (100.0)
I/σ(I)	12.2 (2.3)	13.7 (4.5)
R_{means}[b]	0.065 (0.543)	0.091 (0.516)
Multiplicity	3.5 (3.1)	7.4 (7.4)
Wilson B-factor (Å^2)	50.0	25.5
Refinement		
R-work[c]	0.21	0.19
R-free[d]	0.28	0.23
r.m.s.d		
Bond lengths (Å)	0.013	0.012
Bond angles (°)	1.676	1.722
Ramachandran plot[e] (%)		
Most favored regions	91.8	96.7
Additional allowed regions	7.6	3.3
Generously allowed regions	0.4	0.0
Disallowed regions	0.2	0.0
Average B, all atoms (Å^2)	57.0	31.0
PDB ID	6MNC	6MNE

[a] Data statistics for the outer shell are given in parentheses.

[b] The redundancy-independent R_{merge}/R_{sym}, $R_{means} = \sum_{hkl}\sqrt{\frac{n}{n-1}}\sum_{i=1}^{n}\left|I_{hkl,i} - \langle I_{hkl}\rangle\right| / \sum_{hkl}\sum_i I_{hkl,i}$

[c] $R_{work} = \sum_{hkl}\left||F_{obs}(hkl)| - |F_{calc}(hkl)|\right| / \sum_{hkl}|F_{obs}(hkl)|$

[d] R_{free} = the cross-validation *R* factor for 5% of reflections against which the model was not refined.

[e] Calculated with *PROCHECK*.

Chapitre 4 Remarkable steroid-converting enzyme and receptor regulations in large number breast tumor samples : molecular correlation and combined therapies

4.1 Résumé

La thérapie endocrinienne est une pierre angulaire contre le cancer du sein hormono-dépendant (BC), représenté par les inhibiteurs de l'aromatase (IA). Récemment, l'accumulation d'œstradiol dans les articulations et la dégradation de la dihydrotestostérone stimulant la croissance du BC ont été démontrées par la 17beta-hydroxystéroïde déshydrogénase réductrice dans des études *in vitro* et *in vivo*, indiquant une voie indépendante de la synthèse des œstrogènes. Dans la présente étude, la base de données de séquençage de l'ARN de la cohorte The Cancer Genome Atlas Breast Invasive Carcinoma (*N*=1079) a été extraite, qui comprenait les tissus mammaires normaux post-ménopauses (*N*=56) et les récepteurs mammaires. Les expressions différentielles et la corrélation de l'expression génique ont été analysées par le test *U* de Mann-Whitney et le test rho de Spearman. Nos résultats appuient une nouvelle thérapie ciblant la 17β-HSD7 réductrice et la thérapie combinée ciblant la 11β-HSD2 et la 17β-HSD7.

4.2 Abstract

Endocrine therapy is a cornerstone against hormone-dependent breast-cancer (BC), represented by aromatase inhibitors (AIs). Despite the effectiveness of AI-treatment, resistance often occurs. Recently, the joint estradiol accumulation and dihydrotestosterone degradation stimulating BC growth has been demonstrated by reductive 17beta-hydroxysteroid dehydrogenases in vitro and in vivo, indicating an aromatase-independent pathway for estrogen-synthesis. A systematic study of the expression and correlation of steroid enzymes in clinical samples becomes critical. In the present study, the RNA sequencing dataset of The Cancer Genome Atlas Breast Invasive Carcinoma (TCGA-BRCA) cohort (N=1079) was retrieved through Genomic Data Commons (GDC) data portal, which included post-menopausal normal breast tissues (N=56) and estrogen receptor positive breast tumors (N=526). Differential expressions and gene expression correlation were analyzed by Mann–Whitney *U* test and Spearman's rho test. Differential expression analysis showed significant up-regulation of reductive 17β-HSD7 (2.61-fold, p=5.57E-26) in BC, supporting its sex-hormone effect. Besides, suppression of 11β-HSD1 expression (-8.33-fold, p=1.51E-23) and elevation of 11β-HSD2 expression (2.30-fold, p=2.17E-09), provide a low glucocorticoid level environment diminishing BC anti-proliferation effects. Furthermore, 3α-HSDs were significantly down-regulated (−1.51-fold, p=0.002; −8.18-fold, p=1.63E-28; −35.07-fold, p=2.56E-29; −30.38-fold, p=5.08E-30 for type 1-4 respectively), while 5α-reductases

significantly up-regulated (1.35-fold, p=3.42E-05; 3.11-fold, p=1.33E-11; 1.68-fold, p=1.56E-15 for type 1-3 respectively) in BC compared with normal tissues, reducing cell proliferation suppressers 4-pregnenes, increasing cell proliferation stimulators 5α-pregnanes. Expression correlation analysis indicates significant correlations between 11β-HSD1 with 3α-HSD4 (r_s=0.55, p=7.42E-41). Significant expression correlations between 3α-HSDs were also observed. A 3D schema vividly presents the regulation of steroid enzymes, extensively demonstrating their roles in BC. Our strategy can also contribute to other cancers. Our results support novel therapy targeting the reductive 17β-HSD7 and the combined therapy targeting 11β-HSD2 and 17β-HSD7.

4.3 Introduction

Breast cancer (BC) is the most commonly diagnosed cancer in women in North America, and the second leading cause of cancer death in women[1]. Molecular therapies for BC have developed rapidly during the recent decades and two milestone treatments for hormone-receptor-positive BC have been achieved: the selective estrogen receptor modulators (SERMs) represented by tamoxifen and aromatase inhibitors (AIs) such as letrozole and anastrozole[2]. However, significant side effects have occurred in response to AI treatment and resistance was evident in approximately 37% of patients during AI therapy[3]. Several hypotheses have been proposed to explain the mechanism of AI resistance, including constitutive estrogen receptor (ER) α activation caused by growth factor receptor pathways[4]; activation of growth-signaling pathways independent of estrogens and ERα[5]; and aromatase-independent estrogen biosynthesis pathway such as sulfatase pathway involving the generation of dehydroepiandrosterone (DHEA) and estradiol (E2) from dehydroepiandrosterone sulfate (DHEAS) and estrone sulfate (E1S) through steroid sulfatase (STS), and androst-5-ene-3β,17β-diol (5-diol) from DHEA, 5α-androstane-3β,17β-diol (3β-diol) from dihydrotestosterone (DHT) through 17β-hydroxysteroid dehydrogenase type1 and type 7 (17β-HSD1,7)[2, 6-7]. Moreover, recent studies have demonstrated the important role of glucocorticoids (GCs, predominantly cortisol in humans and corticosterone in rodents) in human BC development. GCs, primarily involved in the regulation of glucose metabolism, inflammation inhibition and immune suppression[8], not only exert important effects on the development and functions of the mammary gland[9], but also act as inhibitors of human BC cell proliferation[10]. And the expression modulation of 11β-hydroxysteroid dehydrogenases type 1 and type 2 (11β-HSD1,2) in human BC resulted in a low intratumoral GC environment, direct contribute to AI resistance. Furthermore, progesterone metabolites 4-pregnenes and 5α-pregnanes possess important effects on the control of BC development[11]. The maintaining of a high 5α-pregnanes/4-pregnenes ratio through down-regulation of 3α-hydroxysteroid dehydrogenases (3α-HSDs) and up-regulation of 5α-reductases (5αRs) expression provide a favorable environment for cancer cell growth, contributing to AI resistance.

In the present study, with The Cancer Genome Atlas Breast Invasive Carcinoma (TCGA-BRCA) RNA sequencing dataset from clinical samples, we analyzed the differential expression and expression correlation of key steroid-converting enzymes directly involved in the modulation of estrogen and androgen, cortisol and cortisone, 4-pregnene and 5α-pregnane, together with their related receptors. The in depth understanding of the joint control of breast cancer by related steroid-hormones will lay down the base for more efficient combined endocrine therapies.

4.4 Materials and Methods

Ethics statement

The usage of RNA sequencing data from TCGA in this study meets the data use policies set by TCGA (https://cancergenome.nih.gov/abouttcga/policies/ethicslawpolicy).

RNA sequencing dataset

TCGA is a community resource project and the TCGA database is currently the largest database of cancer genetic information of over 30 kinds of human tumours[12]. TCGA database contains a large number of RNA-seq data from clinical samples and provides most complete clinical information of each patient, thus is widely used in many studies[13-14]. To avoid introducing errors when merging RNA-seq data from different cohorts, here we choose to use the RNA-seq data from the TCGA database. In this study, we focused on the transcriptome profiling of primary tumor in post-menopausal ER+ female BC patients, and cases that did not meet this criterion were excluded from the analysis. RNA sequencing dataset of TCGA-BRCA cohort (n=1097) was downloaded through the Genomic Data Commons (GDC) data portal service. The gene level expression values in the dataset were generated through the GDC mRNA quantification analysis pipeline by first aligning reads to the GRCh38 reference genome and then by quantifying the mapped reads, which finally normalized to fragments per kilobase of transcript per million mapped reads (FPKM). Due to the highly skewed nature of RNA-seq data, the FPKM values were then log2-transformed to bring them closer to normal distribution. Since we were focused on the transcriptome profiling of primary tumor in post-menopausal ER+ female BC patients, totally 526 tumor samples and 56 normal breast samples were used in following analysis. Moreover, in the analysis of differential expression of key steroid converting enzyme genes between pre- and post-menopausal ER+ BC, totally 163 pre-menopausal cases were included.

Statistical Analysis

Samples were separated into different groups (such as tumor and normal, pre-menopause and post-menopause) according to the variables used in following analysis, which then displayed in Boxplot to show the

distribution of data among groups. Case with a value larger than 1.5 times of interquartile range (IQR) have been considered as an outlier and excluded from following statistical analysis.

Student's *t*-test and the Mann-Whitney *U* test (also called Wilcoxon rank-sum test) are commonly used in identification of differentially expressed genes in two user-defined groups in statistic analysis[15]. Both tests assume that the data distributions of the two groups have the same shape, and the student's *t*-test additionally assuming normal distributions. However, similar to DNA microarray gene expression data, the assumption of a normal distribution of intensities of every gene in RNA-seq may not be valid even after log transformation[16]. Thus to be conservative and robust, the differential gene expression analysis was evaluated by the Mann–Whitney *U* test (2-tailed). The fold change (FC) was defined as the ratio of means of the two compared groups. Positive FC value indicates up-regulation and negative one indicates down-regulation. For the gene expression correlation coefficient test, Spearman's rank correlation coefficient (2-tailed) was employed. For all statistical analysis, the Benjamini-Hochberg Procedure was performed to decrease the false discovery rate (FDR)[17], as a correction of significance; and a $p<0.05$ was considered statistically significant and represented by*, a $p<0.001$ was represented by**.

4.5 Results

17β-HSD7 over-expressed in post-menopausal ER positive (ER+) BC compared to adjacent normal breast tissues

We first examined the differential expression of 17β-HSD1 (gene HSD17B1) and 17β-HSD7 (gene HSD17B7) based on cancer and normal tissues. A Boxplot of the TCGA-BRCA data showed the distribution of values of both genes in normal and cancer groups (**Figure 4.1A** and **Table 4.1**). The expression levels of 17β-HSD1 remained controversial in literatures, with some reports indicating an up-regulation[18-19] whereas others showing a down-regulation[20-21], but both are modest. These different results may due to their limitated sample size. With large number of clinical samples, the expression level of 17β-HSD1 exhibited no significant difference between ER+ BC and normal adjacent breast tissues in post-menopausal women ($p=0.073$) (**Figure 4.1A** and **Table 4.1**). Although the expression of 17β-HSD1 was not changed during BC development, considering its high specific activity in E1 to E2 conversion, $96 \pm 10\ s^{-1}(\mu M)^{-1}$ at the molecular level[22], but a very significant substrate inhibition[23], its enzyme role in maintaining a high intratumoral concentration of E2 is still worth consideration [24]. Moreover, the enzyme may also contribute to significant 17β-HSD7 regulation (see below). Further analysis showed that the expression level of the enzyme in pre- and post-menopausal groups were similar (**Table 4.2**).

For 17β-HSD7, the immunohistological study conducted by Shehu *et al*. showed the enzyme's high expression in both invasive and *in situ* breast carcinoma[25]. The immunoreactivity of 17β-HSD7 was detected in 20 of 41 cases (49%) in BC and 24 of 41 cases (58%) in non-malignant adjacent tissues[21]. The results from present study indicated that its expression in ER+ BC was significantly up-regulated in post-menopausal women (2.61-fold, p=6.08E-26) (**Figure 4.1A** and **Table 4.1**). However, there was no significant difference between the expression of 17β-HSD7 in pre- and post-menopausal groups (**Table 4.2**).

11β-HSD1 under-expressed while 11β-HSD2 over-expressed in post-menopausal ER+ BC compared to adjacent normal breast tissues

11β-HSD1 (gene HSD11B1) has been detected in most BC tissues and normal adjacent tissues by Immunohistochemical studies, and its expression was significantly down-regulated in BC specimens compared with normal adjacent tissues[10]. Whereas the expression of 11β-HSD2 (gene HSD11B2) has been detected in 8 out of 12 breast tumor specimens (66%) by western blot[26]. We examined their expression in both normal breast tissues and ER+ BCs in post-menopausal women, in the TCGA-BRCA cohort. A Boxplot showed a clear different data distributions of the two genes in normal and tumor groups (**Figure 4.1B** and **Table 4.1**). Mann-Whitney *U* tests and FC calculation demonstrated the significant down-regulation of 11β-HSD1 (−8.33-fold, p=1.64E-23) and the significant up-regulation of 11β-HSD2 (2.30-fold, p=2.17E-09) in ER+ BCs compared with normal breast tissues (**Table 4.1**). No significant difference in expression level of these two genes was observed between pre- and post-menopausal groups (**Table 4.2**).

3α-HSDs under-expressed in post-menopausal ER+ BC compared to adjacent normal breast tissues

The down-regulation of 3α-HSD4 (also known as 3α(20α)HSD, gene AKR1C1), 3α-HSD3 (gene AKR1C2) and 3α-HSD2 (gene AKR1C3) in human breast tumors as compared to normal breast tissues has been demonstrated by qRT-PCR with a large number of clinical samples[27]. These expression modifications were also observed in BC cells (such as MCF7, T-47D and MDA-MB-231) as compared to normal breast cell MCF-10A[28]. Here we examined 3α-HSDs expression in ER+ BCs in comparison with normal breast tissues. A Boxplot showed the obvious different data distributions of these genes in normal and cancer groups (**Figure 4.1C** and **Table 4.1**). Mann-Whitney *U* tests and FC calculation showed significantly down-regulation of all four isoforms of 3α-HSDs by −1.51-fold (p=0.002), −8.18-fold (p=1.63E-28), −35.07-fold (p=2.56E-29) and −30.38-fold (p=5.08E-30) respectively in breast cancerous tissues as compared with normal breast tissues (**Table 4.1**). Their expression levels in pre- and post-menopausal patients were comparable (**Table 4.2**).

5α-reductases over-expressed in post-menopausal ER+ BC compared to adjacent normal breast tissues

The expression modulation of 5α-reductases (5αRs) in BCs is remaining controversial. *In vitro* experiments with breast cell lines and BC cell lines indicated a significant up-regulation of 5αR1 in cancer cells than normal cells[28]. On the contrary, Zhao *et al.* reported a significant down-regulation of 5αR1 in breast carcinoma compared to adjacent normal tissues[29]. In the present study, the expression status of 5αRs (gene SRD5As) in ER+ BCs and normal breast tissues was displayed with Boxplot, showing obvious different data distributions in normal and cancer groups (**Figure 4.1D** and **Table 4.1**). Mann-Whitney *U* tests and FC calculation indicated significant up-regulation of all three isoforms of SRD5As by 1.35-fold (p=3.42E-05), 3.11-fold (p=1.33E-11) and 1.68-fold (p=1.56E-15) respectively in breast cancerous tissues as compared with normal breast tissues (**Table 4.1**). All three isoforms showed similar expression level in pre- and post-menopausal patients (**Table 4.2**).

Differential expressions of steroid hormone receptors in post-menopausal ER+ BC and adjacent normal breast tissues

To clearly understand the effects of the expression modification of these key steroid enzymes to breast cancer development, we also examined the expression of their related receptors. The data distribution of receptor genes in normal and cancer groups were displayed by a Boxplot (**Figure 4.1E** and **Table 4.1**). Since all cancer samples used in this study were ER+, ERα (gene ESR1) in those samples were over-expressed (4.01-fold, p=6.74E-18) compared to normal breast tissues. The expression of ERα in post-menopausal cases were significantly higher than premenopausal cases (2.21-fold, p=4.43E-21), which significantly increased the estrogen sensitivity of cancer cells.

Androgen receptor (AR) expression was found to be a favorable prognostic indicator of disease outcomes[30]. It can be detected in 61% of BCs and in 75% of ER+ cases, and it is the most commonly expressed hormone receptor in "*in situ*", invasive and metastatic BC[30]. We examined AR differential expression with clinical samples, results showed a significant up-regulation (1.50-fold, p=3.36E-08) in ER+ BCs compared to normal breast tissues (**Table 4.1**). Its expression levels in pre- and post-menopausal patients were comparable (**Table 4.2**).

Progesterone receptor (PR, gene PGR) expression is driven by estrogen-bound ER[31], and its role in BC remains controversial[32]. According to the present study, no statistical difference of expression has been detected between ER+ BCs and normal breast tissues (1.11-fold, p=0.340) (**Table 4.1**). However, in contrast with the ERα, the expression level of PR in post-menopausal women was significantly lower as compared with pre-menopausal ones (-1.57-fold, p=0.048) (**Table 4.2**).

Glucocorticoid receptor (GR, gene NR3C1) appeared in approximately 50-70% of human invasive BC samples through ligand-binding assays, and its levels decrease significantly during cancer progression[33]. In the present study, GR expression in ER+ BCs was significantly down-regulated compared with normal breast tissues (-3.36-fold, p=2.14E-28) (**Table 4.1**). Its expression levels in pre- and post-menopausal patients were comparable (**Table 4.2**).

Expression correlation of key steroid-converting enzymes and related receptors in post-menopausal ER+ BC

To better understand the expression correlation between these key steroid enzymes and related receptors, we further performed a Spearman's rank correlation coefficient test. Totally 526 ER+ cases from post-menopausal women were involved in this study. Results showed that AKR1C1, AKR1C2 and AKR1C3 expression was strongly positively correlated with each other (r=0.886, p=1.29E-173; r=0.698, p=4.80E-76 and r=0.682, p=3.03E-71 respectively) (**Table 4.3** and **Figure 4.2**). This may be related to their location in chromosomes in the same region and may be subjected to similar regulation mechanisms. Besides, the expression of AKR1C1 and AKR1C2 were also positively correlated with HSD11B1 (r=0.548, p=7.42E-41 and r=0.491, p=1.06E-31 respectively) (**Table 4.3** and **Figure 4.2**). Interestingly, ESR1 has some expression correlations with several other genes. It positively correlated with HSD17B7 (r=0.239, p=1.38E-07), AR (r=0.476, p=9.89E-30) and PGR (r=0.382, p=1E-18), whereas negatively correlated with HSD11B1 (r=-0.237, p=1.89E-07), AKR1C1 (r=-0.268, p=2.26E-09), AKR1C2 (r=-0.227, p=7.23E-07), AKR1C3 (r=-0.154, p=0.001), SRD5A1 (r=-0.35, p=1.05E-15) (**Table 4.3**). AR and PGR also positively correlated with each other with an r value of 0.33 (p=5.67E-14). As expected, the expression of HSD11B1 was positively correlated with NR3C1 (r=0.299, p=1.4E-11).

4.6 Discussion

ER activation by estrogens synthesized through multiple aromatase-independent pathways is still one of the major mechanisms of AI-resistance. Besides E1 and E2, androgen metabolites, such as 5-diol and 3β-diol, were also reported to have estrogenic activities. Both of them possess dual and opposite effect on BC growth: they act as stimulators on their own through ER, but counteract the growth-stimulatory effect of E2 through the AR under the physiological concentrations, contributing to AI-resistance[34]. 5-diol was synthesized from DHEA by 17β-HSD1, and 3β-diol could be converted from DHT by both 17β-HSD1 and 17β-HSD7[6, 35]. With mRNA-sequencing data from a large number of clinical samples, we observed a significant up-regulation of 17β-HSD7 in ER+ BCs in post-menopausal women compared with normal breast tissues, while no significant change has been observed for 17β-HSD1. However, 17β-HSD1 may still contribute to the maintaining of E2 level due to the high enzyme activity. Moreover, the remarkable regulation of 17β-HSD7 by 17β-HSD1 via E2 modulations in BC cells has recently been demonstrated [36]. Inhibition of 17β-HSD7 in breast cancer cells led to E2

decrease and DHT accumulation, resulting in a cell cycle arrest and feedback down-regulation of the enzyme[35, 37]. Thus the significant over-expression of 17β-HSD7 in ER+ BC directly contributes to the high levels of intratumoral estrogens and low levels of intratumoral androgens (**Figure 4.3**). This was consistent with the report by Stanczyk *et al*. that androgen levels were generally lower in cancerous tissue than in benign tissue[38]. The possible use of 17β-HSD7 as target for ER+ BC treatment awaits the study of the enzyme role in cholesterol biosynthesis. Furthermore, we also observed a significant higher expression of ER in post-menopausal BC patients than in premenopausal BC patients, which may remarkably increase the estrogen sensitivity of cancer cells.

The stimulating effect of estrogens on BC proliferation is modulated by GCs. It has been reported that GCs inhibited estrogen responses, and the activation of GR by DEX can attenuate estrogen responses through the induction of the expression of estrogen sulfotransferase (SULT1E1)[39]. GCs inhibited the proliferative activity of MCF-7 cells in the presence of GR, and also have the ability to block the stimulatory effect of E2 on MCF-7 cell proliferation[40]. In T47D BC cells, GCs inhibited cell migration by disrupting the cytoskeletal dynamic organization[41]. In peripheral tissues, the concentrations of intracellular GCs were modulated by the 11β-HSD enzymes. It has been reported that GR-rich normal tissues express 11β-HSD1, while cancerous tissues express 11β-HSD2[42], and high GR expression has been reported to be associated with better prognosis than low or no GR expression[43]. The significant down-regulation of 11β-HSD1 and GR whereas the up-regulation of 11β-HSD2 in breast cancerous tissues was demonstrated by clinical samples in the present study, in which we also observed that the expression of 11β-HSD1 was negatively correlated with ERα but positively correlated with GR. The up-regulation of 11β-HSD2 may be due to the stimulation of E2, since there is an estrogen response element (ERE) located in the promoter of the gene according to the human ERE databases reported by Bourdeau *et al.*[44]. The down-regulation of 11β-HSD1 and GR together with the up-regulation of 11β-HSD2 consequentially led to a lower intratumoral cortisol level as well as a decreased GC signal in cells, diminishing the anti-inflammation effect and anti-proliferative effect of GCs. This contributed to the favorable tumor growth environment, and relieved the estrogen deprivation stress coursed by aromatase inhibition (**Figure 4.3**). 11β-HSD2 acts as an enzymatic shield maintaining and facilitating BC cell growth, and the inhibition of 11β-HSD2 activity elevates the anti-proliferative effect of GCs on BC cells[45].

More and more evidence indicate that the metabolites rather than progesterone itself played important roles in AI-resistant of BC[11, 28, 46-47]. Progesterone was metabolized to 5α-pregnane-3,20-dione (5αP) by 5α-reductase or to 3α-hydroxy-4-pregnen-20-one (3αHP) and 4-pregnen-20α-ol-3-one (20αDHP) by 3α-HSDs in breast tumors[28]. 5αP has been demonstrated to be able to promote BC cell proliferation and detachment *in vitro* and tumor formation *in vivo* regardless of the presence or absence of ER or PR[48], whereas 3αHP and 20αDHP suppress proliferation and detachments of MCF-7 cells, and those effects were mediated through their

receptors[49]. Through the down-regulation of 5αP receptor, 3αHP and 20αDHP suppress mitogenic and metastatic activity in BC cells[50]. However, the genes encoded these receptors have not been reported yet. Experiments also indicated that 3αHP and 20αDHP decreased ER levels or block the stimulation of E2 and 5αP on ER expression in MCF-7 cells in a dose-dependent manner[51]. 3α-HSDs are responsible for the conversion of progesterone to 4-pregnenes, while 5αRs metabolize progesterone and 4-pregnenes to 5α-pregnanes. In the present study, we observed significant down-regulation of 3α-HSDs and up-regulation of 5αRs in ER+ BC patients. This selective expression loss of AKR1Cs in breast tumors may augment progesterone signaling by its nuclear receptors[52], or more importantly, may suppress the formation of mitogen/metastasis inhibitors 3αHP and promote the formation of cancer stimulator 5αP[27-28]. The expression of AKR1C1 and AKR1C2 in human breast carcinoma cells was positively correlated with disease-free and overall survival; and the expression status of AKR1C1 in tumor cells was proposed as an independent prognostic marker[53]. Moreover, these significant expression modifications of 3α-HSDs and 5αRs lead to lower levels of 3αHP and 20αDHP, and higher level of 5αP (**Figure 4.3**), consequentially stimulating cancer cell proliferation, providing an escape pathway for AI-resistance.

Beside all the steroid-converting enzymes analysed in the present work, aromatase is still one of the most important enzyme associated with estrogen-dependent BC development. With large number of clinical samples, our study showed a down-regulation of the enzyme in ER+ BC with statistical significance (-1.70-fold, p=0.002).

4.7 Conclusion

The dual role on E2 and DHT by 17β-HSD7 was recently reported in detail and the enzyme inhibition yields successful reduction of cell proliferation and xenograft tumor shrinkage of the estrogen-dependent cancer[35, 37]. The significant up-regulation of the enzyme in ER+ BC strongly suggests it a novel target for endocrine treatment. Furthermore, different combinatory use of inhibitors targeting dual steroid hormones may yield novel endocrine therapeutic approaches. The inhibition of 17β-HSD7 will not only decrease the E2 level and restore the DHT level, but will also arrest the cell cycle in the G_0/G_1 phase and trigger apoptosis[35]. The decreased E2 level will relieve its suppression to 11β-HSD1 expression. Combined with the use of an 11β-HSD2 inhibitor will lead to the restoration of cortisol levels, that may subsequently elevate endogenous anti-inflammatory and anti-proliferative effects. We are confident that the understanding of expression and regulation of steroid enzymes and their receptors, as well as their correlation, will facilitate BC mechanism study and novel therapy design.

Conflict of Interest

The authors declare that they have no conflict of interest.

Acknowledgements

The work has been supported by the Canadian Institute of Health Research (CIHR) grant to Lin SX *et al*. (MOP97017). We acknowledge Dr. Muriel Steel for her editing of the manuscript.

4.8 Reference

1. Siegel, R. L.; Miller, K. D.; Jemal, A., Cancer Statistics, 2017. *CA Cancer J Clin* **2017,** *67* (1), 7-30.

2. Lin, S. X.; Chen, J.; Mazumdar, M.; Poirier, D.; Wang, C.; Azzi, A.; Zhou, M., Molecular Therapy of Breast Cancer: Progress and Future Directions. *Nat. Rev. Endocrinol.* **2010,** *6* (9), 485-493.

3. Ma, C. X.; Reinert, T.; Chmielewska, I.; Ellis, M. J., Mechanisms of aromatase inhibitor resistance. *Nature reviews. Cancer* **2015,** *15* (5), 261-75.

4. Santen, R. J.; Song, R. X.; Masamura, S.; Yue, W.; Fan, P.; Sogon, T.; Hayashi, S.; Nakachi, K.; Eguchi, H., Adaptation to estradiol deprivation causes up-regulation of growth factor pathways and hypersensitivity to estradiol in breast cancer cells. *Adv Exp Med Biol* **2008,** *630* (19-34).

5. Sabnis, G.; Brodie, A., Adaptive changes results in activation of alternate signaling pathways and resistance to aromatase inhibitor resistance. *Mol Cell Endocrinol* **2011,** *340* (2), 142-7.

6. Aka, J. A.; Mazumdar, M.; Chen, C. Q.; Poirier, D.; Lin, S. X., 17beta-Hydroxysteroid Dehydrogenase Type 1 Stimulates Breast Cancer by Dihydrotestosterone Inactivation in Addition to Estradiol Production. *Mol. Endocrinol.* **2010,** *24* (4), 832-845.

7. Hanamura, T.; Niwa, T.; Gohno, T.; Kurosumi, M.; Takei, H.; Yamaguchi, Y.; Ito, K.; Hayashi, S., Possible Role of the Aromatase-Independent Steroid Metabolism Pathways in Hormone Responsive Primary Breast Cancers. *Breast Cancer Res. Treat.* **2014,** *143* (1), 69-80.

8. Porterfield, S. P., Adrenal gland. *Endocrine physiology* **1996,** *Chap 7*, 139–146.

9. Lyons, W. R., Hormonal synergism in mammary growth. *Proc R Soc Lond B Biol Sci* **1958,** *149* (936), 303-25.

10. Lu, L.; Zhao, G.; Luu-The, V.; Ouellet, J.; Fan, Z.; Labrie, F.; Pelletier, G., Expression of 11beta-hydroxysteroid dehydrogenase type 1 in breast cancer and adjacent non-malignant tissue. An immunocytochemical study. *Pathol Oncol Res* **2011,** *17* (3), 627-32.

11. Wiebe, J. P.; Lewis, M. J.; Cialacu, V.; Pawlak, K. J.; Zhang, G., The role of progesterone metabolites in breast cancer: potential for new diagnostics and therapeutics. *J Steroid Biochem Mol Biol* **2005,** *93* (2-5), 201-8.

12. Tomczak, K.; Czerwinska, P.; Wiznerowicz, M., The Cancer Genome Atlas (TCGA): an immeasurable source of knowledge. *Contemp Oncol (Pozn)* **2015,** *19* (1A), A68-77.

13. Cancer Genome Atlas Research, N., The Molecular Taxonomy of Primary Prostate Cancer. *Cell* **2015,** *163* (4), 1011-25.

14. Cai, L.; Li, Q.; Du, Y.; Yun, J.; Xie, Y.; DeBerardinis, R. J.; Xiao, G., Genomic regression analysis of coordinated expression. *Nat Commun* **2017,** *8* (1), 2187.

15. Deng, J.; Calvert, V.; Pierobon, M., Microarray data analysis: comparing two population means. *Methods Mol Biol* **2012,** *823*, 325-46.

16. Thomas, R.; de la Torre, L.; Chang, X.; Mehrotra, S., Validation and characterization of DNA microarray gene expression data distribution and associated moments. *BMC Bioinformatics* **2010,** *11*, 576.

17. McDonald, J. H., Handbook of Biological Statistics (3rd ed.). *Sparky House Publishing* **2014**, pp 254-260.

18. Miyoshi, Y.; Ando, A.; Shiba, E.; Taguchi, T.; Tamaki, Y.; Noguchi, S., Involvement of up-regulation of 17beta-hydroxysteroid dehydrogenase type 1 in maintenance of intratumoral high estradiol levels in postmenopausal breast cancers. *Int J Cancer* **2001,** *94* (5), 685-9.

19. Sasano, H.; Frost, A. R.; Saitoh, R.; Harada, N.; Poutanen, M.; Vihko, R.; Bulun, S. E.; Silverberg, S. G.; Nagura, H., Aromatase and 17 beta-hydroxysteroid dehydrogenase type 1 in human breast carcinoma. *J Clin Endocrinol Metab* **1996,** *81* (11), 4042-6.

20. Oduwole, O. O.; Li, Y.; Isomaa, V. V.; Mäntyniemi, A.; Pulkka, A. E.; Soini, Y.; Vihko, P. T., 17beta-hydroxysteroid dehydrogenase type 1 is an independent prognostic marker in breast cancer. *Cancer Res* **2004,** *64* (20), 7604-9.

21. Song, D.; Liu, G.; Luu-The, V.; Zhao, D.; Wang, L.; Zhang, H.; Xueling, G.; Li, S.; Desy, L.; Labrie, F.; Pelletier, G., Expression of aromatase and 17beta-hydroxysteroid dehydrogenase types 1, 7 and 12 in breast cancer. An immunocytochemical study. *J Steroid Biochem Mol Biol* **2006,** *101* (2-3), 136-44.

22. Jin, J. Z.; Lin, S. X., Human estrogenic 17beta-hydroxysteroid dehydrogenase: predominance of estrone reduction and its induction by NADPH. *Biochem Biophys Res Commun* **1999,** *259* (2), 489-93.

23. Gangloff, A.; Garneau, A.; Huang, Y. W.; Yang, F.; Lin, S. X., Human oestrogenic 17β-hydroxysteroid dehydrogenase specificity: Enzyme regulation through an NADPH-dependent substrate inhibition towards the highly specific oestrone reduction. *Biochem J* **2001,** *356*, 269-276.

24. Miller, W. R.; Hawkins, R. A.; Forrest, A. P., Significance of aromatase activity in human breast cancer. *Cancer Res* **1982,** *42* (8 Suppl), 3365s-3368s.

25. Shehu, A.; Albarracin, C.; Devi, Y. S.; Luther, K.; Halperin, J.; Le, J.; Mao, J.; Duan, R. W.; Frasor, J.; Gibori, G., The stimulation of HSD17B7 expression by estradiol provides a powerful feed-forward mechanism for estradiol biosynthesis in breast cancer cells. *Mol Endocrinol* **2011,** *25* (5), 754-66.

26. Koyama, K.; Myles, K.; Smith, R.; Krozowski, Z., Expression of the 11beta-hydroxysteroid dehydrogenase type II enzyme in breast tumors and modulation of activity and cell growth in PMC42 cells. *J Steroid Biochem Mol Biol* **2001,** *76* (1-5), 153-9.

27. Lewis, M. J.; Wiebe, J. P.; Heathcote, J. G., Expression of progesterone metabolizing enzyme genes (AKR1C1, AKR1C2, AKR1C3, SRD5A1, SRD5A2) is altered in human breast carcinoma. *BMC Cancer* **2004,** *4*, 27.

28. Wiebe, J. P.; Lewis, M. J., Activity and expression of progesterone metabolizing 5alpha-reductase, 20alpha-hydroxysteroid oxidoreductase and 3alpha(beta)-hydroxysteroid oxidoreductases in tumorigenic (MCF-7, MDA-MB-231, T-47D) and nontumorigenic (MCF-10A) human breast cancer cells. *BMC Cancer* **2003,** *3*, 9.

29. Zhao, G.; Lu, L.; Luu-The, V.; Fan, Z.; Labrie, F.; Pelletier, G., Expression of 5alpha-reductase type 1 in breast cancer and adjacent non-malignant tissue: an immunohistochemical study. *Horm Mol Biol Clin Investig* **2010,** *3* (2), 411-5.

30. Vera-Badillo, F. E.; Chang, M. C.; Kuruzar, G.; Ocana, A.; Templeton, A. J.; Seruga, B.; Goldstein, R.; Bedard, P. L.; Tannock, I. F.; Amir, E., Association between androgen receptor expression, Ki-67 and the 21-gene recurrence score in non-metastatic, lymph node-negative, estrogen receptor-positive and HER2-negative breast cancer. *J Clin Pathol* **2015,** *68* (10), 839-43.

31. Kim, J. J.; Kurita, T.; Bulun, S. E., Progesterone action in endometrial cancer, endometriosis, uterine fibroids, and breast cancer. *Endocr Rev* **2013,** *34* (1), 130-62.

32. Kuhl, H.; Schneider, H. P., Progesterone--promoter or inhibitor of breast cancer. *Climacteric* **2013,** *16 Suppl 1*, 54-68.

33. Abduljabbar, R.; Negm, O. H.; Lai, C. F.; Jerjees, D. A.; Al-Kaabi, M.; Hamed, M. R.; Tighe, P. J.; Buluwela, L.; Mukherjee, A.; Green, A. R.; Ali, S.; Rakha, E. A.; Ellis, I. O., Clinical and biological significance of glucocorticoid receptor (GR) expression in breast cancer. *Breast Cancer Res Treat* **2015,** *150* (2), 335-46.

34. Chen, J.; Wang, W. Q.; Lin, S. X., Interaction of Androst-5-ene-3beta,17beta-diol and 5alpha-androstane-3beta,17beta-diol with estrogen and androgen receptors: a combined binding and cell study. *J Steroid Biochem Mol Biol* **2013,** *137*, 316-21.

35. Wang, X.; Gerard, C.; Theriault, J. F.; Poirier, D.; Doillon, C. J.; Lin, S. X., Synergistic control of sex hormones by 17beta-HSD type 7: a novel target for estrogen-dependent breast cancer. *J Mol Cell Biol* **2015,** *7* (6), 568-79.

36. Han, H.; Thériault, J. F.; Chen, G.; Lin, S. X., Substrate Inhibition of 17beta-HSD1 in living cells and regulation of 17beta-HSD7 by 17beta-HSD1 knockdown. *J Steroid Biochem Mol Biol* **2017,** *S0960-0760* (17), 10.1016/j.jsbmb.2017.05.011.

37. Zhang, C. Y.; Wang, W. Q.; Chen, J.; Lin, S. X., Reductive 17beta-hydroxysteroid dehydrogenases which synthesize estradiol and inactivate dihydrotestosterone constitute major and concerted players in ER+ breast cancer cells. *J Steroid Biochem Mol Biol* **2015,** *150*, 24-34.

38. Stanczyk, F. Z.; Mathews, B. W.; Sherman, M. E., Relationships of sex steroid hormone levels in benign and cancerous breast tissue and blood: A critical appraisal of current science. *Steroids* **2015,** *99* (Pt A), 91-102.

39. Gong, H.; Jarzynka, M. J.; Cole, T. J.; Lee, J. H.; Wada, T.; Zhang, B.; Gao, J.; Song, W. C.; DeFranco, D. B.; Cheng, S. Y.; Xie, W., Glucocorticoids antagonize estrogens by glucocorticoid receptor-mediated activation of estrogen sulfotransferase. *Cancer Res* **2008,** *68* (18), 7386-93.

40. Hegde, S. M.; Kumar, M. N.; Kavya, K.; Kumar, K. M.; Nagesh, R.; Patil, R. H.; Babu, R. L.; Ramesh, G. T.; Sharma, S. C., Interplay of nuclear receptors (ER, PR, and GR) and their steroid hormones in MCF-7 cells. *Mol Cell Biochem* **2016,** *422* (1-2), 109-120.

41. Meng, X.-G.; Yue, S.-W., Dexamethasone Disrupts Cytoskeleton Organization and Migration of T47D Human Breast Cancer Cells by Modulating the AKT/mTOR/RhoA Pathway. *Asian Pacific Journal of Cancer Prevention* **2015,** *15* (23), 10245-10250.

42. Rabbitt, E. H.; Gittoes, N. J. L.; Stewart, P. M.; Hewison, M., 11β-Hydroxysteroid dehydrogenases, cell proliferation and malignancy. *The Journal of Steroid Biochemistry and Molecular Biology* **2003,** *85* (2-5), 415-421.

43. West, D. C.; Pan, D.; Tonsing-Carter, E. Y.; Hernandez, K. M.; Pierce, C. F.; Styke, S. C.; Bowie, K. R.; Garcia, T. I.; Kocherginsky, M.; Conzen, S. D., GR and ER Coactivation Alters the Expression of Differentiation Genes and Associates with Improved ER+ Breast Cancer Outcome. *Mol Cancer Res* **2016,** *14* (8), 707-19.

44. Bourdeau, V.; Deschenes, J.; Metivier, R.; Nagai, Y.; Nguyen, D.; Bretschneider, N.; Gannon, F.; White, J. H.; Mader, S., Genome-wide identification of high-affinity estrogen response elements in human and mouse. *Mol Endocrinol* **2004,** *18* (6), 1411-27.

45. Hundertmark, S.; Bühler, H.; Rudolf, M.; Weitzel, H. K.; Ragosch, V., Inhibition of 11 beta-hydroxysteroid dehydrogenase activity enhances the antiproliferative effect of glucocorticoids on MCF-7 and ZR-75-1 breast cancer cells. *J Endocrinol* **1997,** *155* (1), 171-80.

46. Wiebe, J. P.; Muzia, D.; Hu, J.; Szwajcer, D.; Hill, S. A.; Seachrist, J. L., The 4-pregnene and 5alpha-pregnane progesterone metabolites formed in nontumorous and tumorous breast tissue have opposite effects on breast cell proliferation and adhesion. *Cancer Res* **2000,** *60* (4), 936-43.

47. Wiebe, J. P.; Muzia, D., The endogenous progesterone metabolite, 5a-pregnane-3,20-dione, decreases cell-substrate attachment, adhesion plaques, vinculin expression, and polymerized F-actin in MCF-7 breast cancer cells. *Endocrine* **2001,** *16* (1), 7-14.

48. Wiebe, J. P.; Rivas, M. A.; Mercogliano, M. F.; Elizalde, P. V.; Schillaci, R., Progesterone-induced stimulation of mammary tumorigenesis is due to the progesterone metabolite, 5alpha-dihydroprogesterone (5alphaP) and can be suppressed by the 5alpha-reductase inhibitor, finasteride. *J Steroid Biochem Mol Biol* **2015,** *149*, 27-34.

49. Wiebe, J. P.; Zhang, G.; Welch, I.; Cadieux-Pitre, H. A., Progesterone metabolites regulate induction, growth, and suppression of estrogen- and progesterone receptor-negative human breast cell tumors. *Breast Cancer Res* **2013,** *15* (3), R38.

50. Pawlak, K. J.; Zhang, G.; Wiebe, J. P., Membrane 5alpha-pregnane-3,20-dione (5alphaP) receptors in MCF-7 and MCF-10A breast cancer cells are up-regulated by estradiol and 5alphaP and down-regulated by the progesterone metabolites, 3alpha-dihydroprogesterone and 20alpha-dihydroprogesterone, with associated changes in cell proliferation and detachment. *J Steroid Biochem Mol Biol* **2005,** *97* (3), 278-88.

51. Pawlak, K. J.; Wiebe, J. P., Regulation of estrogen receptor (ER) levels in MCF-7 cells by progesterone metabolites. *J Steroid Biochem Mol Biol* **2007,** *107* (3-5), 172-9.

52. Ji, Q.; Aoyama, C.; Nien, Y. D.; Liu, P. I.; Chen, P. K.; Chang, L.; Stanczyk, F. Z.; Stolz, A., Selective loss of AKR1C1 and AKR1C2 in breast cancer and their potential effect on progesterone signaling. *Cancer Res* **2004,** *64* (20), 7610-7.

53. Wenners, A.; Hartmann, F.; Jochens, A.; Roemer, A. M.; Alkatout, I.; Klapper, W.; van Mackelenbergh, M.; Mundhenke, C.; Jonat, W.; Bauer, M., Stromal markers AKR1C1 and AKR1C2 are prognostic factors in primary human breast cancer. *Int J Clin Oncol* **2016,** *21* (3), 548-56.

Figures and Legends

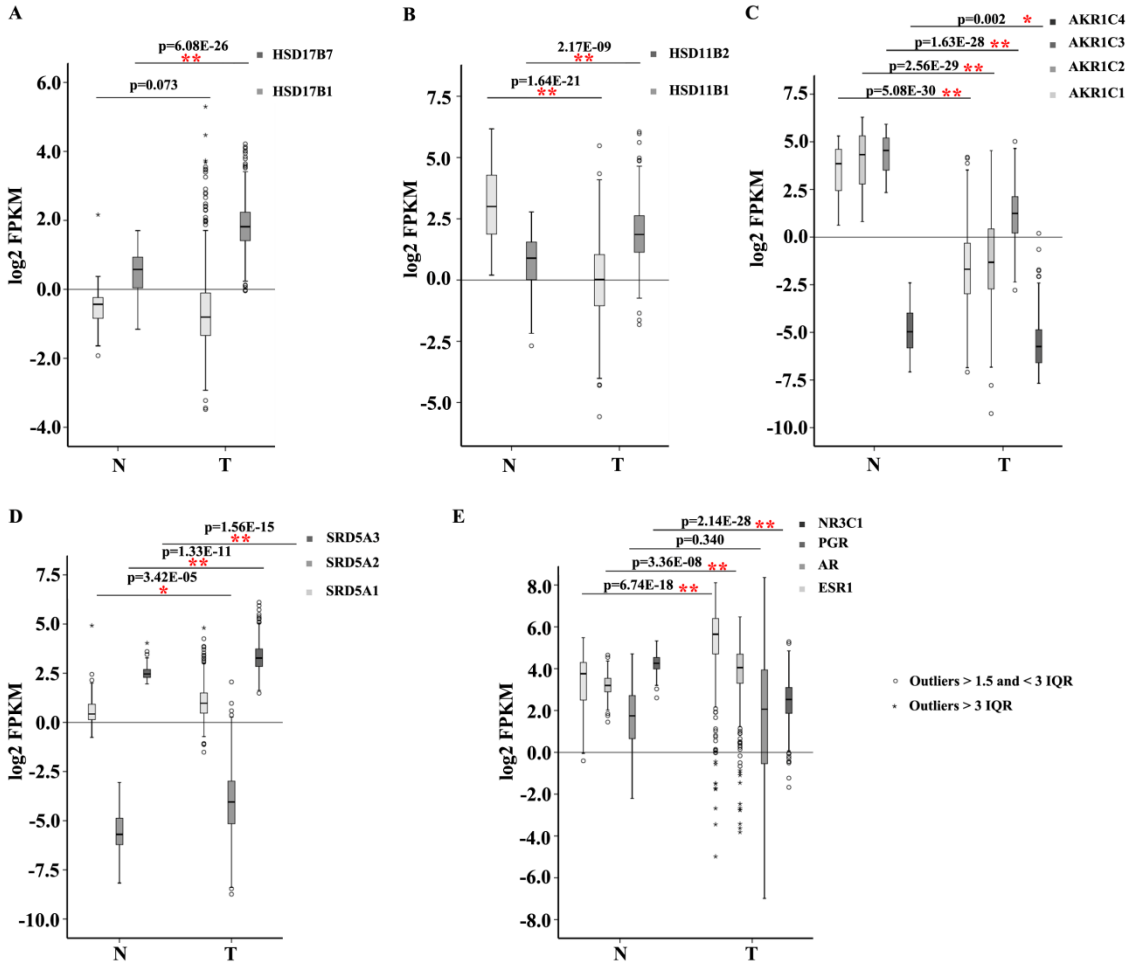

Figure 4.1. Boxplot display gene expression distribution of several key steroid-converting enzymes and related receptors in normal breast and ER+ BC in post-menopausal women. N, normal adjacent breast tissue. T, primary breast tumor. IQR, Interquartile Range. *, p<0.05 (2-tailed). **, p<0.001 (2-tailed).

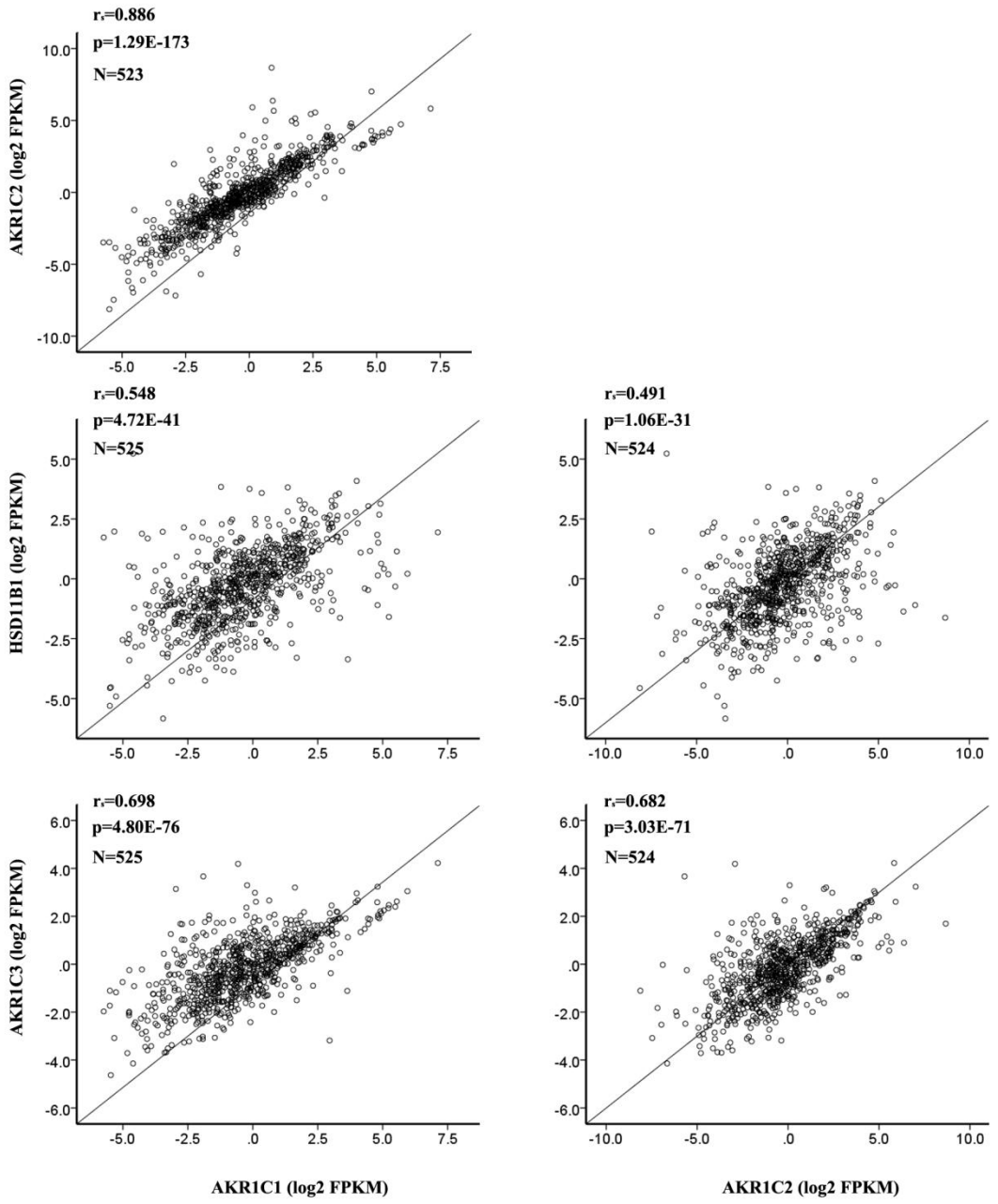

Figure 4.2. Scatter plot of gene expression correlation between AKR1C1, AKR1C2, AKR1C3 and HSD11B1. Relationships between genes were examined using Spearman's rank correlation coefficient test, and the correlation coefficient (r_s), p values and case numbers were indicated.

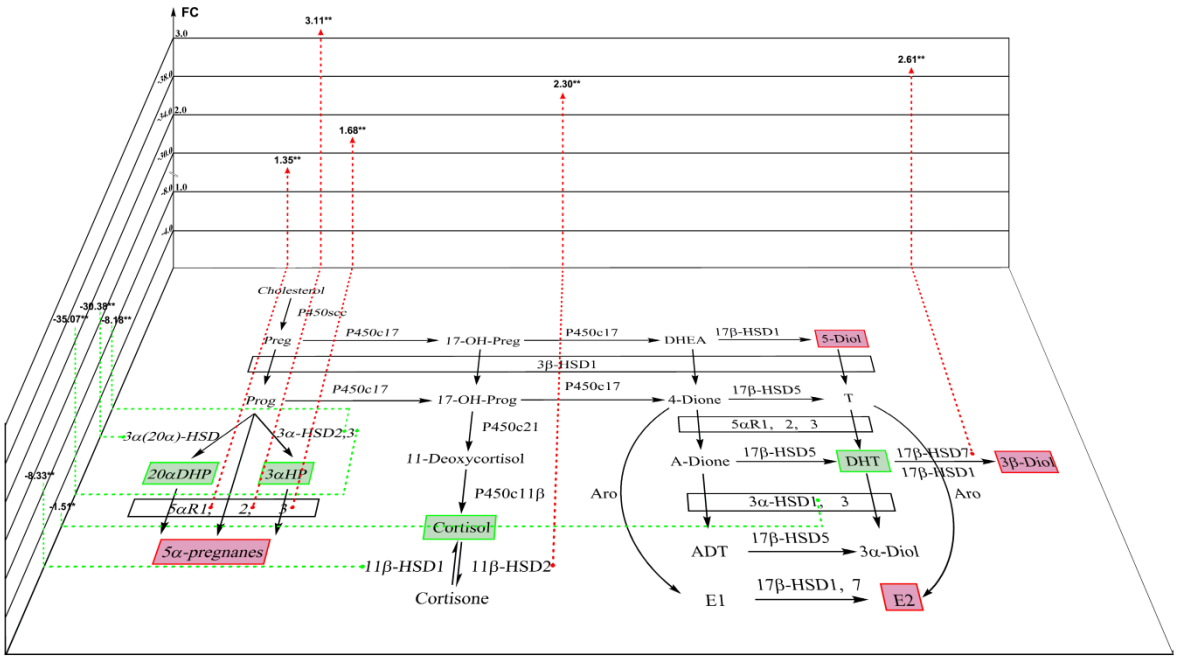

Figure 4.3. Schematic representation of important regulation of steroid-converting enzymes in BC based on a large number of clinical samples from TCGA cohort. The Red arrows indicate up-regulation; the green arrows indicate down-regulation; the red squares indicate cancer stimulators; the green squares indicate cancer suppressers. *, fold change was significant at the 0.05 level; **, fold change was significant at the 0.001 level with Mann–Whitney *U* test (2-tailed). FC, fold change; DHEA, dehydroepiandrosterone; 4-Dione, androstenedione; A-Dione, 5α-androstanedione; ADT, androsterone; E1, estrone; E2, estradiol; T, testosterone; 5-Diol, androst-5-ene-3β,17β-diol; DHT, dihydrotestosterone; 3β-diol, 5α-androstane-3β,17β-diol; 3αHP, 3α-hydroxy-4-pregnen-20-one; 20αDHP, 4-pregnen-20α-ol-3-one.

Tables

Table 4.1. Differential expression of several key steroid-converting enzymes in post-menopausal ER+ BC vs. normal breast tissue.

Gene (Protein)	Case Number		$FPKM_{mean}$		*p*	FC
	N	T	N	T		
HSD17B1 (17β-HSD1)	56	526	0.71	0.67	0.073	-1.06
HSD17B7 (17β-HSD7)	56	526	1.37	3.58	6.08E-26**	2.61
HSD11B1 (11β-HSD1)	56	526	8.33	1.00	1.64E-23**	-8.33
HSD11B2 (11β-HSD2)	56	526	1.62	3.73	2.17E-09**	2.30
AKR1C1 (3α-HSD4)	56	525	9.52	0.31	5.08E-30**	-30.38
AKR1C2 (3α-HSD3)	56	524	13.65	0.39	2.56E-29**	-35.07
AKR1C3 (3α-HSD2)	56	526	17.82	2.18	1.63E-28**	-8.18
AKR1C4 (3α-HSD1)	44	326	0.03	0.02	0.002*	-1.51
SRD5A1 (5αR1)	56	526	1.53	2.06	3.42E-05**	1.35
SRD5A2 (5αR2)	53	510	0.02	0.06	1.33E-11**	3.11
SRD5A3 (5αR3)	56	526	5.92	9.95	1.56E-15**	1.68
ESR1(ERα)	56	526	9.94	39.87	6.74E-18**	4.01
AR	56	526	9.15	13.77	3.36E-08**	1.50
PGR (PR)	56	526	2.73	3.03	0.340	1.11
NR3C1(GR)	56	526	18.25	5.43	2.14E-28**	-3.36

N_N, number of normal breast tissue samples. N_T, number of breast tumor tissue samples. FC, fold change, positive value indicates up-regulation in tumor tissues and negative indicates down-regulation. *, $p<0.05$; **, $p<0.001$ with Mann–Whitney *U* test (2-tailed). 95% CI, 95% confidence intervals.

Table 4.2. Differential expression of several key steroid-converting enzymes between post- and pre-menopausal ER+ BC.

Gene (Protein)	N_{pre}	N_{post}	*p*	FC
HSD17B1 (17β-HSD1)	163	526	0.222	1.16
HSD17B7 (17β-HSD7)	163	526	0.707	1.03
HSD11B1 (11β-HSD1)	163	526	0.689	-1.04
HSD11B2 (11β-HSD2)	163	526	0.095	1.13
AKR1C1 (3α-HSD4)	163	525	0.576	1.15
AKR1C2 (3α-HSD3)	163	524	0.558	1.10
AKR1C3 (3α-HSD2)	163	526	0.683	-1.04
AKR1C4 (3α-HSD1)	101	326	0.448	1.13
SRD5A1 (5αR1)	163	526	0.071	-1.14
SRD5A2 (5αR2)	160	510	0.754	-1.06
SRD5A3 (5αR3)	163	526	0.819	1.00
ESR1(ERα)	163	526	4.43E-21	2.21**
AR	163	526	0.362	1.10
PGR (PR)	163	526	0.048	-1.57*
NR3C1(GR)	163	526	0.332	-1.09

N_{pre}, number of pre-menopausal ER+ BC cases. N_{post}, number of post-menopausal ER+ BC cases. FC, fold change, positive value indicates up-regulation in post-menopausal ER+ BC and negative indicates down-regulation. *, $p<0.05$; **, $p<0.001$ with Mann–Whitney *U* test (2-tailed). 95% CI, 95% confidence intervals.

Table 4.3. Spearman's rank correlation coefficient test of several key steroid-converting enzymes in ER+ BC.

Genes		HSD17B7	HSD11B1	HSD11B2	AKR1C1	AKR1C2	AKR1C3	AKR1C4	SRD5A1	SRD5A2	SRD5A3	AR	ESR1	PGR	NR3C1
HSD17B1	r_s	0.04	0.02	0.00	0.01	0.01	0.03	-0.10	-0.05	-0.03	-0.133*	-0.04	-0.090*	0.202**	-0.04
	p	0.58	0.82	0.99	0.85	0.91	0.68	0.12	0.45	0.70	0.01	0.53	0.09	1.24E-05	0.54
	N	526	526	526	525	524	526	326	526	510	526	526	526	526	526
HSD17B7	r_s		-0.157*	0.151*	-0.137*	-0.122*	-0.01	0.03	-0.190**	0.122*	0.03	0.190**	0.239**	0.351**	-0.095*
	p		0.001	0.002	0.005	0.01	0.86	0.71	4.75E-05	0.01	0.68	4.75E-05	1.38E-07	7.96E-16	0.07
	N		526	526	525	524	526	326	526	510	526	526	526	526	526
HSD11B1	r_s			-0.128*	**0.548****	0.491**	0.373**	-0.05	0.151*	-0.04	-0.06	-0.08	-0.237**	0.00	0.299**
	p			0.01	7.42E-41	1.06E-31	6.74E-18	0.53	0.002	0.51	0.31	0.11	1.89E-07	0.98	1.40E-11
	N			526	525	524	526	326	526	510	526	526	526	526	526
HSD11B2	r_s				-0.01	-0.02	0.02	0.03	-0.06	-0.03	0.05	0.00	0.093*	0.00	-0.188**
	p				0.94	0.81	0.75	0.72	0.27	0.71	0.46	0.98	0.07	0.99	5.38E-05
	N				525	524	526	326	526	510	526	526	526	526	526
AKR1C1	r_s					**0.886****	**0.698****	0.03	0.05	0.00	0.03	-0.129*	-0.268**	-0.03	0.172**
	p					1.29E-173	4.80E-76	0.75	0.47	0.98	0.68	0.01	2.26E-09	0.68	2.66E-04
	N					523	525	326	525	509	525	525	525	525	525
AKR1C2	r_s						**0.682****	0.03	0.04	0.04	0.08	-0.07	-0.227**	-0.03	0.168**
	p						3.03E-71	0.75	0.53	0.53	0.12	0.17	7.23E-07	0.69	4.08E-04
	N						524	326	524	508	524	524	524	524	524
AKR1C3	r_s							0.129*	-0.101*	0.00	0.02	-0.01	-0.154*	0.02	0.209**
	p							0.05	0.05	0.98	0.75	0.94	0.001	0.72	6.12E-06
	N							326	526	510	526	526	526	526	526
AKR1C4	r_s								0.01	0.04	-0.02	-0.04	0.09	-0.109	-0.01
	p								0.89	0.68	0.84	0.66	0.21	0.11	0.94
	N								326	318	326	326	326	326	326
SRD5A1	r_s									0.03	-0.05	-0.246**	-0.350**	-0.146*	0.08
	p									0.68	0.43	5.80E-08	1.05E-15	0.002	0.17

	N									510	526	526	526	526	526
SRD5A2	r_s										0.04	-0.02	-0.07	0.02	-0.03
	p										0.62	0.82	0.26	0.82	0.71
	N										510	510	510	510	510
SRD5A3	r_s											-0.02	0.01	-0.181**	-0.155*
	p											0.75	0.91	1.07E-04	0.001
	N											526	526	526	526
AR	r_s												0.476**	0.330**	0.08
	p												9.89E-30	5.67E-14	0.15
	N												526	526	526
ESR1	r_s													0.382**	0.01
	p													1.00E-18	0.84
	N													526	526
PGR	r_s														0.07
	p														0.18
	N														526

r_s, Spearman's rank correlation coefficient. N, number of samples. *, $p<0.05$ (2-tailed). **, $p<0.001$ (2-tailed).

Conclusion

The results reported in this thesis have been discussed in chapter I to IV. In this chapter, we would like to highlight the major points of the previous discussions, and also try to highlight the links between the different results that facilitate the EDDs treatment. Besides, the prospects of the study are indicated.

The new generation 17β-HSD1 inhibitor PBRM forms a covalent bond with the enzyme.

The 17β-HSD1 has a well established role in estrogen-dependent cancer especially in breast cancer, however no candidate inhibitor has eventually reached the clinical trials[88]. The major obstacle in the development of an inhibitor for the 17β-HSD1, which is generally associated with previous series of inhibitors, is the presence of undesirable estrogenic activity. This may be largely due to the fact that 17β-HSD1 has a high affinity for estrogens[67, 132]. Thus the potent inhibitors usually contain an estrogen core making it difficult to eliminate their estrogenic activity[88]. To overcome this obstacle, decades of research accompanied by trial and error as well as structure based rational design were devoted and finally lead to the development of PBRM, which has shown promising efficacy in both breast cancer cells and human tumor xenografts in nude mice[98-99]. It was derived from the most potent 17β-HSD1 inhibitor CC-156, with a substitution of the C3-end hydroxyl group with a bromoethyl group[98]. This modification slightly decreases the inhibitor activity of PBRM to 17β-HSD1 compared to CC-156 with an IC_{50} value of 68nM for the E1 to E2 conversion[99]. However, the presence of a bromide instead of a hydroxyl group at the C3 end of the inhibitor significantly eliminates the binding of PBRM to the estrogen receptor alpha. Moreover, PBRM was further demonstrated to be an irreversible inhibitor of 17β-HSD1[101], which was further proved by the 17β-HSD1-PBRM-NADP+ complex structure reported by Li *et al*[133]. This ternary complex structure reveals a covalent bond between the C-31 of PBRM and the Nε of residue His[221], and is by far the first example of N-alkylation between a human enzyme and a low-reactivity alkyl halide derivative. The successful design of this highly specific irreversible inhibitor opens the door to a new design of alkyl halide-based specific covalent inhibitors and ligands as potential therapeutic agents.

Residues His[221] is responsible for the substrate inhibition of 17β-HSD1.

As an important enzyme in the biosynthesis of estradiol, 17β-HSD1 has been studied since the late 1950s[134]. Although the major function of the enzyme is the reversible 17β oxido-reduction of steroids[135], it can also, to a much lower extent, catalyse the 3β oxido-reduction of steroids[79], suggesting the existence of a different substrate recognition mechanism than previously proposed. Indeed, crystal structures of 17β-HSD1 in complexes with androgens such as testosterone, demonstrated the existence of a normal and a reversely orientated binding mode in the substrate binding cavity[63, 77, 136]. In the reverse binding mode, the A-ring of the steroid facing toward the catalytic triad while the D-ring binds to the recognition end of the cavity. No reverse

orientation has been observed in the E2 complexes so far. Besides, no 17β-HSD1-E1 complex has been reported prior to us. The previous reported alternative binding mode of steroid in 17β-HSD1 lead us to assess the possible binding mode of E1 in the enzyme as well as its impact on the observed substrate inhibition of the enzyme[137]. Thus we co-crystallized the 17β-HSD1 in complex with E1. Moreover, previous experiments showed that cofactor NADPH has a significant role in the binding affinity of 17β-HSD1 to E1[67], while NADPH and NADH possess profound different effect in the substrate inhibition of the enzyme[137]. To illustrate the role of NADPH on substrate binding of 17β-HSD1, we also solved the ternary complex structures containing the cofactor analog NADP+. From the binary and ternary complex structures, we indeed observed the reversely oriented E1 in all complexes, and the dead-end complex 17β-HSD1-E1-NADP+ can be responsible for the observed substrate inhibition of the enzyme. As comparison with previously reported E2/testosterone/DHT complexes, we propose His[221] is involved in the substrate inhibition mechanism. This residue is responsible for the E1 binding mode discrimination through the favorable hydrogen bond with the 17-carbonyl group of the steroid. The non-productive E1 binding mode observed in all 17β-HSD1 complexes suggest that this particular steroid can adapt more than one orientation. Moreover, at the high E1 concentrations that we used in the crystallization trials, the reverse binding mode is favored. This reverse binding orientation of E1 in 17β-HSD1 which lead to a dead-end complex is quite similar as the alternative binding modes of testosterone and 4-Androstene-3,17-dione (4-dione) in their 5β-reductase (AKR1D1) complex structures[138-139]. The two steroids in the 5β-reductase complexes are not inserted into the substrate binding cavity with their A ring toward the catalytic site as observed in the progesterone and cortisone complexes, instead they are bound with a "backward" orientation which forming into dead-end complexes[138-139].

Rational design of 17β-HSD1 inhibitor based on substrate inhibition mechanism

Interestingly, the E1 molecule in both E1 binary and ternary complex crystal structures reported here were observed in a reversed binding mode, indicating the energy favoring of the reverse binding mode of the steroid. Thus it prompts us to design novel inhibitor by using the *SeeSAR*[140]. The O-3 of estradiol is essential for its binding to ERα[141]. On the basis of substrate inhibition mechanism, we conducted a structural modification at O-3 of E1 in an attempt to modulate interaction with residues at the catalytic site of 17β-HSD1, especially the Tyr[155] as observed in CC-156 complex[142], and to reduce the undesired residual estrogenic activity. An extra benzylamide ring was added to the O-3 of E1 resulting in the formation of a novel compound 3-(((8*R*,9*S*,13*S*,14*S*)-13-methyl-17-oxo-7,8,9,11,12,13,14,15,16,17-decahydro-6*H*-cyclopenta [*a*]phenanthren-3-yl)oxy)benzamide (SX7). Binding analysis using *SeeSAR* showed that the E1 moiety of SX7 adopts a reverse binding mode, whereas the benzylamide moiety of the inhibitor interacts with 17β-HSD1 in a similar pattern as CC-156 did. The binding affinity of SX7 to the enzyme calculated by the Hydrogen bond and Dehydration (HYDE)[143] shown a high estimated affinity (43nM). A docking study against ERα ligand binding

domain showed the unfavourable binding of the new compound. Further laboratory experiments need to be performed to investigate its inhibitory properties as well as the estrogenic activity.

Significant modification in gene expression and correlation analysis of gene expression suggests novel therapy for breast cancer treatment.

The common goal of endocrine therapy for EDDs treatment is to reduce the production of estrogens, especially the most potent one estradiol, or to block the stimulation of estrogens through binding with the estrogen receptor. The two concepts yield two milestone represented by aromatase inhibitor and tamoxifen[64]. However, significant side effects have occurred in response to AI treatment and resistance was evident in approximately 37% of patients during AI therapy[144]. It was demonstrated that dynamic changes in the genome usually accompanied with tumorigenesis[145]. The modulation of the expression of genes determined the availability of steroid-converting enzymes which consequentially affect the concentration of related steroid hormones. Thus, it is reasonable to identify potential target through the statistically analysis of differentially expressed genes with RNA-seq dataset. The results from the TCGA-BRCA cohort analysis showed significant down-regulation of 3α-HSDs and up-regulation of 5α-reductases, resulting in the decreasing of cell proliferation suppresser 4-pregnenes and increasing of cell proliferation stimulators 5α-pregnanes. Besides, a significant up-regulation of 17β-HSD7 and 11β-HSD2, accompanied by a significant down-regulation of 11β-HSD1 were observed. This resulted in the accumulation of E2 and reduction of cortisol, favoring an environment for BC proliferation. Thus we propose a novel therapy targeting the reductive 17β-HSD7 and the new combined therapy targeting 11β-HSD2 and 17β-HSD7.

In this thesis, we have investigated the interactions of 17β-HSD1 at the atomic level with three inhibitors (EM-139, 2-MeO-CC-156 and PBRM) through crystallographic methods. We demonstrated that the steroid core of the reversible inhibitor EM-139 is responsible for the major interactions with 17β-HSD1, whereas the bulky 7α-alkyl moiety of the inhibitor, which is essential for its anti-estrogenic activity, compromises its inhibitory effect on the enzyme. The other reversible inhibitor 2-MeO-CC-156, which is derived from CC-156 with a reduced intrinsic estrogenic activity but also a decrease inhibitory potency, compromised its potential for further development. The addition of a bromoethyl side chain at position C-3 of CC-156 produced a potent and non-estrogenic covalent inhibitor PBRM, which interacts similarly to CC-156 with 17β-HSD1. The structural analysis of 17β-HSD1-PBRM-$NADP^+$ complex clearly shows the formation of a covalent bond between His^{221} and the bromoethyl side chain of the inhibitor, providing insight into molecular interactions that favor the binding and subsequent N-alkylation event in the enzyme catalytic site. Also, the bromoethyl group at position C-3 of the PBRM warrants its non-estrogenic profile, slows down its metabolism, and secures its specific action of 17β-HSD1 through the formation of a covalent bond with Nε of residue His^{221}. Furthermore, structural

analysis of E1 binary and ternary complexes demonstrates the reverse binding mode of E1, which is stabilized by residue His^{221} and led to the formation of dead-end complex. Based on this substrate inhibition mechanism, we employed the *in silico* method to design a 17β-HSD1 inhibitor, yielding a novel compound SX7 with a high estimated binding affinity to the enzyme. Our present studies provide profound details in the structure-function and inhibitor-enzyme relations of 17β-HSD1, facilitating further development of inhibitors of the enzyme for clinical purposes. Besides, with large number of clinical samples, RNA sequencing data analysis demonstrates the significant up-regulation of 17β-HSD7 and 11β-HSD2. We thus propose a novel combined therapy targeting 11β-HSD2 and 17β-HSD7.

Bibliographie

1. Torre, L. A.; Bray, F.; Siegel, R. L.; Ferlay, J.; Lortet-Tieulent, J.; Jemal, A., Global cancer statistics, 2012. *CA Cancer J Clin* **2015,** *65* (2), 87-108.

2. Siegel, R. L.; Miller, K. D.; Jemal, A., Cancer statistics, 2018. *CA Cancer J Clin* **2018,** *68* (1), 7-30.

3. Jemal, A.; Siegel, R.; Ward, E.; Hao, Y.; Xu, J.; Murray, T.; Thun, M. J., Cancer statistics, 2008. *CA Cancer J Clin* **2008,** *58* (2), 71-96.

4. Jemal, A.; Siegel, R.; Ward, E.; Hao, Y.; Xu, J.; Thun, M. J., Cancer statistics, 2009. *CA Cancer J Clin* **2009,** *59* (4), 225-49.

5. Jemal, A.; Siegel, R.; Xu, J.; Ward, E., Cancer statistics, 2010. *CA Cancer J Clin* **2010,** *60* (5), 277-300.

6. Siegel, R.; Ward, E.; Brawley, O.; Jemal, A., Cancer statistics, 2011: the impact of eliminating socioeconomic and racial disparities on premature cancer deaths. *CA Cancer J Clin* **2011,** *61* (4), 212-36.

7. Siegel, R.; Naishadham, D.; Jemal, A., Cancer statistics, 2012. *CA Cancer J Clin* **2012,** *62* (1), 10-29.

8. Siegel, R.; Naishadham, D.; Jemal, A., Cancer statistics, 2013. *CA Cancer J Clin* **2013,** *63* (1), 11-30.

9. Siegel, R.; Ma, J.; Zou, Z.; Jemal, A., Cancer statistics, 2014. *CA Cancer J Clin* **2014,** *64* (1), 9-29.

10. Siegel, R. L.; Miller, K. D.; Jemal, A., Cancer statistics, 2015. *CA Cancer J Clin* **2015,** *65* (1), 5-29.

11. Siegel, R. L.; Miller, K. D.; Jemal, A., Cancer statistics, 2016. *CA Cancer J Clin* **2016,** *66* (1), 7-30.

12. Siegel, R. L.; Miller, K. D.; Jemal, A., Cancer Statistics, 2017. *CA Cancer J Clin* **2017,** *67* (1), 7-30.

13. van Landeghem, A. A.; Poortman, J.; Nabuurs, M.; Thijssen, J. H., Endogenous concentration and subcellular distribution of estrogens in normal and malignant human breast tissue. *Cancer Res* **1985,** *45* (6), 2900-6.

14. Russo, I. H.; Russo, J., Role of hormones in mammary cancer initiation and progression. *J Mammary Gland Biol Neoplasia* **1998,** *3* (1), 49-61.

15. Jonat, W.; Pritchard, K. I.; Sainsbury, R.; Klijn, J. G., Trends in endocrine therapy and chemotherapy for early breast cancer: a focus on the premenopausal patient. *J Cancer Res Clin Oncol* **2006,** *132* (5), 275-86.

16. Beckmann, M. W.; Niederacher, D.; Schnürch, H. G.; Gusterson, B. A.; Bender, H. G., Multistep carcinogenesis of breast cancer and tumour heterogeneity. *Journal of Molecular Medicine* **1997,** *75* (6), 429–439.

17. Liehr, J. G., Is estradiol a genotoxic mutagenic carcinogen? *Endocr Rev* **2000,** *21* (1), 40-54.

18. Henderson, I. C.; Canellos, G. P., Cancer of the breast: the past decade. *N Engl J Med* **1980,** *302* (1), 17-30.

19. Jensen, E. V.; Jordan, V. C., The estrogen receptor: a model for molecular medicine. *Clin Cancer Res* **1980,** *9* (6), 1980-9.

20. Giguère, V.; Tremblay, A.; Tremblay, G. B., Estrogen receptor beta: re-evaluation of estrogen and antiestrogen signaling. *steroids* **1998,** *63*, 335-9.

21. Levin, E. R., Membrane oestrogen receptor alpha signalling to cell functions. *J Physiol* **2009,** *587* (Pt 21), 5019-23.

22. McDonnell, D. P.; Norris, J. D., Connections and regulation of the human estrogen receptor. *Science* **2002,** *296* (5573), 1642-4.

23. Pettersson, K.; Delaunay, F.; Gustafsson, J. A., Estrogen receptor beta acts as a dominant regulator of estrogen signaling. *Oncogene* **2000,** *19* (43), 4970-8.

24. Strom, A.; Hartman, J.; Foster, J. S.; Kietz, S.; Wimalasena, J.; Gustafsson, J. A., Estrogen receptor beta inhibits 17beta-estradiol-stimulated proliferation of the breast cancer cell line T47D. *Proc Natl Acad Sci U S A* **2004,** *101* (6), 1566-71.

25. Treeck, O.; Lattrich, C.; Springwald, A.; Ortmann, O., Estrogen receptor beta exerts growth-inhibitory effects on human mammary epithelial cells. *Breast Cancer Res Treat* **2010,** *120* (3), 557-65.

26. Sorosky, J. I., Endometrial cancer. *Obstet Gynecol* **2012,** *120* (2 Pt 1), 383-97.

27. Bokhman, J. V., Two pathogenetic types of endometrial carcinoma. *Gynecol Oncol* **1983,** *15* (1), 10-7.

28. Banno, K.; Yanokura, M.; Iida, M.; Masuda, K.; Aoki, D., Carcinogenic mechanisms of endometrial cancer: involvement of genetics and epigenetics. *J Obstet Gynaecol Res* **2014,** *40* (8), 1957-67.

29. Sorosky, J. I., Endometrial cancer. *Obstet Gynecol* **2008,** *111* (2 Pt 1), 436-47.

30. Konings, G. F.; Cornel, K. M.; Xanthoulea, S.; Delvoux, B.; Skowron, M. A.; Kooreman, L.; Koskimies, P.; Krakstad, C.; Salvesen, H. B.; van Kuijk, K.; Schrooders, Y. J.; Vooijs, M.; Groot, A. J.; Bongers, M. Y.; Kruitwagen, R. F.; Enitec; Romano, A., Blocking 17beta-hydroxysteroid dehydrogenase type 1 in endometrial cancer: a potential novel endocrine therapeutic approach. *J Pathol* **2018,** *244* (2), 203-214.

31. Fournier, M. A.; Poirier, D., Estrogen formation in endometrial and cervix cancer cell lines: involvement of aromatase, steroid sulfatase and 17beta-hydroxysteroid dehydrogenases (types 1, 5, 7 and 12). *Mol Cell Endocrinol* **2009,** *301* (1-2), 142-5.

32. Giudice, L. C., Clinical practice. Endometriosis. *N Engl J Med* **2010,** *362* (25), 2389-98.

33. Van Gorp, T.; Amant, F.; Neven, P.; Vergote, I.; Moerman, P., Endometriosis and the development of malignant tumours of the pelvis. A review of literature. *Best Pract Res Clin Obstet Gynaecol* **2004,** *18* (2), 349-71.

34. Chene, G.; Ouellet, V.; Rahimi, K.; Barres, V.; Provencher, D.; Mes-Masson, A. M., The ARID1A pathway in ovarian clear cell and endometrioid carcinoma, contiguous endometriosis, and benign endometriosis. *Int J Gynaecol Obstet* **2015,** *130* (1), 27-30.

35. Rizner, T. L., Estrogen metabolism and action in endometriosis. *Mol Cell Endocrinol* **2009,** *307* (1-2), 8-18.

36. Delvoux, B.; Groothuis, P.; D'Hooghe, T.; Kyama, C.; Dunselman, G.; Romano, A., Increased production of 17beta-estradiol in endometriosis lesions is the result of impaired metabolism. *J Clin Endocrinol Metab* **2009,** *94* (3), 876-83.

37. Huhtinen, K.; Stahle, M.; Perheentupa, A.; Poutanen, M., Estrogen biosynthesis and signaling in endometriosis. *Mol Cell Endocrinol* **2012,** *358* (2), 146-54.

38. Groothuis, P. G.; Nap, A. W.; Winterhager, E.; Grummer, R., Vascular development in endometriosis. *Angiogenesis* **2005,** *8* (2), 147-56.

39. de Graaff, A. A.; Dunselman, G. A.; Delvoux, B.; van Kaam, K. J.; Smits, L. J.; Romano, A., B lymphocyte stimulator -817C>T promoter polymorphism and the predisposition for the development of deep infiltrating endometriosis. *Fertil Steril* **2010,** *94* (3), 1108-10.

40. Nyholt, D. R.; Low, S. K.; Anderson, C. A.; Painter, J. N.; Uno, S.; Morris, A. P.; MacGregor, S.; Gordon, S. D.; Henders, A. K.; Martin, N. G.; Attia, J.; Holliday, E. G.; McEvoy, M.; Scott, R. J.; Kennedy, S.

H.; Treloar, S. A.; Missmer, S. A.; Adachi, S.; Tanaka, K.; Nakamura, Y.; Zondervan, K. T.; Zembutsu, H.; Montgomery, G. W., Genome-wide association meta-analysis identifies new endometriosis risk loci. *Nat Genet* **2012,** *44* (12), 1355-9.

41. Bulun, S. E., Endometriosis. *N Engl J Med* **2009,** *360* (3), 268-79.

42. Fedele, L.; Bianchi, S.; Zanconato, G.; Tozzi, L.; Raffaelli, R., Gonadotropin-releasing hormone agonist treatment for endometriosis of the rectovaginal septum. *American Journal of Obstetrics and Gynecology* **2000,** *183* (6), 1462-1467.

43. Goh, J. T. W.; Hall, B. A., Postmenopausal Endometrioma and Hormonal Replacement Therapy. *Aust NZ J Obstet Gynaecol* **1992,** *32* (4), 384-385.

44. Mungenast, F.; Thalhammer, T., Estrogen biosynthesis and action in ovarian cancer. *Front Endocrinol (Lausanne)* **2014,** *5*, 192.

45. Greenlee, R. T.; Murray, T.; Bolden, S.; Wingo, P. A., Cancer statistics, 2000. *CA Cancer J Clin* **2000,** *50* (1), 7-33.

46. Morch, L. S.; Lokkegaard, E.; Andreasen, A. H.; Kruger-Kjaer, S.; Lidegaard, O., Hormone Therapy and Ovarian Cancer. *JAMA* **2009,** *302* (3), 298-305.

47. Lacey, J. V.; Mink, P. J.; Lubin, J. H.; Sherman, M. E.; Troisi, R.; Hartge, P.; Schatzkin, A.; Schairer, C., Menopausal hormone replacement therapy and risk of ovarian cancer. *Journal of the American Medical Association* **2002,** *288* (3), 334-341.

48. Collaborative Group On Epidemiological Studies Of Ovarian, C.; Beral, V.; Gaitskell, K.; Hermon, C.; Moser, K.; Reeves, G.; Peto, R., Menopausal hormone use and ovarian cancer risk: individual participant meta-analysis of 52 epidemiological studies. *Lancet* **2015,** *385* (9980), 1835-42.

49. Langdon, S. P.; Crew, A. J.; Ritchie, A. A.; Muir, M.; Wakeling, A.; Smyth, J. F.; Miller, W. R., Growth inhibition of oestrogen receptor-positive human ovarian carcinoma by anti-oestrogens in vitro and in a xenograft model. *Eur J Cancer* **1994,** *30* (5), 682-686.

50. Schuler, S.; Ponnath, M.; Engel, J.; Ortmann, O., Ovarian epithelial tumors and reproductive factors: a systematic review. *Archives of Gynecology and Obstetrics* **2013,** *287* (6), 1187–1204.

51. Labrie, F., All sex steroids are made intracellularly in peripheral tissues by the mechanisms of intracrinology after menopause. *J Steroid Biochem Mol Biol* **2015,** *145*, 133-8.

52. Hua, K.; Feng, W.; Cao, Q.; Zhou, X.; Lu, X.; Feng, Y., Estrogen and progestin regulate metastasis through the PI3K/AKT pathway in human ovarian cancer. *Int J Oncol* **2008,** *33* (5), 959-67.

53. Simpson, E. R., Sources of estrogen and their importance. *The Journal of Steroid Biochemistry and Molecular Biology* **2003,** *86* (3-5), 225-230.

54. Endoh, A.; Kristiansen, S. B.; Casson, P. R.; Buster, J. E.; Hornsby, P. J., The zona reticularis is the site of biosynthesis of dehydroepiandrosterone and dehydroepiandrosterone sulfate in the adult human adrenal cortex resulting from its low expression of 3 beta-hydroxysteroid dehydrogenase. *J Clin Endocrinol Metab* **1996,** *81* (10), 3558-3565.

55. Longcope, C., Adrenal and gonadal androgen secretion in normal females. *Clin Endocrinol Metab* **1986,** *15* (2), 213-228.

56. Knochenhauer, E.; Azziz, R., Ovarian hormones and adrenal androgens during a woman's life span. *Journal of the American Academy of Dermatology* **2001,** *45* (3), S105-S115.

57. Simpson, E. R., Aromatization of androgens in women: current concepts and findings. *Fertility and Sterility* **2002,** *77*, 6-10.

58. Labrie, F., Extragonadal synthesis of sex steroids: intracrinology. *Ann Endocrinol (Paris).* **2003,** *64* (2), 95-107.

59. Labrie, F., Intracrinology. *Mol Cell Endocrinol* **1991,** *78* (3), C113-8.

60. Kallberg, Y.; Oppermann, U.; Jörnvall, H.; Persson, B., Short-chain dehydrogenases/reductases (SDRs). *European Journal of Biochemistry* **2002,** *269* (18), 4409-4417.

61. Dumont, M.; Luu-The, V.; de Launoit, Y.; Labrie, F., Expression of human 17β-hydroxysteroid dehydrogenase in mammalian cells. *The Journal of Steroid Biochemistry and Molecular Biology* **1992,** *41*, 605-608.

62. Simard, J.; Vincent, A.; Duchesne, R.; Labrie, F., Full Oestrogenic Activity of C19-Δ5 Adrenal Steroids in Rat Pituitary Lactotrophs and Somatotrophs. *Mol. Cell Endocrinol.* **1988,** *55*, 233-242.

63. Aka, J. A.; Mazumdar, M.; Chen, C. Q.; Poirier, D.; Lin, S. X., 17beta-Hydroxysteroid Dehydrogenase Type 1 Stimulates Breast Cancer by Dihydrotestosterone Inactivation in Addition to Estradiol Production. *Mol. Endocrinol.* **2010,** *24* (4), 832-845.

64. Lin, S. X.; Chen, J.; Mazumdar, M.; Poirier, D.; Wang, C.; Azzi, A.; Zhou, M., Molecular Therapy of Breast Cancer: Progress and Future Directions. *Nat. Rev. Endocrinol.* **2010,** *6* (9), 485-493.

65. Hanamura, T.; Niwa, T.; Gohno, T.; Kurosumi, M.; Takei, H.; Yamaguchi, Y.; Ito, K.; Hayashi, S., Possible Role of the Aromatase-Independent Steroid Metabolism Pathways in Hormone Responsive Primary Breast Cancers. *Breast Cancer Res. Treat.* **2014,** *143* (1), 69-80.

66. Lin, S. X.; Yang, F.; Jin, J. Z.; Breton, R.; Zhu, D. W.; Luu-The, V.; Labrie, F., Subunit Identity of the Dimeric 17β-Hydroxysteroid Dehydrogenase from Human Placenta. *J. Biol. Chem.* **1992,** *267*, 16182-16187.

67. Jin, J. Z.; Lin, S. X., Human estrogenic 17beta-hydroxysteroid dehydrogenase: predominance of estrone reduction and its induction by NADPH. *Biochem Biophys Res Commun* **1999,** *259* (2), 489-93.

68. Miyoshi, Y.; Ando, A.; Shiba, E.; Taguchi, T.; Tamaki, Y.; Noguchi, S., Involvement of up-regulation of 17beta-hydroxysteroid dehydrogenase type 1 in maintenance of intratumoral high estradiol levels in postmenopausal breast cancers. *Int J Cancer* **2001,** *94* (5), 685-9.

69. Oduwole, O. O.; Li, Y.; Isomaa, V. V.; Mäntyniemi, A.; Pulkka, A. E.; Soini, Y.; Vihko, P. T., 17beta-hydroxysteroid dehydrogenase type 1 is an independent prognostic marker in breast cancer. *Cancer Res* **2004,** *64* (20), 7604-9.

70. Cornel, K. M.; Kruitwagen, R. F.; Delvoux, B.; Visconti, L.; Van de Vijver, K. K.; Day, J. M.; Van Gorp, T.; Hermans, R. J.; Dunselman, G. A.; Romano, A., Overexpression of 17beta-hydroxysteroid dehydrogenase type 1 increases the exposure of endometrial cancer to 17beta-estradiol. *J Clin Endocrinol Metab* **2012,** *97* (4), E591-601.

71. Mori, T.; Ito, F.; Matsushima, H.; Takaoka, O.; Koshiba, A.; Tanaka, Y.; Kusuki, I.; Kitawaki, J., Dienogest reduces HSD17beta1 expression and activity in endometriosis. *J Endocrinol* **2015,** *225* (2), 69-76.

72. Blomquist, C. H.; Bonenfant, M.; McGinley, D. M.; Posalaky, Z.; Lakatua, D. J.; Tuli-Puri, S.; Bealka, D. G.; Tremblay, Y., Androgenic and estrogenic 17β-hydroxysteroid dehydrogenase/17-ketosteroid reductase in human ovarian epithelial tumors: evidence for the type 1, 2 and 5 isoforms. *The Journal of Steroid Biochemistry and Molecular Biology* **2002,** *81* (4), 343-351.

73. Puranen, T.; Poutanen, M.; Peltoketo, H.; Vihko, P. T.; Vihko, R. K., Site-directed mutagenesis of the putative active site of human 17β-hydroxysteroid dehydrogenase type 1. *Biochemical Journal* **1994,** *304*, 289-93.

74. Zhu, D. W.; Lee, X.; Breton, R.; Ghosh, D.; Pangborn, W.; Duax, W. L.; Lin, S. X., Crystallization and Preliminary X-ray Diffraction Analysis of the Complex of Human Placental 17β-Hydroxysteroid Dehydrogenase with NADP+. *J. Mol. Biol.* **1993,** *234* (1), 242-244.

75. Ghosh, D.; Pletnev, V. Z.; Zhu, D. W.; Wawrzak, Z.; Duax, W. L.; Pangborn, W.; Labrie, F.; Lin, S. X., Structure of human estrogenic 17 beta-hydroxysteroid dehydrogenase at 2.20 A resolution. *Structure* **1995,** *3* (5), 503-13.

76. Azzi, A.; Rehse, P. H.; Zhu, D. W.; Campbell, R. L.; Labrie, F.; Lin, S. X., Crystal Structure of Human Estrogenic 17β-Hydroxysteroid Dehydrogenase Complexed with 17β-Estradiol. *Nat. Struct. Biol.* **1996,** *3*, 665-668.

77. Gangloff, A.; Shi, R.; Nahoum, V.; Lin, S. X., Pseudo-Symmetry of C19 Steroids, Alternative Binding Orientations, and Multispecificity in Human Estrogenic 17beta-Hydroxysteroid Dehydrogenase. *FASEB J.* **2003,** *17* (2), 274-276.

78. Nahoum, V.; Gangloff, A.; Shi, R.; Lin, S. X., How estrogen-specific proteins discriminate estrogens from androgens: a common steroid binding site architecture. *FASEB J* **2003,** *17* (10), 1334-1336.

79. Puranen, T.; Poutanen, M.; Ghosh, D.; Vihko, P.; Vihko, R., Characterization of Structural and Functional Properties of Human 17β-Hydroxysteroid Dehydrogenase Type 1 Using Recombinant Enzymes and Site-Directed Mutagenesis. *Molecular Endocrinology* **1997,** *11* (1), 77-86.

80. Mazza, C.; Breton, R.; Housset, D.; Fontecilla-Camps, J. C., Unusual charge stabilization of NADP+ in 17beta-hydroxysteroid dehydrogenase. *Journal of Biological Chemistry* **1998,** *273* (14), 8145-52.

81. Han, Q.; Campbell, R. L.; Gangloff, A.; Huang, Y. W.; Lin, S. X., Dehydroepiandrosterone and Dihydrotestosterone Recognition by Human Estrogenic 17β-Hydroxysteroid Dehydrogenase. *J. Biol. Chem.* **2000,** *275*, 1105-1111.

82. Huang, Y. W.; Pineau, I.; Chang, H. J.; Azzi, A.; Bellemare, V.; Laberge, S.; Lin, S. X., Critical Residues for the Specificity of Cofactors and Substrates in Human Estrogenic 17β-Hydroxysteroid

Dehydrogenase 1: Variants Designed from the Three-Dimensional Structure of the Enzyme. *Mol. Endocrinol.* **2001,** *15* (11), 2010-2020.

83. Nashev, L. G.; Atanasov, A. G.; Baker, M. E.; Odermatt, A., Cysteine-10 on 17 beta -Hydroxysteroid Dehydrogenase 1 Has Stabilizing Interactions in the Cofactor Binding Region and Renders Sensitivity to Sulfhydryl Modifying Chemicals. *Int J Cell Biol* **2013,** *2013*, 769536.

84. Negri, M.; Recanatini, M.; Hartmann, R. W., Insights in 17β-HSD1 Enzyme Kinetics and Ligand Binding by Dynamic Motion Investigation. *PLoS ONE* **2010,** *5* (8).

85. Betz, G., Reaction Mechanism of 17β-Estradiol Dehydrogenase Determined by Equilibrium Rate Exchange. *J Biol Chem* **1971,** *246*, 2063-2068.

86. Marchais-Oberwinkler, S.; Henn, C.; Moller, G.; Klein, T.; Negri, M.; Oster, A.; Spadaro, A.; Werth, R.; Wetzel, M.; Xu, K.; Frotscher, M.; Hartmann, R. W.; Adamski, J., 17beta-Hydroxysteroid Dehydrogenases (17beta-HSDs) as Therapeutic Targets: Protein Structures, Functions, and Recent Progress in Inhibitor Development. *J. Steroid Biochem. Mol. Biol.* **2011,** *125* (1-2), 66-82.

87. Ghosh, D.; Vihko, P., Molecular mechanisms of estrogen recognition and 17-keto reduction by human 17β-hydroxysteroid dehydrogenase 1. *Chemico-Biological Interactions* **2001,** *130-132*, 637-650.

88. Lin, S. X.; Poirier, D.; Adamski, J., A Challenge for Medicinal Chemistry by the 17β-Hydroxysteroid Dehydrogenase Superfamily: An Integrated Biological Function and Inhibition Study. *Curr. Top. Med. Chem.* **2013,** *13* (10), 1164-1171.

89. Salah, M.; Abdelsamie, A. S.; Frotscher, M., Inhibitors of 17beta-hydroxysteroid dehydrogenase type 1, 2 and 14: Structures, biological activities and future challenges. *Mol Cell Endocrinol* **2018**.

90. Tremblay, M. R.; Poirier, D., Overview of a Rational Approach to Design Type I 17beta-Hydroxysteroid Dehydrogenase Inhibitors without Estrogenic Activity: Chemical Synthesis and Biological Evaluation. *J. Steroid Biochem. Mol. Biol.* **1998,** *66* (4), 179-191.

91. Poirier, D., Contribution to the development of inhibitors of 17beta-hydroxysteroid dehydrogenase types 1 and 7: key tools for studying and treating estrogen-dependent diseases. *J Steroid Biochem Mol Biol* **2011,** *125* (1-2), 83-94.

92. Poirier, D.; Dionne, P.; Auger, S., A 6β-(thiaheptanamide) derivative of estradiol as inhibitor of 17β-hydroxysteroid dehydrogenase type 1. *J Steroid Biochem Mol Biol* **1998,** *64*, 83-90.

93. Tremblay, M. R.; Boivin, R. P.; Luu-The, V.; Poirier, D., Inhibitors of type 1 17beta-hydroxysteroid dehydrogenase with reduced estrogenic activity: modifications of the positions 3 and 6 of estradiol. *J Enzyme Inhib Med Chem* **2005,** *20* (2), 153-63.

94. Lin, S. X.; Baltzinger, M.; Remy, P., Fast kinetic study of yeast phenylalanyl-tRNA synthetase: An efficient discrimination between tyrosine and phenylalanine at the level of the aminoacyladenylate·enzyme complex. *Biochemistry* **1983,** *22* (3), 681-9.

95. Poirier, D.; Boivin, R. P.; Tremblay, M. R.; Bérubé, M.; Qiu, W.; Lin, S. X., Estradiol-adenosine hybrid compounds designed to inhibit type 1 17beta-hydroxysteroid dehydrogenase. *J Med Chem* **2005,** *48* (26), 8134-47.

96. Fournier, D.; Poirier, D.; Mazumdar, M.; Lin, S. X., Design and synthesis of bisubstrate inhibitors of type 1 17β-hydroxysteroid dehydrogenase: Overview and perspectives. *European Journal of Medicinal Chemistry* **2008,** *43* (11), 2298-2306.

97. Laplante, Y.; Cadot, C.; Fournier, M. A.; Poirier, D., Estradiol and estrone C-16 derivatives as inhibitors of type 1 17beta-hydroxysteroid dehydrogenase: blocking of ER+ breast cancer cell proliferation induced by estrone. *Bioorganic & medicinal chemistry* **2008,** *16* (4), 1849-60.

98. Maltais, R.; Ayan, D.; Poirier, D., Crucial Role of 3-Bromoethyl in Removing the Estrogenic Activity of 17beta-HSD1 Inhibitor 16beta-(m-Carbamoylbenzyl)estradiol. *ACS Med. Chem. Lett.* **2011,** *2* (9), 678-681.

99. Ayan, D.; Maltais, R.; Roy, J.; Poirier, D., A New Nonestrogenic Steroidal Inhibitor of 17beta-Hydroxysteroid Dehydrogenase Type I Blocks the Estrogen-Dependent Breast Cancer Tumor Growth Induced by Estrone. *Mol. Cancer Ther.* **2012,** *11* (10), 2096-2104.

100. Maltais, R.; Ayan, D.; Trottier, A.; Barbeau, X.; Lague, P.; Bouchard, J. E.; Poirier, D., Discovery of a Non-Estrogenic Irreversible Inhibitor of 17beta-Hydroxysteroid Dehydrogenase Type 1 from 3-Substituted-16beta-(m-carbamoylbenzyl)-estradiol Derivatives. *J. Med. Chem.* **2014,** *57* (1), 204-222.

101. Trottier, A.; Maltais, R.; Ayan, D.; Barbeau, X.; Roy, J.; Perreault, M.; Poulin, R.; Lague, P.; Poirier, D., Insight into the Mode of Action and Selectivity of PBRM, a Covalent Steroidal Inhibitor of 17beta-Hydroxysteroid Dehydrogenase Type 1. *Biochem. Pharmacol.* **2017,** *144*, 149-161.

102. Rice, S.; Whitehead, S. A., Phytoestrogens and breast cancer--promoters or protectors? *Endocr Relat Cancer* **2006,** *13* (4), 995-1015.

103. Whitehead, S. A.; Rice, S., Endocrine-disrupting chemicals as modulators of sex steroid synthesis. *Best Pract Res Clin Endocrinol Metab* **2006,** *20* (1), 45-61.

104. Yu, Y.; Deck, J. A.; Hunsaker, L. A.; Deck, L. M.; Royer, R. E.; Goldberg, E.; Vander Jagt, D. L., Selective active site inhibitors of human lactate dehydrogenases A4, B4, and C4. *Biochem Pharmacol* **2001,** *62* (1), 81-9.

105. Brown, W. M.; Metzger, L. E.; Barlow, J. P.; Hunsaker, L. A.; Deck, L. M.; Royer, R. E.; Vander Jagt, D. L., 17-beta-Hydroxysteroid dehydrogenase type 1: computational design of active site inhibitors targeted to the Rossmann fold. *Chem Biol Interact* **2003,** *143-144*, 481-91.

106. Messinger, J.; Hirvela, L.; Husen, B.; Kangas, L.; Koskimies, P.; Pentikainen, O.; Saarenketo, P.; Thole, H., New inhibitors of 17beta-hydroxysteroid dehydrogenase type 1. *Mol Cell Endocrinol* **2006,** *248* (1-2), 192-8.

107. Frotscher, M.; Ziegler, E.; Marchais-Oberwinkler, S.; Kruchten, P.; Neugebauer, A.; Fetzer, L.; Scherer, C.; Muller-Vieira, U.; Messinger, J.; Thole, H.; Hartmann, R. W., Design, synthesis, and biological evaluation of (hydroxyphenyl)naphthalene and -quinoline derivatives: potent and selective nonsteroidal inhibitors of 17beta-hydroxysteroid dehydrogenase type 1 (17beta-HSD1) for the treatment of estrogen-dependent diseases. *J Med Chem* **2008,** *51* (7), 2158-69.

108. Kruchten, P.; Werth, R.; Marchais-Oberwinkler, S.; Frotscher M, H., R. W., Development of a biological screening system for the evaluation of highly active and selective 17beta-HSD1-inhibitors as potential therapeutic agents. *Mol Cell Endocrinol* **2009,** *301*, 154-157.

109. Marchais-Oberwinkler, S.; Wetzel, M.; Ziegler, E.; Kruchten, P.; Werth, R.; Henn, C.; Hartmann, R. W.; Frotscher, M., New drug-like hydroxyphenylnaphthol steroidomimetics as potent and selective 17beta-hydroxysteroid dehydrogenase type 1 inhibitors for the treatment of estrogen-dependent diseases. *J Med Chem* **2011,** *54* (2), 534-47.

110. Bey, E.; Marchais-Oberwinkler, S.; Kruchten, P.; Frotscher, M.; Werth, R.; Oster, A.; Algul, O.; Neugebauer, A.; Hartmann, R. W., Design, synthesis and biological evaluation of bis(hydroxyphenyl) azoles as potent and selective non-steroidal inhibitors of 17beta-hydroxysteroid dehydrogenase type 1 (17beta-HSD1) for the treatment of estrogen-dependent diseases. *Bioorganic & medicinal chemistry* **2008,** *16* (12), 6423-35.

111. Bey, E.; Marchais-Oberwinkler, S.; Negri, M.; Kruchten, P.; Oster, A.; Klein, T.; Spadaro, A.; Werth, R.; Frotscher, M.; Birk, B.; Hartmann, R. W., New insights into the SAR and binding modes of

bis(hydroxyphenyl)thiophenes and -benzenes: influence of additional substituents on 17beta-hydroxysteroid dehydrogenase type 1 (17beta-HSD1) inhibitory activity and selectivity. *J Med Chem* **2009,** *52* (21), 6724-43.

112. Kruchten, P.; Werth, R.; Bey, E.; Oster, A.; Marchais-Oberwinkler, S.; Frotscher, M.; Hartmann, R. W., Selective inhibition of 17beta-hydroxysteroid dehydrogenase type 1 (17betaHSD1) reduces estrogen responsive cell growth of T47-D breast cancer cells. *J Steroid Biochem Mol Biol* **2009,** *114* (3-5), 200-6.

113. Oster, A.; Hinsberger, S.; Werth, R.; Marchais-Oberwinkler, S.; Frotscher, M.; Hartmann, R. W., Bicyclic substituted hydroxyphenylmethanones as novel inhibitors of 17beta-hydroxysteroid dehydrogenase type 1 (17beta-HSD1) for the treatment of estrogen-dependent diseases. *J Med Chem* **2010,** *53* (22), 8176-86.

114. Abdelsamie, A. S.; Bey, E.; Gargano, E. M.; van Koppen, C. J.; Empting, M.; Frotscher, M., Towards the evaluation in an animal disease model: Fluorinated 17beta-HSD1 inhibitors showing strong activity towards both the human and the rat enzyme. *Eur J Med Chem* **2015,** *103*, 56-68.

115. Abdelsamie, A. S.; van Koppen, C. J.; Bey, E.; Salah, M.; Borger, C.; Siebenburger, L.; Laschke, M. W.; Menger, M. D.; Frotscher, M., Treatment of estrogen-dependent diseases: Design, synthesis and profiling of a selective 17beta-HSD1 inhibitor with sub-nanomolar IC50 for a proof-of-principle study. *Eur J Med Chem* **2017,** *127*, 944-957.

116. Labrie, C.; Martel, C.; Dufour, J. M.; Lévesque, C.; Mérand, Y.; Labrie, F., Novel compounds inhibit estrogen formation and action. *Cancer Res* **1992,** *52* (3), 610-5.

117. Poirier, D., Inhibitors of 17β-Hydroxysteroid Dehydrogenases. *Current Medicinal Chemistry* **2003,** *10* (6), 453-77.

118. Zhang, C. Y.; Wang, W. Q.; Chen, J.; Lin, S. X., Reductive 17beta-hydroxysteroid dehydrogenases which synthesize estradiol and inactivate dihydrotestosterone constitute major and concerted players in ER+ breast cancer cells. *J Steroid Biochem Mol Biol* **2015,** *150*, 24-34.

119. Törn, S.; Nokelainen, P.; Kurkela, R.; Pulkka, A.; Menjivar, M.; Ghosh, S.; Coca-Prados, M.; Peltoketo, H.; Isomaa, V.; Vihko, P., Production, purification, and functional analysis of recombinant human and mouse 17β-hydroxysteroid dehydrogenase type 7. *Biochemical and Biophysical Research Communications* **2003,** *305* (1), 37-45.

120. Keller, B.; Ohnesorg, T.; Mindnich, R.; Gloeckner, C. J.; Breitling, R.; Scharfe, M.; Moeller, G.; Blocker, H.; Adamski, J., Interspecies comparison of gene structure and computational analysis of gene regulation of 17beta-hydroxysteroid dehydrogenase type 1. *Mol Cell Endocrinol* **2006,** *248* (1-2), 168-71.

121. Marijanovic, Z.; Laubner, D.; Moller, G.; Gege, C.; Husen, B.; Adamski, J.; Breitling, R., Closing the gap: identification of human 3-ketosteroid reductase, the last unknown enzyme of mammalian cholesterol biosynthesis. *Mol Endocrinol* **2003,** *17* (9), 1715-25.

122. Shehu, A.; Mao, J.; Gibori, G. B.; Halperin, J.; Le, J.; Devi, Y. S.; Merrill, B.; Kiyokawa, H.; Gibori, G., Prolactin receptor-associated protein/17beta-hydroxysteroid dehydrogenase type 7 gene (Hsd17b7) plays a crucial role in embryonic development and fetal survival. *Mol Endocrinol* **2008,** *22* (10), 2268-77.

123. Breitling, R.; Krazeisen, A.; Moeller, G.; Adamski, J., 17β-hydroxysteroid dehydrogenase type 7 — an ancient 3-ketosteroid reductase of cholesterogenesis. *Molecular and Cellular Endocrinology* **2001,** *171*, 199-204.

124. Wang, X.; Gerard, C.; Theriault, J. F.; Poirier, D.; Doillon, C. J.; Lin, S. X., Synergistic control of sex hormones by 17beta-HSD type 7: a novel target for estrogen-dependent breast cancer. *J Mol Cell Biol* **2015,** *7* (6), 568-79.

125. Theriault, J. F.; Lin, S. X., The dual sex hormone specificity for human reductive 17beta-hydroxysteroid dehydrogenase type 7: Synergistic function in estrogen and androgen control. *J Steroid Biochem Mol Biol* **2019,** *186*, 61-65.

126. Reuter, J. A.; Spacek, D. V.; Snyder, M. P., High-throughput sequencing technologies. *Mol Cell* **2015,** *58* (4), 586-97.

127. Churko, J. M.; Mantalas, G. L.; Snyder, M. P.; Wu, J. C., Overview of high throughput sequencing technologies to elucidate molecular pathways in cardiovascular diseases. *Circ Res* **2013,** *112* (12), 1613-23.

128. Wan, M.; Wang, J.; Gao, X.; Sklar, J., RNA Sequencing and its Applications in Cancer Diagnosis and Targeted Therapy. *North American Journal of Medicine and Science* **2014,** *7* (4), 156-162.

129. Tomczak, K.; Czerwinska, P.; Wiznerowicz, M., The Cancer Genome Atlas (TCGA): an immeasurable source of knowledge. *Contemp Oncol (Pozn)* **2015,** *19* (1A), A68-77.

130. Cancer Genome Atlas, N., Comprehensive molecular portraits of human breast tumours. *Nature* **2012,** *490* (7418), 61-70.

131. Cai, L.; Li, Q.; Du, Y.; Yun, J.; Xie, Y.; DeBerardinis, R. J.; Xiao, G., Genomic regression analysis of coordinated expression. *Nat Commun* **2017,** *8* (1), 2187.

132. Huang, X. F.; Luu-The, V., Gene structure, chromosomal localization and analysis of 3-ketosteroid reductase activity of the human 3(α → β)-hydroxysteroid epimerase. *Biochimica et Biophysica Acta* **2001,** *1520*, 124-130.

133. Li, T.; Maltais, R.; Poirier, D.; Lin, S. X., Combined Biophysical Chemistry Reveals a New Covalent Inhibitor with a Low-Reactivity Alkyl Halide. *J Phys Chem Lett* **2018**, 5275-5280.

134. Langer, L. J.; Engel, L. L., Human placental estradiol-17β dehydrogenase. *J Biol Chem* **1958,** *233*, 583-588.

135. Luu-The, V.; Zhang, Y.; Poirier, D.; Labrie, F., Characteristics of human types 1, 2 and 3 17β-hydroxysteroid dehydrogenase activities: Oxidation/reduction and inhibition. *Journal of Steroid Biochemistry and Molecular Biology* **1995,** *55*, 581-587.

136. Shi, R.; Lin, S. X., Cofactor Hydrogen Bonding onto the Protein Main Chain is Conserved in the Short Chain Dehydrogenase/Reductase Family and Contributes to Nicotinamide Orientation. *J. Biol. Chem.* **2004,** *279* (16), 16778-16785.

137. Gangloff, A.; Garneau, A.; Huang, Y. W.; Yang, F.; Lin, S. X., Human oestrogenic 17β-hydroxysteroid dehydrogenase specificity: Enzyme regulation through an NADPH-dependent substrate inhibition towards the highly specific oestrone reduction. *Biochem J* **2001,** *356*, 269-276.

138. Di Costanzo, L.; Drury, J. E.; Penning, T. M.; Christianson, D. W., Crystal Structure of Human Liver Δ4-3-Ketosteroid 5β-Reductase (AKR1D1) and Implications for Substrate Binding and Catalysis. *Journal of Biological Chemistry* **2008,** *283* (24), 16830-16839.

139. Faucher, F.; Cantin, L.; Luu-The, V.; Labrie, F.; Breton, R., Crystal Structures of Human Δ4-3-Ketosteroid 5β-Reductase (AKR1D1) Reveal the Presence of an Alternative Binding Site Responsible for Substrate Inhibition. *Biochemistry* **2008,** *47* (51), 13537–13546.

140. *SeeSAR version 7.3; BioSolveIT GmbH, Sankt Augustin, Germany, 2018*.

141. Brzozowski, A. M.; Pike, A. C.; Dauter, Z.; Hubbard, R. E.; Bonn, T.; Engström, O.; Ohman, L.; Greene, G. L.; Gustafsson, J. A.; Carlquist, M., Molecular basis of agonism and antagonism in the oestrogen receptor. *Nature* **1997,** *389* (6652), 753-8.

142. Mazumdar, M.; Fournier, D.; Zhu, D. W.; Cadot, C.; Poirier, D.; Lin, S. X., Binary and Ternary Crystal Structure Analyses of a Novel Inhibitor with 17beta-HSD type 1: A Lead Compound for Breast Cancer Therapy. *Biochem. J.* **2009,** *424* (3), 357-366.

143. Schneider, N.; Lange, G.; Hindle, S.; Klein, R.; Rarey, M., A Consistent Description of Hydrogen Bond and Dehydration Energies in Protein-Ligand Complexes: Methods Behind the HYDE Scoring Function. *J. Comput. Aided. Mol. Des.* **2013,** *27* (1), 15-29.

144. Ma, C. X.; Reinert, T.; Chmielewska, I.; Ellis, M. J., Mechanisms of aromatase inhibitor resistance. *Nature reviews. Cancer* **2015,** *15* (5), 261-75.

145. Hanahan, D.; Weinberg, R. A., Hallmarks of cancer: the next generation. *Cell* **2011,** *144* (5), 646-74.

Annexe A Cold-active extracellular lipase: expression in Sf9 insect cells, homogenization, and catalysis

2.1 Résumé

Les lipases actives à froid font l'objet d'une attention particulière de nos jours, car elles sont de plus en plus utilisées dans diverses industries, telles que la synthèse chimique fine, la transformation des aliments et les détergents à lessive. Dans cette étude, un gène de lipase extracellulaire provenant de la *Yarrowia lipolytica* (LIPY8) a été cloné et exprimé par le système d'expression baculovirus. La lipase recombinante (LipY8p) a été purifiée en chromatographies, donnant un facteur de purification de 25,7 fois avec une activité spécifique de 1102,9 U/mg pour l'huile d'olive. L'enzyme était la plus active à un pH 7,5 et à 17°C. Son activité maximale est en vers des esters à chaîne moyenne (C10). L'activité de la lipase était affectée par les métaux de transition, les détergents et les solvants organiques. Ces propriétés enzymatiques confèrent à cette lipase un potentiel considérable pour les applications biotechnologiques.

2.2 Abstract

Cold-active lipases are gaining special attention nowadays as they are increasingly used in various industries such as fine chemical synthesis, food processing, and washer detergent. In the present study, an extracellular lipase gene from Yarrowia lipolytica (LIPY8) was cloned and expressed by baculovirus expression system. The recombinant lipase (LipY8p) was purified using chromatographic techniques, resulting in a purification factor of 25.7-fold with a specific activity of 1102.9U/mg toward olive oil. The apparent molecular mass of purified LipY8p was 40kDa. The enzyme was most active at pH 7.5 and 17ºC. It exhibited maximum activity toward medium chain (C10) esters. The presence of transition metals such as Zn^{2+}, Cu^{2+}, and Ni^{2+} strongly inhibited the enzyme activity, whereas it was enhanced by EDTA. The lipase activity was affected by detergents and was elevated by various organic solvents at 10% (v/v). These enzymatic properties make this lipase of considerable potential for biotechnological applications.

2.3 Introduction

Lipase (EC 3.1.1.3) enzymes are able to hydrolyze triacylglycerol to glycerol and long-chain fatty acids, in addition to the reverse reaction of ester synthesis using a broad range of unnatural substrates. The amount of water in the reaction medium can influence lipase behavior [1-2]. As a consequence of their useful features, such as independence from cofactors, broad range of substrate specificity, chemoselectivity, regioselectivity, stereoselectivity and stability in organic solvents, they have been used in various biotechnological applications, including organic synthesis, detergent manufacturing, food processing, biodiesel production, the chemical industry and biomedical sciences [3-6].

Lipases from different sources have been characterized and commercialized for industrial utilities. However, with intensification of global warming and the energy crisis, the development of cold-active lipases has attracted increased attention. Cold-adapted lipases possess relatively high catalytic activities at a low temperature range between 0 and 30ºC whereas normal lipases exhibit dramatically reduced or no catalytic activities [6-7]. Thus, cold-active lipases are desirable in many areas for their lower energy costs, reduced microbial contamination in industrial processes, reduced chemical side-reactions and product stabilization [8-10]. Cold-active lipases primarily originate from psychrophilic and psychrotrophic microorganisms, which exist in low temperature environments such as deep seawater and Antarctic/polar regions [11-16].

In a previous study, we isolated and characterized the *LipY* lipase from a psychrotrophic *Yarrowia lipolytica* (Bohaisea-9145), which exhibited high catalytic activity at low temperatures[17]. We also cloned the *LIPY8* lipase gene from this strain, which was previously reported by Song *et al*. [18]. Preliminary experiments indicated that the cold-active feature of the encoded extracellular lipase LipY8p has not been fully characterized. In this paper, we heterologously overexpressed the *LIPY8* gene in a baculovirus expression system, followed by purification and careful characterization of the recombinant lipase, with the aim of facilitating the industrial utility of this cold-active lipase.

2.4 Materials and Methods

Materials

Plasmid pUC57-LipY8 containing the *LIPY8* gene (GenBank accession number DQ200800) without the N-terminal signal peptide coding sequence was obtained from Dr. Sun's laboratory. Enzymes used for manipulating DNA, such as Pfu polymerase, T4 DNA ligase, *EcoR*I and *Not*I were purchased from NEB (Canada). All primers were synthesized by IDT-DNA (Canada). The Bac-to-Bac Baculovirus Expression System kit, which includes the pFastBac1 vector, the *E. coli* competent cell DH10Bac and CellfectinII reagent was from Invitrogen (Canada). *Spodoptera frugiperda* insect cell line Sf9 and Sf-900 III SFM serum-free media

were purchased from ThermoFisher Scientific (Canada). I-MAX serum-free media was from Wisent (Canada). Ni-NTA agarose resin was from ThermoFisher Scientific (Canada). Mono Q HR 5/5 columns were obtained from GE Healthcare (USA). The different lipase substrates were purchased from Sigma and Alfa Aesar. All reagents were of analytical grade. All curve fitting were performed using GraphPad Prism version 7 for Windows, GraphPad Software, La Jolla California USA, www.graphpad.com. This protein sequence alignment figure was generated with MEGA 7 software [19].

Construction of pFastBacSP6His Vector

The original pFastBac1 vector from Invitrogen does not have a signal peptide and is unsuitable for secreted protein expression. Based on pFastBac1, the signal peptide coding sequence (MGGLLLAAFLALVSVPRAQA) from human lipocalin-6 (NCBI code NM_198946) was added downstream of the polyhedron promoter (P_{PH}), followed with a 6His purification tag. This reconstructed vector was named pFastBacSP6His.

Construction of Recombinant Transfer Vector

The *LIPY8* gene was amplified using a primer pair designed for the pFastBacSP6His vector. The signal peptide coding sequence of the *LIPY8* gene was deleted from this construct. The sequence of the forward primer (F) was 5'- GCGCGAATTCGCGGGCGTGAGCCAGGGT -3', the added *EcoR*I restriction site is underlined. The reverse primer (R) was 5'- GCGCCTCGAGTTATGCGGCCGCGTTTTC -3' bearing an *Xho*I restriction site (underlined). The PCR was performed using 32 cycles of: denaturation at 94˚C for 30s, an annealing step at 63˚C for 30s, extension at 72˚C for 1.5 min followed by a 5-min final extension at 72˚C. The amplified product separated on a 1% agarose gel, purified by gel-extraction kit (Qiagen, Canada) and digested with *EcoR*I and *Xho*I, was ligated into the *EcoR*I-*Xho*I sites of the pFastBacSP6His vector. The recombinant vector pFastBacSP6His–LipY8 was transformed into competent *E.coli* DH5α cells. The integrity of the recovered plasmid was confirmed by restriction endonuclease digestion with *EcoR*I and *Xho*I, and sequencing (service provided by the genome sequencing and genotyping platform of the research center of University Laval) using the primers described above. The recombinant pFastBacSP6His–LipY8 plasmid was extracted from DH5α cells and transformed into competent *E.coli* DH10Bac cells. The cells were spread on blue/white selective LB agar plates containing 50µg/ml kanamycin, 7 µg/ml gentamicin, 10 µg/ml tetracycline, 100 µg/ml Bluo-gal and 40 µg/ml IPTG, and incubated overnight at 37˚C. Recombinant Bacmid-LipY8 DNA was isolated and integration of the target gene into the Bacmid DNA was detected by PCR using the pUC/M13 forward and pUC/M13 reverse primers as described by the Bac-to-Bac Baculovirus Expression System kit user manual.

Cell Culture and Virus Preparation

The Sf9 cells were grown as monolayers at 27ºC in Sf-900 III SFM or I-MAX serum-free media. Purified recombinant Bacmid DNA was used to transfect monolayers of Sf9 cells with Cellfectin II reagent to produce the low-titer P1 viral stock, which was then used to generate a high-titer P2 viral stock through a second infection of Sf9 cells. The titer of the baculoviral stocks was determined by plaque assay. Two percent (v/v) fetal bovine serum was added to all viral stocks, which were stored at 4ºC and protected from light. The wild-type Bacmid DNA was subjected to the same procedures and served as a negative control for lipase expression.

Lipase Overexpression and Purification

Sf9 cells were infected with recombinant or wild-type virus at a multiplicity of infection (MOI) > 10. One-milliliter aliquots of the expression culture were collected every 24 h for 7 days for determination of the optimal expression period using the activity tests described below.

All purification performances were carried out at 4ºC unless otherwise stated. The cells and debris were precipitated by centrifugation at 500 *g* for 10 min. The supernatant was collected and Tris buffer pH 8.0 was added to a final concentration of 50 mM. Ammonium sulfate powder was added gradually with constant agitation to 75% saturation over a 2-h period. Protein pellets were collected by centrifugation at 3,200 g for 30 min, and dialyzed overnight against 20 mM Tris-HCl, pH 8.0, with constant agitation.

For Ni-NTA affinity chromatography, 50 ml of concentrated lipase solution was loaded onto a Ni-NTA column (10 ml, 1.6 × 5 cm) equilibrated with buffer A (20 mM Tris-HCl pH 8.0). The lipase was eluted by a stepwise imidazole gradient with increasing concentration in buffer A. The eluted fraction was collected and the solution buffer was changed to buffer B (50 mM Tris pH 7.5, 20% (v/v) glycerol, 50 mM NaCl, 1 mM ethylenediaminetetraacetic acid (EDTA) by repeated concentration and dilution with Centricon filtration units (EMD Millipore, Canada)[20].

Ion-exchange chromatography was performed on an AKTA Explorer FPLC system (GE, USA) with a Mono Q HR 5/5 column. Lipase solution was loaded onto the column equilibrated with buffer B, and was eluted with a linear salt gradient using 1 M NaCl (pH 7.5).

SDS-PAGE

Sodium dodecyl sulfate polyacrylamide gel electrophoresis (SDS-PAGE) was performed on a 12% polyacrylamide gel on a vertical mini gel apparatus (Bio-Rad, Canada). Molecular mass markers were obtained from Bio-Rad. Proteins were stained with Coomassie Brilliant Blue R250 (Bio-Rad, Canada).

Lipase Deglycosylation

The pOPH6 plasmid containing the PNGase F gene was purchased from addgene.org. The PNGase F protein was purified as described by Loo *et al.*[21]. Enzymatic deglycosylation was performed at 30°C for 30 h using 1.2 mg of 1 mg/ml purified LipY8 with 125 ug of purified PNGase F. PNGase F was then removed by Mono Q HR 5/5 column.

Lipase Assay

Lipase activity was measured spectrophotometrically (410 nm) using *p*-nitro phenyl dodecanoate (*p*NPL) as substrate by the method described by Winkler and Stuckmann[22]. In brief, 100 µl of substrate stock solution (0.3% (w/v) *p*NPL) was added to 1 ml standard reaction buffer (50 mM Na_2HPO_4 pH 7.5, 0.2% (w/v) Na deoxycholate, 0.1% (w/v) gum arabic) and incubated in a water bath with constant shaking at 200 rpm at 22ºC for 5 min. The reaction was initiated by the addition of 2 µl of enzymes and terminated by the addition of 1.2 ml acetone-ethanol (1:1) solution. The reaction duration was 2 min, and the release of *p*NP was recorded at 410 nm using a UV/Vis spectrophotometer (UV70, Beckman Coulter, USA). Enzyme activity was calculated by constructing a standard curve with *p*NP under the same buffer conditions as the reaction. One unit (U) of lipase activity was defined as the amount of enzyme that liberated 1 µmol of *p*NP per min under standard assay conditions.

Lipase activity was also measured by the fluorescence-based rhodamine B (RhB) assay using olive oil emulsion[23] with some modifications. An RhB-olive oil emulsion mixture (RhB-OOe) containing 50 mM Na_2HPO_4 (pH 7.5), 1% (w/v) gum arabic, 0.001% (w/v) RhB, and 2% (v/v) olive oil was emulsified with a DrinkMaster for 5 min, and then the pH was adjusted. The enzymatic assays were performed in a 45 mm × 12.5 mm quartz cuvette with magnetic stirring at pH 7.5 and 22°C using a fluorescence spectrofluorometer (HORIBA Fluorolog, USA). The enzymatic reactions were initiated by the addition of 2 µl of enzyme solution to 1 ml of emulsion. The liberated fatty acids were calculated from the fluorescence emitted at 580 nm (excitation wavelength is 350 nm). The reaction emulsion with heat-denatured enzyme solution was measured in the same way and used as a blank control. A standard curve for oleic acid in the presence of RhB and gum arabic was prepared, and a linear regression was performed allowing the calculation of lipase activity. The fluorescence emission changes were converted into the hydrolysis rate using polynomial equations. One unit (U) of lipase activity was defined as the amount of enzyme releasing 1 µmol of fatty acid per min under the assay conditions.

Effect of Temperature and pH on Lipase Activity and Stability

The activity of the lipase at different temperatures and pH was determined by a *p*NP release assay using *p*NPL as substrate. To investigate temperature stability, the lipase solution was incubated for 1 h at different temperatures ranging from 0 to 45ºC. For pH stability the lipase solution was incubated for 1 h at different pH at 22ºC. Buffers used for different pH values included 50 mM sodium phosphate buffer (pH 6–8), 50 mM Tris-HCl (pH 8.5, 9), 50 mM CHES (pH 9.5), and 50 mM CAPS (pH 10). Residual activity was measured by *p*NP release assay using *p*NPL as substrate.

Substrate Specificity

For the determination of substrate specificity, several *p*-Nitro phenyl esters including *p*NP-acetate (*p*NPA, C2), *p*NP-butyrate (*p*NPB, C4), *p*NP-decanoate (*p*NPD, C10), *p*NP-dodecanoate (*p*NPL, C12), *p*NP-myristate (*p*NPM, C14), and *p*NP-palmitate (*p*NPP, C16) were used as substrates.

Effect of Metal Ions and Inhibitors on Lipase Activity

The *p*NP release assay was used to determine the effect of metal ions and inhibitors on lipase activity. The reaction buffer was preloaded with different chemicals at the desired final concentrations.

Effect of Detergents on Lipase Activity and Stability

The effects of detergents on enzyme activity and stability were evaluated by *p*NP release assay using *p*NPL as substrate. For the effect on lipase activity, different detergents were pre-loaded into the reaction buffer. To determine lipase stability, the purified enzyme was pre-incubated with various detergents for 2–72 h at 22ºC and the residual activity was determined by standard assay. Several detergents were used in this study including SDS, Triton-X100, Tween 20, NP40, n-Dodecyl-β-D-Maltoside (β-DDM), n-octyl-β-D-glucoside (β-OG) and octaethylene glycol monododecyl ether ($C_{12}E_8$).

Effect of Organic Solvents on Lipase Activity and Stability

Seven different organic solvents including methanol, ethanol, isopropanol, acetone, Dimethyl sulfoxide (DMSO), Dimethylformamide (DMF) and ethyl ether were used to determine their effects on lipase activity and stability. The lipase residual activity was measured by *p*NP release assay using *p*NPL as substrate. To determine the effects on enzyme activity, the standard reaction buffer was prepared with the addition of different solvents to yield the desired final solvent concentrations (10 or 20% v/v). For the lipase stability test the enzymes were incubated with different solvents (20% v/v) for 2 h at 22ºC, and the residual activity was measured.

2.5 Results and Discussion

Protein Sequence Analysis

LipY8p contains 371 amino acids (AAs) with a 28-AAs signal sequence, resulting in a 343-AAs mature protein. The lipase engineering database search indicated that the lipase belongs to the abH23 superfamily with a highly conserved GX pattern in the amino acid sequence[24]. Sequence alignment between LipY8 and the closely related *Y. lipolytica* lipase genes exhibited 99.2% identity with LipY (Uniprot: E0Z5H2), 99.2% with Lip8 (Uniprot: Q872L3), 78.1% with Lip7 (Uniprot: Q872L4) and 40.9% with Lip2 (Uniprot: Q9P8F7). Blast analysis with the Uniprot database revealed homology of LipY8 to several yeast lipases such as those from *Candida galli* (CgLIP8, 91.3%; CgLIP7, 77.5%), *Candida deformans* (CdLIP3, 90.7%; CdLIP2, 71%), and *Candida alimentaria* (CaLIP7, 66%) (**Figure 1**). The conserved GHSLG(G/A)A motif characteristic of the triacylglycerol hydrolases, shared by the filamentous fungi lipase family[25], was found at position ~190. The lipase catalytic triad containing the serine, aspartic acid, and histidine residues were located at conserved positions. Eight highly conserved Cys residues were also found at conserved positions in all of these lipases and are hypothesized to form disulfide bridges (**Figure 1**).

Cloning and Recombinant Baculovirus Preparation

Pichia Pastoris has historically been the first choice for over expression of yeast genes[26]. However, here we secretly expressed the *LIPY8* gene in baculovirus-infected insect cells, which also providing sufficient post-translational modification. The 1038-bp *LIPY8* gene fragment was successfully amplified by PCR from plasmid pUC57-LipY8 using a primer pair designed for the pFastBacSP6His vector. The target gene was subcloned downstream of the P_{PH} promoter of the pFastBacSP6His vector in-frame with the N-terminal signal sequence and 6His tag. After amplification in *E. coli* strain DH5α, the pFastBacSP6His-LipY8 recombinant plasmid was then introduced into the *E. coli* host strain DH10Bac. Integration of the target gene was confirmed by PCR and further confirmed by sequencing using the primers described above. The recombinant Bacmid DNA was extracted and transfected into Sf9 cells with Cellfectin reagent. After 4 or 5 days of incubation, the P1 viral stock was prepared and further amplified to generate the P2 stock. The viral plaque assay indicated the titer of P2 viral stock reached approximately 3.7×10^8 pfu/ml.

Expression of Recombinant LipY8p Lipase

The Sf9 cells were infected with recombinant virus from the P2 viral stock. The time course of recombinant extracellular lipase production was monitored by analyzing the activity of the culture medium every 24 h for up to 7 days (**Figure 2**). The initial lipase activity resulted from the introduction of the enzyme from the viral stock. Maximum lipase activity was attained 3 days post infection when cell viability decreased to around 75%.

Thereafter, lipase activity stabilized until at least 7 days post infection, indicating strong resistance to protein degradation. The maximal value of lipase specific activity in culture medium reached 17.37 U/mg by *p*-Nitro phenyl (*p*NP) release assay at 3 days post infection. No activity was detected in the wild-type virus-infected cell group.

Purification of Recombinant LipY8p Lipase

Lipase homogenization was achieved using ammonium sulfate precipitation followed by Ni-NTA affinity and Mono Q anion exchange chromatography. In brief, the lipase solution obtained from dialysis after ammonium sulfate precipitation was applied to a Ni-NTA column. Stepwise elution with increasing concentrations of imidazole in buffer A was carried out. Peak 3 with the highest lipase activity was collected (**Figure 3A**). The active fractions were pooled and applied to a Mono Q HR 5/5 column. A linear gradient of increasing NaCl concentration from zero to 1 M was performed over 100 min and LipY8p was eluted at about 10 mS/cm conductivity, resulting in a homogenous preparation as evaluated by SDS-PAGE (**Figure 3B** and **C**). The purification process resulted in an approximate 25.7-fold purification factor and a final recovery of 23.2% of the enzyme protein with a molecular mass of 40 kDa and specific activity of 446.85 U/mg by *p*NP release assay (**Table 1**).

The LipY8p lipase is a glycoprotein and endoglycosidase treatment of the heterologously expressed lipase in *Pichia pastoris* showed a 2 kDa decrease in molecular mass [18]. A similar result was observed for the lipase expressed by insect cells: the molecular mass of the heterologously expressed lipase was reduced by approximately 2 kDa after treatment with PNGase F (**Figure 3C**). Glycosylation is essential for the activity of a secretory expressed glycoprotein [27], and deglycosylation was reported to have a significant effect on enzyme activity [28-30]. However, the residual activity of the LipY8p lipase following deglycosylation retained 90.1 ± 1.3% activity of the untreated protein.

Effect of Temperature and pH on Lipase Activity and Stability

The insect cells expressing LipY8p lipase exhibited an extraordinary cold-active property that was not observed in previous report [18]. Cold-active lipases show optimal reaction temperatures at lower than 30ºC [31]. LipY8p had optimal activity at a temperature of 17ºC and retained 70.6% of the highest activity at 8ºC, which is similar to the reported cold-active lipases from *P. lynferdii* NRRL Y-7723, *Geotrichum* sp. SYBC WU-3 and *Candida albicans* [7, 31-32]. The optimal temperature of LipY8p is lower than many reported cold-active lipases [10, 12, 14, 33-38], but higher than the lipase from *Microbacterium luteolum* [39]. Moreover, similar to these reported cold-active lipases[7, 31], the activity of LipY8p drastically declined as the temperature rose above 25ºC and approached inactivity at temperatures above 45ºC (**Figure 4A**). However, LipY8p showed less thermo stability

than the cold-active lipases from *P. lynferdii* NRRL Y-7723, *Geotrichum* sp. SYBC WU-3 and *Candida albicans* [7, 31-32]. Its activity was essentially maintained from 0 to 30ºC temperature, whereas a sharp decrease in stability was observed as temperatures rose above 35ºC (**Figure 4A**).

The majority of cold-active microbial lipases exhibit optimal activity at near neutral or alkaline conditions [36]. LipY8p showed considerable stability over the pH ranges 5–9 with optimal activity at pH 7.5 (**Figure 4B**), which is similar to the lipases from *Rhizomucor endophyticus* [36] and Candida zeylanoides [33]. The wide range of stability of the lipase indicated its potential use in both acidic and alkaline conditions.

Substrate Specificity of Lipase

To investigate the substrate specificity of LipY8p, various lengths of *p*-Nitro phenyl esters were used as the substrates. The lipase showed the highest specific activity toward *p*-nitro phenyl decanoate (*p*NPD) (C10) (relative activity of 155.0%) at 791.3 ± 9.5 U/mg. *p*-nitro phenyl palmitate (*p*NPP) (C16), *p*-nitro phenyl myristate (*p*NPM) (C14) and *p*-nitro phenyl butyrate (*p*NPB) (C4) were equally utilized as substrates. The shorter carbon chain ester (C2) was poorly hydrolyzed (**Figure 5**). This indicated that LipY8p preferred medium chain esters[18], which is a typical property of the GX class lipase [24]. Similar results were reported for cold-active lipase from *Pseudomonas proteolytica* (GBPI_Hb61)[10] and *Pseudomonas* sp. strain KB700A[40]. However LipY8p lipase exhibited much higher hydrolysis activity toward olive oil with a specific activity of 1102.9 U/mg (**Figure 6**), which was much higher than the AMS8 lipase (394.43U/mg) from Antarctic *Pseudomonas* sp.[37].

Effect of Metal Ions and Inhibitors on Lipase Activity

Lipase activity was assayed in the presence of various metal ions at 1 mM concentrations (**Table 2**). Remarkable inhibition of the enzyme activity was observed in the presence of various transition metals such as Zn^{2+}, Cu^{2+}, as well as Ni^{2+}. Similarly, cold-active lipases from *Psychrobacter cryohalolentis* $K5^T$ [38] were reported to be inhibited by these three metals, and lipase from Antarctic *Pseudomonas* (AMS8 lipase)[37] and *Pseudomonas* sp. Strain B11-1[12] were inhibited by Zn^{2+}, Cu^{2+} and Fe^{2+}. The lipase activities were fairly stable in the presence of Mg^{2+} and Ca^{2+}, and activated by K^+ (118.4 ± 5.8%). In contrast, the presence of EDTA (1 mM) resulted in a considerable stimulation of lipase activity (136.1 ± 4.5%), and the inhibitory effect of Ni^{2+} was eliminated by the addition of EDTA, indicating that the lipase was not a metalloenzyme. Similar results were reported for the YlLip2 lipase from *Yarrowia lipolytica* [41] and the lipase from *Psychrobacter cryohalolentis* $K5^T$ [38]. In contrast, certain cold-active lipases require metal ions as the enzyme cofactor[40]. Of interest are the failed attempts to inhibit lipase activity through reduction of disulfide bonds in the protein despite sequence analysis revealing that the protein may contain several conserved disulfide bonds (**Figure 1**). The addition of

different concentrations of β-mercaptoethanol (β-ME) to the reaction buffer gave rise to significant activation of lipase activity. However, the simultaneous addition of 1 mM β-ME and 0.1% (w/v) n-octyl-β-D-glucoside (β-OG) led to a marked inactivation of the enzyme (77.2 ± 2.1%). This observation indicated that additional destabilizing factors, such as a detergent, were necessary for the reductant to gain access to the disulfide bond[42]. The activation effect of β-ME on enzyme activity was also reported with lipases from the *P. aeruginosa* mutant[43] and *S. bambergiensis* OC 25-4[44] where lipase activity was enhanced by 19.6% and 8%, respectively, after treatment with a concentration of 0.1% (v/v) β-ME. This can be explained by the requirement for sulfhydryl groups for lipase activity[43]. As a serine protease inhibitor, phenylmethylsulfonyl fluoride (PMSF) (1 mM and 4 mM) showed significant inhibitory effects with 80.1% and 47.6% residual activities, respectively, demonstrating that the lipase is of the serine hydrolase type[45].

Effect of Detergents on Lipase Activity and Stability

Detergents such as Tween-20 and Triton-X100 are commonly used as emulsifying agents to improve the emulsion of substrates, thereby making the substrate more accessible. However, the present of detergents in the reaction system may affect the catalytic activity of lipase depending on the concentration used. At a concentration of 0.1% (v/v or w/v), the detergents SDS, Triton-X100, NP40, Tween-20 and β-DDM strongly inhibited LipY8p activity. β-OG had a mild positive effect at 0.1% w/v (105.5 ± 2.2%), but significantly inhibited lipase activity as the concentration increased to 0.3% w/v (2.2 ± 0.1%). The inhibitory effect was also observed with $C_{12}E_8$ at 0.001% w/v (63.1 ± 5.2%) and 0.002% w/v (7.9 ± 1.4%) (**Table 3**). These results can likely be attributed to the hydrophobic property of the long chains of these detergents making them act as substrates and therefore competitive inhibitors of the enzyme [46].

Although most of the tested detergents have inhibitory effect on LipY8p activity when present in the reaction buffer system, almost all of them exhibited activating effect on the enzyme activity when be added into the enzyme stock for pre-incubation. When LipY8p was pre-incubated with 0.1% (v/v or w/v) Triton-X100 (128.1 ± 4.1%), β-OG (147.1 ± 0.3%), or $C_{12}E_8$ (144.2 ± 5.5%) for 2 h at 22ºC, we observed a strong activation of lipase activity (**Table 4**). This positive effect on lipase activity was retained for up to 72 h for Triton-X100 and longer for β-OG and $C_{12}E_8$ (**Table 4**). Thus, this indicates that the detergents were able to weaken the hydrophobic interaction within the lipase protein, resulting in disaggregation and stabilization of the enzyme[47]. However, as the incubation time increased, the denaturation effects of these detergents became dominant and the enzyme activity decreased. Pre-incubating of lipase with 0.1% (w/v) β-DDM produced a sharp decrease in lipase activity (39.9 ± 3.3%), and the destabilization effect was more pronounced with SDS, NP40 and Tween-20 at the same concentration (**Table 4**). This suggested that the lipase showed greater sensitivity to these detergents, which may have induced conformational changes and denaturation of the protein [48].

Effect of Organic Solvents on Lipase Activity and Stability

Enzymes could be used to perform reactions in organic solvents that are not possible in aqueous systems. However, activity and stability of enzymes in organic solvents show a strong dependence on the nature of the enzymes[49]. As proteins, enzymes tend to lose their activity in solutions containing higher than 10–20% organic co-solvents[50]. Thus, reaction buffers containing 10% or 20% (v/v) various organic solvents were used to examine their effects on lipase activity and stability. LipY8p activity was dramatically increased by the presence of 20% (v/v) DMSO (416.9 ± 22.7%) during the reaction. A similar phenomenon was also observed for *P. fluorescens* lipase whose activity increased up to 4.0-fold in the presence of 50% (v/v) DMSO[51]. This significant activation of lipase activity may be attributed to a conformational change and increased flexibility of the protein caused by the solvent. Activation of lipase activity was also observed with 20% (v/v) methanol (180.3 ± 1.7%). Similar effects were recorded for ethanol (266.7 ± 5.4%), acetone (361.5 ± 11.3%) as well as isopropanol (174.4 ± 5.3%) at concentrations of 10% (v/v). These became inhibitory as the concentration increased to 20% (v/v) (**Table 5**). The effects of organic solvents on lipase stability are recorded in **Table 6**. The enzyme lost almost 90% activity after exposure to 20% (v/v) ethyl ether or Dimethylformamide (DMF) at 22ºC for 2 h, and activity was virtually eliminated following addition of acetone, ethanol or isopropanol. However, LipY8p exhibited relatively higher stability in methanol and DMSO retaining 72.8 ± 1.4% and 88.1 ± 4.6% residual activity, respectively, after treatment. These results suggest that longer chain length alcohols have a stronger inhibitory effect. Binding of a thin layer of water molecules to the surface is essential for the enzyme protein to maintain its native conformation[41]. Water is a particular solvent type that shows lower affinity toward the protein surface in comparison to water-miscible organic solvents [52]. Water patches on the protein surface are formed by a limited number of directly-bound water molecules and also by water–water interactions. Thus, the presence of water-miscible organic solvents deprives the enzyme of bound water leading to enzyme inactivation. Lipases show diversity in their tolerance to water-miscible organic solvents [46]. The cold-active lipase from *Pseudomonas proteolytica* (GBPI_Hb61) showed decreased stability after a 30-min exposure to various water-miscible organic solvents, with the exception of methanol (103.5%) [10].

2.6 Conclusion

In the present work, we report the cloning and expression of the *LIPY8* gene by baculovirus expression system, as well as purification and characterization of the enzyme. The results from this study revealed that the purified recombinant enzyme was highly active in cold temperatures ranging from 8 to 21ºC with maximal activity at 17ºC. The lipase showed high stability over a wide range of pH values from 5 to 9 with optimal activity at 7.5. The enzyme also exhibited stability in the presence of a selection of inhibitors, metal ions, detergents and organic solvents. It is particularly interesting that the LipY8p expressed by insect cells showed a marked difference in enzymatic characterization with regard to optimal pH values and temperatures to that

expressed by *Pichia Pastoris* reported by Song *et al*. These differences also exist between LipY8p and LipY despite both originating from marine *Y. lipolytica* and sharing high sequence identity. To the best of our knowledge, with regard to closely related lipases of LipY8p, only the 3D structure of *Y. lipolytica* Lip2 lipase (40.9% identity) has been solved. Thus, solving the 3D structure of LipY8p will shed light on the enzyme structure and function, and also contribute to the understanding of enzymatic activities at low temperatures as well as their optimization for biotechnological applications.

Acknowledgments

We thank Dr. Muriel Steel for her editing of the manuscript.

Funding

This work was with the International collaboration program (PSR-SIIRI) supported by and the Ministry of Economy, Science and Innovation of Quebec, Canada (MESI) and the Ministry of Science and Technology of China.

Conflict of interest statement

The authors declare that they have no conflict of interest.

2.7 Reference

1. Jaeger, K. E.; Eggert, T., Lipases for biotechnology. *Curr Opin Biotechnol* 2002, *13* (4), 390-7.

2. Gupta, R.; Gupta, N.; Rathi, P., Bacterial lipases: an overview of production, purification and biochemical properties. *Appl Microbiol Biotechnol* **2004,** *64* (6), 763-81.

3. Haldane, J. B. S., Enzymes (Monographs on Biochemistry). *Longmans, Green and Co.* **1930**, pp. 102.

4. Gitlesen, T.; Bauer, M.; Adlercreutz, P., Adsorption of lipase on polypropylene powder. *Biochim Biophys Acta* **1997,** *1345* (2), 188-96.

5. Hasan, F.; Shah, A. A.; Hameed, A., Industrial applications of microbial lipases. *Enzyme and Microbial Technology* **2006,** *39* (2), 235-251.

6. Joseph, B.; Ramteke, P. W.; Thomas, G., Cold active microbial lipases: some hot issues and recent developments. *Biotechnol Adv* **2008,** *26* (5), 457-70.

7. Bae, J.-H.; Kwon, M.-H.; Kim, I.-H.; Hou, C. T.; Kim, H.-R., Purification and characterization of a cold-active lipase from Pichia lynferdii Y-7723: pH-dependant activity deviation. *Biotechnology and Bioprocess Engineering* **2014,** *19* (5), 851-857.

8. Gerday, C.; Aittaleb, M.; Bentahir, M.; Chessa, J. P.; Claverie, P.; Collins, T.; D'Amico, S.; Dumont, J.; Garsoux, G.; Georlette, D.; Hoyoux, A.; Lonhienne, T.; Meuwis, M. A.; Feller, G., Cold-adapted enzymes: from fundamentals to biotechnology. *Trends Biotechnol* **2000,** *18* (3), 103-7.

9. Siddiqui, K. S.; Cavicchioli, R., Cold-adapted enzymes. *Annu Rev Biochem* **2006,** *75*, 403-33.

10. Jain, R.; Pandey, A.; Pasupuleti, M.; Pande, V., Prolonged Production and Aggregation Complexity of Cold-Active Lipase from Pseudomonas proteolytica (GBPI_Hb61) Isolated from Cold Desert Himalaya. *Mol Biotechnol* **2017,** *59* (1), 34-45.

11. Feller, G.; Thiry, M.; Gerday, C., Nucleotide sequence of the lipase gene lip2 from the antarctic psychrotroph Moraxella TA144 and site-specific mutagenesis of the conserved serine and histidine residues. *DNA Cell Biol* **1991,** *10* (5), 381-8.

12. Choo, D. W.; Kurihara, T.; Suzuki, T.; Soda, K.; Esaki, N., A cold-adapted lipase of an Alaskan psychrotroph, Pseudomonas sp. strain B11-1: gene cloning and enzyme purification and characterization. *Appl Environ Microbiol* **1998,** *64* (2), 486-91.

13. Kulakova, L.; Galkin, A.; Nakayama, T.; Nishino, T.; Esaki, N., Cold-active esterase from Psychrobacter sp. Ant300: gene cloning, characterization, and the effects of Gly→Pro substitution near the active site on its catalytic activity and stability. *Biochimica et Biophysica Acta (BBA) - Proteins and Proteomics* **2004,** *1696* (1), 59-65.

14. Suzuki, T.; Nakayama, T.; Kurihara, T.; Nishino, T.; Esaki, N., Cold-active lipolytic activity of psychrotrophic Acinetobacter sp. strain no. 6. *J Biosci Bioeng* **2001,** *92* (2), 144-8.

15. Zhang, J.; Lin, S.; Zeng, R., Cloning, expression, and characterization of a cold-adapted lipase gene from an antarctic deep-sea psychrotrophic bacterium, Psychrobacter sp 7195. *J Microbiol Biotechnol* **2007,** *17* (4), 604-10.

16. Russell, N. J., Molecular adaptations in psychrophilic bacteria: potential for biotechnological applications. *Adv Biochem Eng Biotechnol* **1998,** *61*, 1-21.

17. Sheng, J.; Wang, F.; Wang, H.; Sun, M., Cloning, characterization and expression of a novel lipase gene from marine psychrotrophic Yarrowia lipolytica. *Annals of Microbiology* **2011,** *62* (3), 1071-1077.

18. Song, H. T.; Jiang, Z. B.; Ma, L. X., Expression and purification of two lipases from Yarrowia lipolytica AS 2.1216. *Protein Expr Purif* **2006,** *47* (2), 393-7.

19. Kumar, S.; Stecher, G.; Tamura, K., MEGA7: Molecular Evolutionary Genetics Analysis Version 7.0 for Bigger Datasets. *Mol Biol Evol* **2016,** *33* (7), 1870-4.

20. Zhu, D. W.; Azzi, A.; Rehse, P.; Lin, S. X., The Crystallogenesis of a Human Estradiol Dehydrogenase-Substrate Complex. *J. Cryst. Growth* **1996,** *168*, 275-279.

21. Loo, T.; Patchett, M. L.; Norris, G. E.; Lott, J. S., Using secretion to solve a solubility problem: high-yield expression in Escherichia coli and purification of the bacterial glycoamidase PNGase F. *Protein Expr Purif* **2002,** *24* (1), 90-8.

22. Winkler, U. K.; Stuckmann, M., Glycogen, hyaluronate, and some other polysaccharides greatly enhance the formation of exolipase by Serratia marcescens. *J Bacteriol* **1979,** *138* (3), 663-70.

23. Zottig, X.; Meddeb-Mouelhi, F.; Beauregard, M., Development of a high-throughput liquid state assay for lipase activity using natural substrates and rhodamine B. *Anal Biochem* **2016,** *496*, 25-9.

24. Pleiss, J.; Fischer, M.; Peiker, M.; Thiele, C.; Schmid, R. D., Lipase engineering database: Understanding and exploiting sequence–structure–function relationships. *Journal of Molecular Catalysis B: Enzymatic* **2000,** *10* (5), 491-508.

25. Bigey, F.; Tuery, K.; Bougard, D.; Nicaud, J. M.; Moulin, G., Identification of a triacylglycerol lipase gene family in Candida deformans: molecular cloning and functional expression. *Yeast* **2003,** *20* (3), 233-48.

26. Daly, R.; Hearn, M. T., Expression of heterologous proteins in Pichia pastoris: a useful experimental tool in protein engineering and production. *J Mol Recognit* **2005,** *18* (2), 119-38.

27. Stahnke, G.; Davis, R. C.; Doolittle, M. H.; Wong, H.; Schotz, M. C.; Will, H., Effect of N-linked glycosylation on hepatic lipase activity. *J Lipid Res* **1991,** *32* (3), 477-84.

28. Liu, Y.; Xie, W.; Yu, H., Enhanced activity of Rhizomucor miehei lipase by deglycosylation of its propeptide in Pichia pastoris. *Curr Microbiol* **2014,** *68* (2), 186-91.

29. Yang, M.; Yu, X. W.; Zheng, H.; Sha, C.; Zhao, C.; Qian, M.; Xu, Y., Role of N-linked glycosylation in the secretion and enzymatic properties of Rhizopus chinensis lipase expressed in Pichia pastoris. *Microb Cell Fact* **2015,** *14*, 40.

30. Goettig, P., Effects of Glycosylation on the Enzymatic Activity and Mechanisms of Proteases. *Int J Mol Sci* **2016,** *17* (12).

31. Cai, Y.; Wang, L.; Liao, X.; Ding, Y.; Sun, J., Purification and partial characterization of two new cold-adapted lipases from mesophilic Geotrichum sp. SYBC WU-3. *Process Biochemistry* **2009,** *44* (7), 786-790.

32. Lan, D. M.; Yang, N.; Wang, W. K.; Shen, Y. F.; Yang, B.; Wang, Y. H., A novel cold-active lipase from Candida albicans: cloning, expression and characterization of the recombinant enzyme. *Int J Mol Sci* **2011,** *12* (6), 3950-65.

33. Canak, I.; Berkics, A.; Bajcsi, N.; Kovacs, M.; Belak, A.; Teparic, R.; Maraz, A.; Mrsa, V., Purification and Characterization of a Novel Cold-Active Lipase from the Yeast Candida zeylanoides. *J Mol Microbiol Biotechnol* **2015,** *25* (6), 403-11.

34. Li, M.; Yang, L. R.; Xu, G.; Wu, J. P., Screening, purification and characterization of a novel cold-active and organic solvent-tolerant lipase from Stenotrophomonas maltophilia CGMCC 4254. *Bioresour Technol* **2013,** *148*, 114-20.

35. Yan, Q.; Duan, X.; Liu, Y.; Jiang, Z.; Yang, S., Expression and characterization of a novel 1,3-regioselective cold-adapted lipase from Rhizomucor endophyticus suitable for biodiesel synthesis. *Biotechnol Biofuels* **2016,** *9*, 86.

36. Duan, X.; Zheng, M.; Liu, Y.; Jiang, Z.; Yang, S., High-level expression and biochemical characterization of a novel cold-active lipase from Rhizomucor endophyticus. *Biotechnol Lett* **2016,** *38* (12), 2127-2135.

37. Ganasen, M.; Yaacob, N.; Rahman, R. N.; Leow, A. T.; Basri, M.; Salleh, A. B.; Ali, M. S., Cold-adapted organic solvent tolerant alkalophilic family I.3 lipase from an Antarctic Pseudomonas. *Int J Biol Macromol* **2016,** *92*, 1266-1276.

38. Novototskaya-Vlasova, K. A.; Petrovskaya, L. E.; Rivkina, E. M.; Dolgikh, D. A.; Kirpichnikov, M. P., Characterization of a cold-active lipase from Psychrobacter cryohalolentis K5(T) and its deletion mutants. *Biochemistry (Mosc)* **2013,** *78* (4), 385-94.

39. Joseph, B.; Shrivastava, N.; Ramteke, P. W., Extracellular cold-active lipase of Microbacterium luteolum isolated from Gangotri glacier, western Himalaya: Isolation, partial purification and characterization. *Journal of Genetic Engineering and Biotechnology* **2012,** *10* (1), 137-144.

40. Rashid, N.; Shimada, Y.; Ezaki, S.; Atomi, H.; Imanaka, T., Low-temperature lipase from psychrotrophic Pseudomonas sp. strain KB700A. *Appl Environ Microbiol* **2001,** *67* (9), 4064-9.

41. Yu, M.; Qin, S.; Tan, T., Purification and characterization of the extracellular lipase Lip2 from Yarrowia lipolytica. *Process Biochemistry* **2007,** *42* (3), 384-391.

42. Liebeton, K.; Zacharias, A.; Jaeger, K. E., Disulfide bond in Pseudomonas aeruginosa lipase stabilizes the structure but is not required for interaction with its foldase. *J Bacteriol* **2001,** *183* (2), 597-603.

43. Bisht, D.; Yadav, S. K.; Darmwal, N. S., An oxidant and organic solvent tolerant alkaline lipase by P. aeruginosa mutant: downstream processing and biochemical characterization. *Braz J Microbiol* **2014,** *44* (4), 1305-14.

44. Ugur, A.; Sarac, N.; Boran, R.; Ayaz, B.; Ceylan, O.; Okmen, G., New Lipase for Biodiesel Production: Partial Purification and Characterization of LipSB 25-4. *ISRN Biochem* **2014,** *2014*, 289749.

45. Salleh, A. B.; Rahman, R. N. Z. R. A.; Basri, M., New Lipases and Proteases. *Nova Biomedical* **2006**, pp 63-76.

46. Glogauer, A.; Martini, V. P.; Faoro, H.; Couto, G. H.; Muller-Santos, M.; Monteiro, R. A.; Mitchell, D. A.; de Souza, E. M.; Pedrosa, F. O.; Krieger, N., Identification and characterization of a new true lipase isolated through metagenomic approach. *Microb Cell Fact* **2011,** *10*, 54.

47. Borkar, P. S.; Bodade, R. G.; Rao, S. R.; Khobragade, C. N., Purification and characterization of extracellular lipase from a new strain: Pseudomonas aeruginosa SRT 9. *Braz J Microbiol* **2009,** *40* (2), 358-66.

48. Salameh, M. A.; Wiegel, J., Effects of Detergents on Activity, Thermostability and Aggregation of Two Alkalithermophilic Lipases from Thermosyntropha lipolytica. *Open Biochem J* **2010,** *4*, 22-8.

49. Torres, S.; Castro, G., Non- aqueous biocatalysis in homogenous systems. *Food Technol Biotechnol* **2004,** *42*, 271-277.

50. Gupta, M. N.; Batra, R.; Tyagi, R.; Sharma, A., Polarity Index: The Guiding Solvent Parameter for Enzyme Stability in Aqueous-Organic Cosolvent Mixtures. *Biotechnol Prog* **1997,** *13*, 284-288.

51. Tsuzuki, W.; Ue A Kitamura, Y., Effect of dimethylsulfoxide on hydrolysis of lipase. *Biosci Biotechnol Biochem* **2001,** *65* (9), 2078-82.

52. Kulschewski, T.; Pleiss, J., Binding of Solvent Molecules to a Protein Surface in Binary Mixtures Follows a Competitive Langmuir Model. *Langmuir* **2016,** *32* (35), 8960-8.

Figures and Legends

Figure 1. Multiple sequence alignments between LipY8p and highly homologous lipases from *Y. lipolytica* (LIPY, E0Z5H2; LIP8, Q872L3; LIP7, Q872L4; LIP2, Q9P8F7), *Candida galli* (CgLIP8, A0A078BRV6; CgLIP7, A0A078BNS3), *Candida deformans* (CdLIP3, Q875G8; CdLIP2, Q875G9) and *Candida alimentaria* (CaLIP7, A0A078BMP3). Cysteine residues are marked in gray and conserved residues of the active site including serine, aspartic acid and histidine are marked in black.

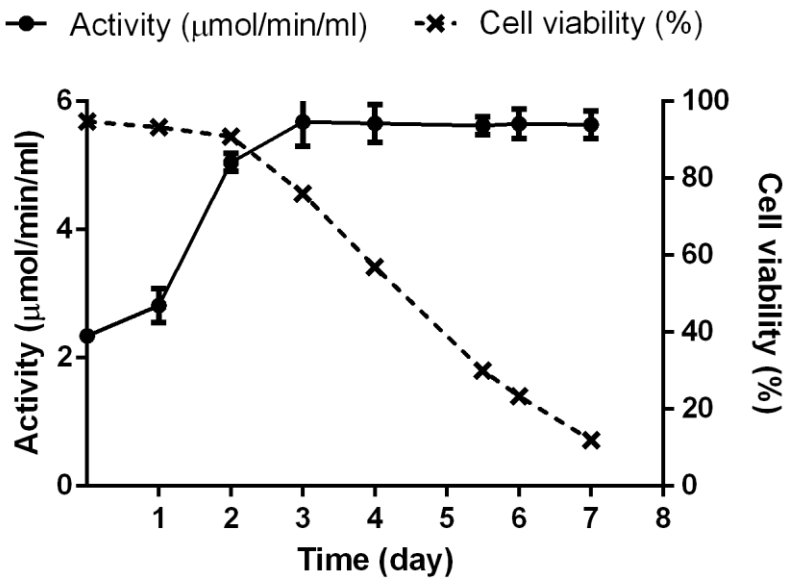

Figure 2. Time course of LipY8p expression and Sf9 cell viability. Lipase activity reached a plateau three days after infection with virus.

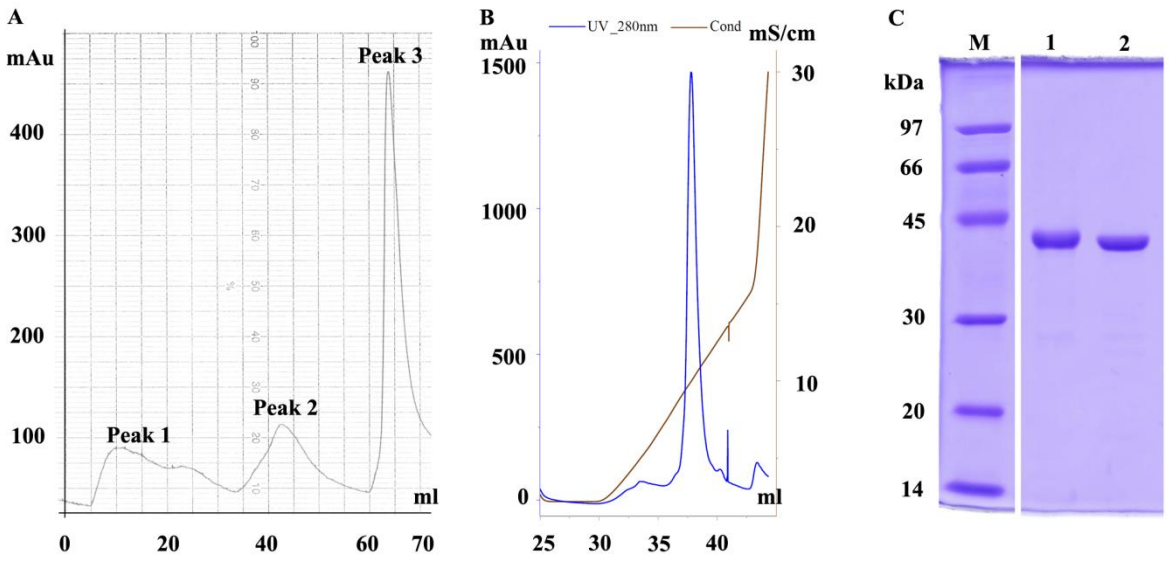

Figure 3. Purification of the recombinant LipY8p lipase. (A) Ni-NTA affinity chromatography. Peak1, peak2 and peak3 were eluted by buffer A containing 5 mM, 20 mM and 150 mM imidazole, respectively; (B) Mono Q anion exchange. LipY8p was eluted at around 10 mS/cm conductivity. (C) SDS-PAGE analysis of purified LipY8p. M, protein marker; 1, purified LipY8p; 2, LipY8p after deglycosylation.

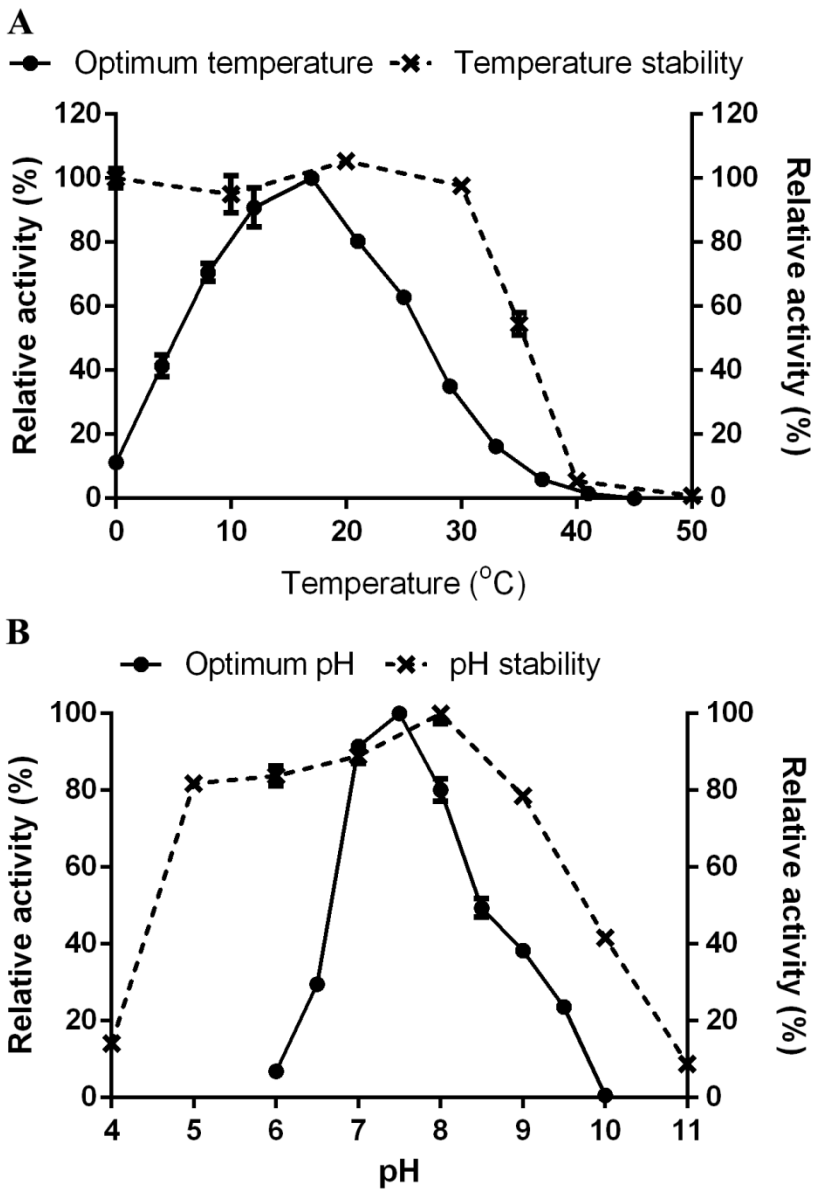

Figure 4. Optimum temperature (A) and optimum pH (B) on activity and stability of LipY8p lipase.

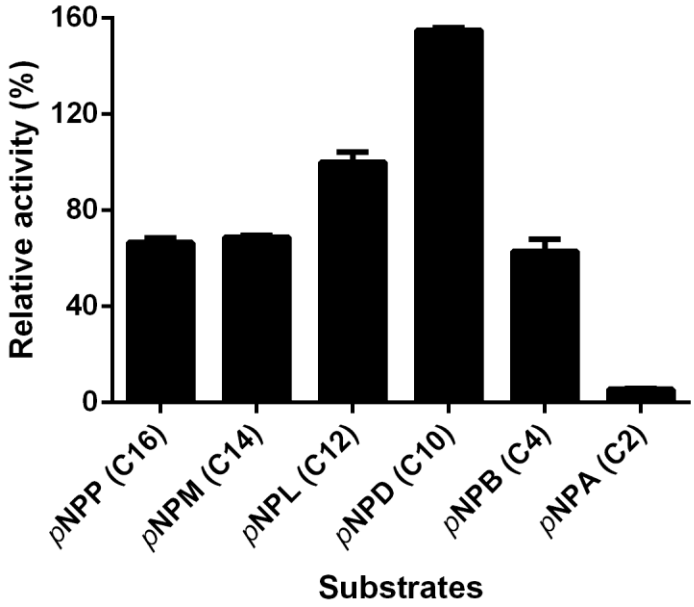

Figure 5. Substrate specificity of LipY8p lipase against different chain length *p*NP esters. Activity of *p*NP dodecanoate (*p*NPL) was considered as 100%. *p*NPP, *p*NP palmitate; *p*NPM, *p*NP myristate; *p*NPD, *p*NP decanoate; *p*NPB, *p*NP butyrate; *p*NPA, *p*NP acetate.

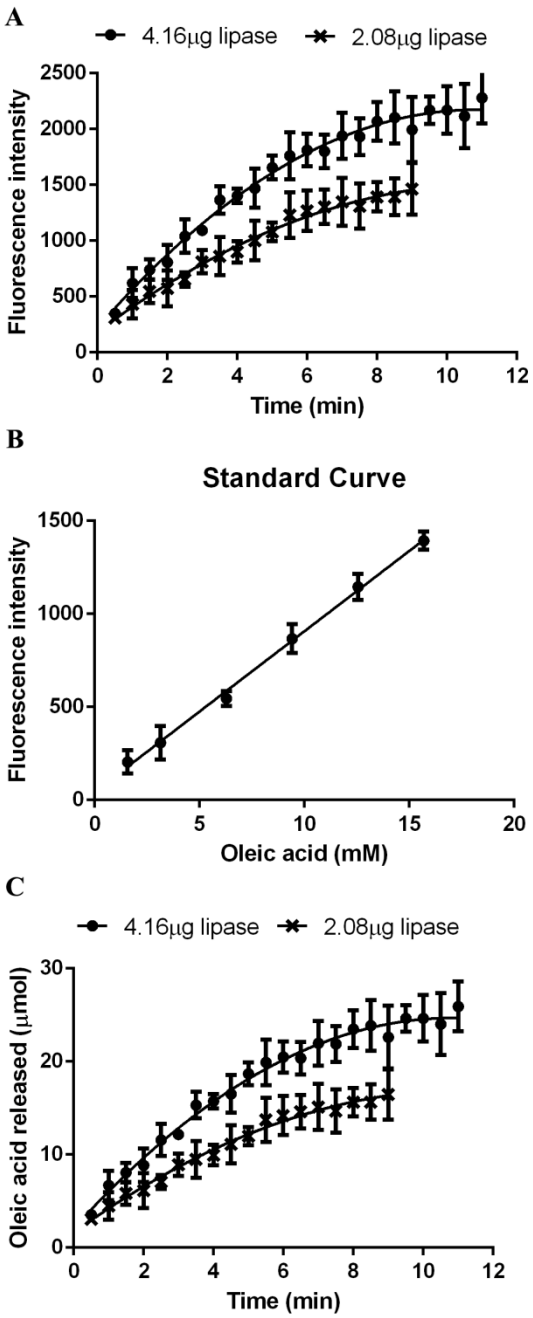

Figure 6. Quantification of fatty acid released by LipY8p hydrolysis of olive oil. (A) Hydrolysis of olive oil in RhB-OOe leads to fluorescence emission. (B) Standard curve prepared with RhB-OOe using 3–18 mM oleic acid. (C) Quantification of fatty acid released by LipY8p hydrolysis of olive oil. The excitation wavelength was set to 350 nm, and fluorescence emission was recorded at 580 nm. Each measurement was performed three times, and standard deviations were indicated.

Tables

Table 1. A summary of LipY8p lipase purification

Purification steps	Protein (mg)	Lipase activity (kU[a])	Specific activity (U/mg)	Yield (%)	Purification (fold)
Culture medium	104.37	1.81	17.37	100	1
Ammonium sulfate	61.93	1.57	25.36	86.63	1.46
Ni-NTA column	3.61	0.64	177.08	35.30	10.19
Mono Q column	0.94	0.42	446.85	23.19	25.72

[a] Activity test was carried out by spectrophotometer in phosphate buffer pH 7.5 at 17ºC, using pNPL as substrate. One unit (U) of enzyme activity was defined as the amount of enzyme required for the liberation of 1.0 µmol p-nitrophenol per min under the assay conditions.

Table 2. Effect of metal ions and inhibitors on lipase activity

Compounds	Concentration (mM)	Residual activity (%)
Control	none	100 ± 1.18
β-ME	1	117.6 ± 1.22
	5	129.8 ± 8.32
	10	125.8 ± 1.69
PMSF	1	80.1 ± 2.22
	4	47.6 ± 3.92
KCl	1	118.4 ± 5.83
$CaCl_2$	1	96.3 ± 3.99
$MgCl_2$	1	96.8 ± 1.50
$ZnSO_4$	1	1.2 ± 0.10
$CuCl_2$	1	12.5 ± 0.02
$NiSO_4$	1	51.8 ± 2.11
EDTA	1	136.1 ± 4.49

Table 3. Effect of detergents on lipase activity when present in reaction buffer

Detergents	Concentration (v/v or w/v)	Residual activity (%)
Control	none	100 ± 1.18
SDS	0.1%	0.89 ± 0.16
Triton-X100	0.1%	-
NP40	0.1%	-
Tween-20	0.1%	0.14 ± 0.02
β-OG	0.1%	105.5 ± 2.18
	0.3%	2.2 ± 0.10
β-DDM	0.1%	-
$C_{12}E_8$	0.001%	63.1 ± 5.16
	0.002%	7.9 ± 1.38

-, Activity undetectable.

Table 4. Effect of detergents on lipase activity and stability when present in enzyme stock solution

Detergents	Concentration (v/v or w/v)	Residual activity (%)	Incubation time (h)
Control	none	100 ± 1.85	2
SDS	0.1%	-	2
Triton-X100	0.1%	128.1 ± 4.05	2
	0.1%	140.2 ± 4.15	24
	0.1%	110.4 ± 2.75	48
	0.1%	96.4 ± 4.44	72
NP40	0.1%	-	2
Tween-20	0.1%	-	2
β-OG	0.1%	147.1 ± 0.25	2
	0.1%	124.7 ± 4.19	24
	0.1%	119.2 ± 2.83	48
	0.5%	143.9 ± 4.12	2
	0.5%	127.7 ± 1.58	24
	0.5%	121.6 ± 2.49	48
β-DDM	0.1%	39.9 ± 3.29	2
$C_{12}E_8$	0.1%	144.2 ± 5.50	2
	0.01%	140.0 ± 2.85	2
	0.1%	140.8 ± 3.56	24
	0.1%	130.0 ± 1.88	48

-, Activity undetectable.

Table 5. Effect of organic solvents on lipase activity

Solvents	Concentration (v/v)	Residual activity (%)
Control	none	100 ± 7.15
Iso-propanol	10%	174.4 ± 5.27
	20%	5.2 ± 0.29
Methanol	20%	180.3 ± 1.71
Ethanol	10%	266.7 ± 5.4
	20%	50.1 ± 3.51
Acetone	10%	361.5 ± 11.3
	20%	38.7 ± 2.09
DMSO	20%	416.9 ± 22.7

Table 6. Stability of lipase in different organic solvents

Solvents	Concentration (v/v)	Residual activity (%)
Control	none	100 ± 2.24
Methanol	20%	72.81 ± 1.37
Ethanol	20%	0.90 ± 0.03
Acetone	20%	1.38 ± 0.04
Iso-propanol	20%	-
DMSO	20%	88.05 ± 4.64
DMF	20%	13.21 ± 0.13
Ethyl Ether	20%	10.86 ± 0.16

-, Activity undetectable.